สภาวะสำหรับอิเลคโตรพอลิเมอไรเซชันของไพรอลเพื่อการสร้างไมโครอิเลคโทรดอาร์เรย์ภายในฟีนอลไบโอเซนเซอร์

นางสาวปานใจ รุจิสมนภา

วิทยานิพนธ์นี้เป็นส่วนหนึ่งของการศึกษาตามหลักสูตรปริญญาวิศวกรรมศาสตรมหาบัณฑิต
สาขาวิชาวิศวกรรมเคมี ภาควิชาวิศวกรรมเคมี
คณะวิศวกรรมศาสตร์ จุฬาลงกรณ์มหาวิทยาลัย
ปีการศึกษา 2552

ลิขสิทธิ์ของจุฬาลงกรณ์มหาวิทยาลัย

ศูนย์วิทยทรัพยากร
จุฬาลงกรณ์มหาวิทยาลัย

PYRROLE ELECTROPOLYMERIZATION CONDITIONS FOR FABRICATION OF MICROELECTRODE ARRAY WITHIN PHENOL BIOSENSOR

Miss Panjai Rujisomnapa

A Thesis Submitted in Partial Fulfillment of the Requirements
for the Degree of Master of Engineering Program in Chemical Engineering
Department of Chemical Engineering
Faculty of Engineering
Chulalongkorn University
Academic Year 2009
Copyright of Chulalongkorn University

Thesis Title	PYRROLE ELECTROPOLYMERIZATION CONDITIONS FOR FABRICATION OF MICROELECTRODE ARRAY WITHIN PHENOL BIOSENSOR
By	Miss Panjai Rujisomnapa
Field of Study	Chemical Engineering
Thesis Advisor	Associate Professor Seeroong Prichanont, Ph.D.
Thesis Co-Advisor	Chanchana Thanachayanont, Ph.D.

Accepted by the Faculty of Engineering, Chulalongkorn University in Partial Fulfillment of the Requirements for the Master's Degree

.....Dean of the Faculty of Engineering

(Associate Professor Boonsom Lerdhirunwong, Dr.Ing.)

THESIS COMMITTEE

..... Chairperson

(Associate Professor Muenduen Phisalaphong, Ph.D.)

.....Thesis Advisor

(Associate Professor Seeroong Prichanont, Ph.D.)

.....Thesis Co-Advisor

(Chanchana Thanachayanont, Ph.D.)

.....Examiner

(Assistant Professor Varong Pavarajarn, Ph.D.)

.....External Examiner

(Associate Professor Manop Suphantharika, Ph.D.)

ปานใจ รุจิสมนภา : สภาวะสำหรับอิเลคโตรพอลิเมอไรเซชันของไพรอลเพื่อการสร้างไมโครอิเลคโทรดอาร์เรย์ภายในฟีนอลไบโอเซนเซอร์ (PYRROLE ELECTROPOLYMERIZATION CONDITIONS FOR FABRICATION OF MICROELECTRODE ARRAY WITHIN PHENOL BIOSENSOR) อ.ที่ปรึกษาวิทยานิพนธ์หลัก : รศ. ดร. สีรุ้ง ปรีชานนท์, อ.ที่ปรึกษาวิทยานิพนธ์ร่วม : ดร. ชัณชนา ธนชยานันท์, 121 หน้า

งานวิจัยนี้ศึกษาการตรึงเอนไซม์ฮอร์สแรดิชเปอร์ออกซิเดสร่วมกันกับพอลิไพรอลลงบนไมโครอิเลคโทรดอาร์เรย์ที่สร้างด้วยวิธีโซโนเคมิคอล สำหรับตรวจวัดสารฟีนอล โดยสร้างบนอิเลคโทรดชนิดกลาสซีคาร์บอน เอนไซม์และพอลิไพรอลจะถูกเคลือบบนไมโครอิเลคโทรดที่ถูกโซนิเคทที่เวลา 25 นาทีบนฟิล์มของพอลิไดอะมิโนเบนซีนซึ่งเป็นพอลิเมอร์ไม่นำไฟฟ้า และศึกษาสภาวะที่ใช้ในการเคลือบด้วยวิธีอิเลคโตรพอลิเมอร์ไรเซชัน ดังนี้ จำนวนรอบการเคลือบ, อัตราเร็วในการสแกน, ความเข้มข้นของไพรอล และเอนไซม์ ตามลำดับ จากการศึกษาพบว่าไมโครอิเลคโทรดไบโอเซนเซอร์ที่ให้กระแสได้ดีที่สุดในงานวิจัยนี้ควรตรึง ฮอร์สแรดิชเปอร์ออกซิเดสร่วมกับ พอลิไพรอลที่ความเข้มข้น 250 ยูนิต/มิลลิลิตร และ 0.05 โมลาร์ ตามลำดับ ใช้อัตราการสแกนเท่ากับ 20 มิลลิโวลต์/วินาที และเคลือบเป็นจำนวน 20 รอบ

ไบโอเซนเซอร์นี้มีช่วงความเป็นเส้นตรงของฟีนอลที่ 2-100 ไมโครโมลาร์ มีความว่องไวต่อฟีนอลเท่ากับ 0.1053 นาโนแอมแปร์/ไมโครโมลาร์ และมีระดับการตรวจพบต่ำสุดที่ความเข้มข้นฟีนอลเท่ากับ 4.55 ไมโครโมลาร์ โดยกระแสตอบสนองต่อฟีนอลจะเข้าสู่สมดุลภายใน 150 วินาที แต่อย่างไรก็ตามกระแสตอบสนองของเซนเซอร์ที่สร้างขึ้นนี้เหลือเพียง 50% ของกระแสเริ่มต้น หลังจากวัดซ้ำ 10 ครั้ง และลดลง 54% ของกระแสเริ่มต้นหลังเก็บรักษาไว้สองวัน นอกจากนี้ ความสามารถในการผลิตซ้ำมีค่า เบี่ยงเบนมาตรฐานสัมพัทธ์สูงถึง 23.84%

ภาควิชา	วิศวกรรมเคมี	ลายมือชื่อนิสิต ปานใจ รุจิสมนภา
สาขาวิชา	วิศวกรรมเคมี	ลายมือชื่ออาจารย์ที่ปรึกษาวิทยานิพนธ์หลัก
ปีการศึกษา	2552	ลายมือชื่ออาจารย์ที่ปรึกษาวิทยานิพนธ์ร่วม

5170590921 : MAJOR CHEMICAL ENGINEERING
KEYWORDS: MICROELECTRODE ARRAY / HORSERADISH PEROXIDASE / POLYPYRROLE /POLYDIAMINOBENZENE/ PHENOL BIOSENSOR

PANJAI RUJISOMNAPA: PYRROLE ELECTROPOLYMERIZATION CONDITIONS FOR FABRICATION OF MICROELECTRODE ARRAY WITHIN PHENOL BIOSENSOR. THESIS ADVISOR: ASSOC. PROF. SEEROONG PRICHANONT, Ph.D., THESIS CO-ADVISOR: CHANCHANA THANACHAYANONT, Ph.D., 121 pp.

This research is the study of horseradish peroxidase (HRP) and polypyrrole (PPY) co-immobilization onto sonochemical fabricated microelectrode arrays for phenol detection. This microelectrode was fabricated based on glassy carbon electrode. An enzyme and pyrrole were electropolymerized onto 25min sonicated microelectrode arrays of ablated polydiaminobenzene film. Optimal fabrication conditions of microelectrode arrays for phenol detection were studied, namely, number of cycles and scan rate for pyrrole electropolymerization, pyrrole and HRP concentrations, respectively. Suitable microelectrode biosensors in this research were fabricated from co- electropolymerization of 250 U/ml HRP and 0.05M pyrrole at 20mV/s scan rate for 20cycles.

Linear range of this biosensor was found in from 2-100 μM. The sensitivity of this biosensor was 0.1053 nA/ μM and the detection limit of 4.55 μM phenol was obtained. The response time of this biosensor was found within 150 s. However, the current response of this biosensor decreased to 50% of the initial current after 10 repeated tests, and lost 54% of its initial response on the second day of storage. Moreover, the R.S.D. of this microelectrode reproducibility was 23.84%

จุฬาลงกรณ์มหาวิทยาลัย

Department: Chemical Engineering	Student's Signature : Panjai Rujisomnapa
Field of Study: Chemical Engineering	Advisor's Signature :
Academic Year: 2009	Co-Advisor's Signature :

ACKNOWLEDGEMENTS

The author would like to sincerely thanks and express her sincere gratitude and appreciation to her advisor, Associate Professor Seeroong Prichanont, for her supervision, encouraging guidance, advice, discussion and helpful suggestions throughout the course of this Master Degree study. Also, she is very grateful to her co-advisor, Mrs.Chanchana Thanachayanont, for material surface suggestions and for helpful of electrode cutting and any techniques. In addition, the author would also be grateful to Associate Professor Muenduen Phisalaphong, as the chairman, Professor Manop Suphantharika, Assistant Professor Varong Pavarajarn as the external and internal members of the thesis committee, respectively. The author also acknowledges to Associate Professor Mana Sriyudthsak from electrical engineering faculty who gave useful suggestions in electrochemical knowledge. The financial supports from the Department of Chemical Engineering and the Graduate School of Chulalongkorn University are gratefully acknowledged.

In addition, the author is grateful to Metrohm Siam Company and their official for helps in equipment, location and suggestions. Especially appreciate for enzyme supporting from Atomic Sci distribute company and expenses reducing of SEM technique from Nanotec. Also, she appreciates to MTEC for electrode cutting and image analyze program.

Special thanks to Miss Lerdluck Keawimol and Mr. Yusran Dao, PhD. and Master Degree students, respectively, of Associate Professor Seeroong Prichanont for suggestion, advice and information and helps. Thanks to Mr. Bancha Ounpanich for electrical techniques. Moreover, thanks to Mrs. Wanwimon Mekboonsonglarb and Mr. Sirawat Saening, technicians of STREC, for many useful suggestions and helps.

Most of all, the author would like to express the highest gratitude to her family who always pay attention to her all the times for suggestions and listen her complaints. The most success of graduation is devoted to my family.

Finally, the author wishes to thank all members of the Biochemical Engineering Research Laboratory and all my friends in the Department of Chemical Engineering for their assistance and warm collaborations.

CONTENTS

PAGE

ABSTRACT (THAI) ..... **iv**

ABSTRACT (ENGLISH) ..... **v**

ACKNOWLEDGEMENTS ..... **vi**

CONTENTS ..... **vii**

LISTS OF TABLES ..... **ix**

LISTS OF FIGURES ..... **x**

CHAPTER

I INTRODUCTION **1**

1.1 Motivation 1

1.2 Objective 2

1.3 Expected benefits 2

1.4 Scopes of the research 2

II THEORY **4**

2.1 Biosensor 4

2.2 Microelectrode array 12

2.3 Horseradish peroxidase (HRP) 16

2.4 Enzyme immobilization 19

2.5 Conducting polymer for fabrication of biosensor 21

III LITERATURE REVIEWS **24**

3.1 Fabrication techniques of microelectrode arrays 24

3.2 Horseradish peroxidase (HRP) biosensor 33

IV MATERIALS AND METHODS **50**

4.1 Materials 51
4.2 Apparatus 51
4.3 Preparation of buffer solution 52
4.4 Electrode preparation 52
4.5 Polymerization and enzyme immobilization of micro-electrode arrays 53
4.6 Cyclic voltammetric and Amperometric phenol sensor 54
4.7 Performance factor of microelectrode biosensor 54
4.8 Characterization of modified electrode 56
4.9 Statistical differences 56

V RESULTS AND DISCUSSIONS **57**

5.1 Microelectrode arrays formation 57
5.2 HRP-PPY biosensor 76
5.3 Performance factors 92

VI CONCLUSIONS AND RECOMMENDATIONS **99**

REFERENCES **101**

APPENDICES **111**

Appendix A Raw data 112
Appendix B Conference 117

VITA **121**

ศูนย์วิทยทรัพยากร
จุฬาลงกรณ์มหาวิทยาลัย

LIST OF TABLES

TABLES **PAGE**

3.1 Researches of microelectrode arrays for enzyme based biosensors from different fabrication methods. 31
3.2 Research of HRP based on amperometric biosensors with different immobilization methods. 37
3.3 Researches of an enzyme entrapment within polypyrrole film by electropolymerization for fabrication HRP biosensor and their electropolymerization conditions. 45
5.1 Average diamiter from formular calculation of pores on surface of each sonicated electrodes. 67
5.2 Optimum conditions for fabrication of HRP-PPY co-immobilixed on microelectrode arrays. 87
5.3 Comparison of performance factors of this research with other researches. 98

ศูนย์วิทยทรัพยากร
จุฬาลงกรณ์มหาวิทยาลัย

LIST OF FIGURES

FIGURES **PAGE**

2.1 Schematic layout of a biosensor (Eggins, 1999). 5

2.2 Cyclic voltammogram with four main parameters (http://upload.wikimedia.org/wikipedia/ Cyclovoltammogram.jpg). 8

2.3 Current-time for constant potential amperometry (www.rsc.org/ej/AN/2007/b611920d/b611920d-f5.gif). 10

2.4 Method of determining the detection limit (Eggins, 1999). 11

2.5 Schematic representation of diffusion layers of concentration profiles developing at arrays of electrodes at different times of the electrochemical perturbation: (a) planar diffusion at short times, (b) hemispherical or cylindrical diffusion at intermediate times, and (c) planar diffusion and overlap of individual diffusion layers at long times (Zoski, 2009). 15

2.6 (a) random array scheme, (b) ordered array scheme, and (c) Three-dimensional arrays from etching method (Zoski, 2009;.Lee et al., 2006). 16

2.7 Mechanism of mediated bioelectrocatalytic reduction of hydrogen peroxide at peroxidase-modified electrodes. M_{ox} and M_{red} are the oxidized and reduced forms of the mediator, respectively (Rosatto et al., 1999). 18

2.8 Mechanism of the direct bioelectrocatalytic reduction of hydrogen-peroxide at peroxidase-modified electrodes (Rosatto et al., 1999). 18

2.9 Schemes of adsorption, covalent bonding, cross-linking and encapsulation methods of an enzyme immobilization, respectively (Blanch and Clark,1997). 21

2.10 Polypyrrole molecule (Cosnier, 1999). 22

3.1 SEM micrographs of (a) PEDOT doped with $LiClO_4$ grown through a polystyrene latex sphere template on the electrode site before removal of polystyrene template (inset showing the high magnification); (b) A microporous film of PEDOT doped with $LiClO_4$ after partially removal of polystyrene template. (inset showing the template was removed partly) (Yang et al, 2004). 25

3.2 Schematic of the electrode array fabrication process. A clean insulating substrate was coated with photoresist, then patterned photolithographically

and developed. The patterned substrate was then metalized and lift-off used to create the electrode array (Revzin et al., 2002). 26
3.3 Schematic of structure of microelectrode arrays. 28
4.1 The experimental chart of this work. 50
4.2 Schematics of polymer insulated electrode and microelectrode array, respectively. 52
4.3 Schematic of sonochemically fabricated polypyrrole/HRP microelectrode array. 54
4.4 The schematic diagram for small GC electrode connection. 55
5.1 Cyclic voltammogram of polydiaminobenzene dihydrocholride electropolymerization for 50 cycles at 20mV/s. 58
5.2 Cyclic voltammograms (vs. Ag/AgCl) in 10mM ferri/ferrocyanide couple solution of (i) bare GCE, (ii) PPD coated GCE, and (iii) a 25 min sonicated PPD/GCE, respectively. Scan rate 20mV/s. 60
5.3 Cyclic voltammograms (vs. Ag/AgCl) in 10mM ferri/ferrocyanide couple solution of (i) 10, (ii) 20, (iii) 25, (iv) 30, (v) 50, and (vi) 90 min sonicated PPD coated GCE, respectively. Scan rate 20mV/s. 61
5.4 AFM images of (a) bare GCE and (b) PPD coated GCE; and SEM images of (c) bare GCE and (d) PPD coated GCE, respectively. 63
5.5 Section analysis from AFM image for the film thickness determination of a 50 cycles PPD coated GCE. 64
5.6 AFM images of sonicated PPD/GCE for (a) 10, (b) 20, (c.1) 25, (d.1) 30, (e.1) 50, and (f.1) 90 min.; (c.2) to (f.2) are distributions of pore's sizes on surfaces of a 25, 30 50, and 90 min sonicated electrodes, respectively. 69
5.7 SEM images of sonicated PPD/GCE with (a) 10, (b) 20, (c) 25, (d) 30, (e) 50, and (f) 90 min. 72
5.8 Schematic diagrams of polymer film sonication (black is GCE and orange is PPD film); (a) non-sonicated PPD/GCE, (b) before 10 min sonicated PPD/GCE, (c) a 10 min sonicated PPD/GCE, (d) a 20 min sonicated PPD/GCE, (e) a 25 min sonicated PPD/GCE, (f) 30, 50 and 90 min sonicated PPD/GCE. 73

5.9 Total number of pores on surface of sonicated electrodes at 25, 30, 50, and 90 min sonication times, respectively. 74
5.10 Mechanism of mediated bioelectrocatalytic reduction of H_2O_2 at HRP based electrodes where M_{ox} and M_{red} are the oxidised and reduced forms of the phenol, respectively (Rosatto et al., 1999). 77
5.11 Comparison of current responses between bare GCE, PPY/GCE, and HRP-PPY/GCE in different solution (pH 7.4) at-0.05V. 79
5.12 Comparison of current responses between bare GCE, PPY/GCE, and HRP-PPY/GCE with various H_2O_2 concentration in 50μM phenol / PBS solution (pH 7.4) at-0.05V. 80
5.13 Cyclic voltammogram of polypoyrrole-horseradish peroxidase electro-polymerization for 15 cycles at 10mV/s. 82
5.14 Effect of number of cyles (vs. Ag/AgCl) on the HRP-PPY electro-polymerization onto 25 min sonicated PPD/GCE responses to amount of 50μM H_2O_2 and 50μM phenol in PBS at -0.05V. Where * represent the significant difference ($p<0.05$) relative to 10 cycle of PPY-HRP electropoltymerization. 83
5.15 Effect of scan rate (vs. Ag/AgCl) on the HRP-PPY electropoly-merization onto 25 min sonicated PPD/GCE responses to amount of 50μM H_2O_2 and 50μM phenol in PBS at -0.05V. Where * represent the significant difference ($p<0.05$) relative to 10 mV/s of PPY-HRP electropoltymerization. 84
5.16 Effect of pyrrole concentration (vs. Ag/AgCl) on the HRP-PPY electropolymerization onto 25 min sonicated PPD/GCE responses to amount of 50μM H_2O_2 and 50μM phenol in PBS at -0.05V. Where * represent the significant difference ($p<0.05$) relative to 0.05M Pyrrole. 86
5.17 Effect of HRP concentration (vs. Ag/AgCl) on the HRP-PPY electropolymerization onto 25 min sonicated PPD/GCE responses to amount of 50μM H_2O_2 and 50μM phenol in PBS at -0.05V. Where * represent the significant difference ($p<0.05$) relative to 250U/ml HRP. 87

5.18 Comparison of amperometry current responses of HRP-PPY/ 25 min sonicated PPD/GCE in different solution (pH 7.4) at-0.05V. 88
5.19 (a) and (b) are AFM and SEM images of HRP-PPY protrusions on arrays of PPD/GCE, respectively; (c) SEM image of 25 min sonicated PPD/GCE without HRP-PPY. 91
5.20 Schematic diagrams of enzyme-polypyrrole protrusion (black is GCE, orange is PPD film, and purple is HRP-PPY protrusion); (a) non-mushroom shape of HRP- PPY protrusion, (b) recessed microelectrode arrays, (c) too small diameter microelectrode arrays, (d) inactive microelectrode arrays (e) merged protrusion. 91
5.21 Calibration curve of amperometric phenol response in 50 μM H_2O_2/ PBS solution (pH 7.4) at -0.05V (vs. Ag/AgCl). Inset: the linear part of the calibration curve. 93
5.22 Amperometric current response of biosensor of 50μM phenol/ 50μM H_2O_2 in PBS solution (pH 7.4) at -0.05V (vs. Ag/AgCl). 94
5.23 Ten amperometric current responses of a same biosensor in 50μM phenol/50μM H_2O_2 / PBS solution (pH 7.4) at -0.05V (vs. Ag/AgCl). 95
5.24 Amperometric current ten biosensors in 50μM phenol/50μM H_2O_2 (pH 7.4) at -0.05V (vs. Ag/AgCl). 96
5.25 Storage stability of a biosensor in 50μM phenol/50μM H_2O_2 / PBS solution (pH 7.4) at -0.05V (vs. Ag/AgCl). 97

ศูนย์วิทยทรัพยากร
จุฬาลงกรณ์มหาวิทยาลัย

CHAPTER I

INTRODUCTION

1.1 Motivation

In the past three decades, microelectrode arrays have been used as devices to examine electroactive species in the field of cellular biology. Many researchers, especially in clinical and biochemical research, applied microelectrode arrays within biosensors for substance determination. These biosensors showed their special characteristics which were greater than conventional biosensors such as small volume in reagents, quick response time, ease of fabrication, and etc (Liu et al., 2005). Although microelectrode arrays can be fabricated by several techniques such as photolithography or laser ablation, but these are costly approaches. Sonochemical fabrication is a simple and inexpensive approach. Previous researches have utilized sonochemically microelectrode arrays containing entrapped enzymes for an amperometric detection of glucose (Barton et al., 2004; Myler et al., 2004), alcohol (Myler et al., 2005) and a range of organophosphate pesticides (Pritchard et al., 2004; Law and Higson, 2005) with extreme sensitivity (10^{-17} M of substance).

Nowadays, interests for environmental monitoring have increased due to the wide expanding of industrial plants as well as heavy uses of chemical reagents. In many cases, such reagents are toxic when they are released to the environment. Phenols are one example of these pollutants that are often found in wastewaters of several industries, including coal conversion, petroleum refining, resins and plastics, metal coating, dyes and other chemicals, food, textiles, mining and dressing, and pulp and paper (Rosatto et al., 1999; Stanca et al., 2003; Korkut et al., 2008). One approach for determination of phenols is uses of amperomatric biosensors which are considered more favorable due to their simplicity, high sensitivity and low costs.

Peroxidases can be used to detect a phenol and a great numbers of phenolic compounds. Horseradish peroxidase (HRP) is a type of peroxidases which can be seen in many macroelectrode biosensor researches for phenol detection. Nevertheless,

microelectrode biosensors have not been found for phenol detection, so it is interesting to use microelectrode arrays containing HRP for detection of phenol and its derivatives.

In this research, the HRP based microelectrode arrays within biosensors were fabricated by sonochemical procedure for detection of phenols. Polypyrrole was used to entrap enzyme by an electropolymerization process, and then the electropolymerization conditions of pyrrole were investigated such as scan rate, monomer concentration, enzyme concentration, and number of scan cycles. The optimum conditions were selected for biosensor fabrication.

1.2 Objective

To study effects of electropolymerization conditions on efficiency of polydiaminobenzene/ polypyrrole/ HRP microelectrode arrays for phenol detection.

1.3 Expected benefits

To define suitable conditions for fabrication of polydiaminobenzene/ polypyrrole/ HRP microelectrode arrays on biosensor and to improve the sensitivity of microelectrode within biosensor for phenol detection.

1.4 Scopes of the research

In this research, glassy carbon electrode (GCE) was used as working electrode, while platinum wire (Pt) and silver/silver chloride ($Ag/AgCl_3$) was used as counter and reference electrodes, respectively. GCEs were electropolymerized with 5mM polydiaminobenzene versus Ag/AgCl between 0 to 1.0V, 20mV/s for 50 cycles. The coated electrodes were then sonicated for 25 min after 2 hours air dried.

1.4.1 Investigate of suitable electrosynthesis conditions of polypyrrole on polydiaminobenzene array for phenol detection using cyclic voltammetry method.

1.4.1.1 Numbers of scan cycles (10, 15, 20, 25, and 30 cycles).

1.4.1.2 Scan rate (5, 10, 20, 30, and 50 mV/s).

1.4.1.3 Pyrrole monomer concentration (0.03, 0.05, 0.07, and 0.09 M).

1.4.1.4 Enzyme concentration (150, 250, 350, and 450 unit/ml).

An enzyme was mixed with pyrrole monomer in phosphate buffer solution (PBS, pH 7.4). Potential cycling was used between 0 to +1.0 V. The temperature for fabrication of microelectrode arrays was fixed at the room temperature.

1.4.2 Physical characterization of microelectrode arrays by Scanning Electron Microscopy (SEM) and Atomic Force Microscope (AFM).

1.4.3 Electrochemical analysis of microelectrode arrays without enzyme were performed with cyclic voltammogram (CV) in 10mM ferri/ferrocyanide at scan rate of 20 mV/s and the potential between -1.0 and 1.0 V. For an enzyme microelectrode, the measurements were performed with amperometry technique in 50μM hydrogen peroxide/ 50 μM phenol/ phosphate buffer solution at -0.05V.

1.4.4 Determine the performance factors of the polydiaminobenzene/ polypyrrole/ horseradish peroxidase microelectrode arrays that are fabricated under suitable conditions.

1.4.4.1 Linear range, sensitivity, and detection limit

1.4.4.2 Response time

1.4.4.3 Reusability (repeatability)

1.4.4.4 Reproducibility

1.4.4.5 Lifetime

ศูนย์วิทยทรัพยากร
จุฬาลงกรณ์มหาวิทยาลัย

CHAPTER II

THEORY

The aim of this chapter was to give a comprehensive understanding of basic theories for microelectrode arrays fabrication. Firstly, the introduction of biosensors and microelectrode arrays will be detailed. The following part describes horseradish peroxidase (HRP), an enzyme that was chosen as a biocatalyst in this research. Moreover, methods of enzyme immobilization and information of a conducting polymer, an immobilized matrix, will also be focused in the final section of this chapter.

2.1 Biosensor

A biosensor is a specific detection device via cooperation between a biological substance and a transducer. A first biosensor was produced by Leland C. Clark in 1962 which was applied for glucose detection. Currently, the widespread uses and development of biosensor technology are increased as seen in several research. Biosensors can be used in many fields such as clinic, military, agriculture, industry and environment because they possess several advantageous characters, for example: high specificity, short response time, ease of use, and high operating stability.

A biosensor consists of two major parts which are a bioreceptor and a transducer as shown in the Fig. 2.1. The bioreceptor is the biological molecules that specify with their target substrate. Examples of biological substances are enzymes, antigens, organelles, cells or tissues, and etc. Biological substance is physically and chemically immobilized or connected with a transducer. The transducer is a device for receiving and converting reaction signals between a bioreceptor and an analyzed substance to an electrical signal. A display output of this signal relates with concentrations of the analyzed substrate, and then an amount of this substrate can be determined.

However, a suitable type of transducers must be selected for each specific application. For examples, a redox reaction can cause the electron transfer in a system, and then an amperometric transducer must be selected to determine this changing.

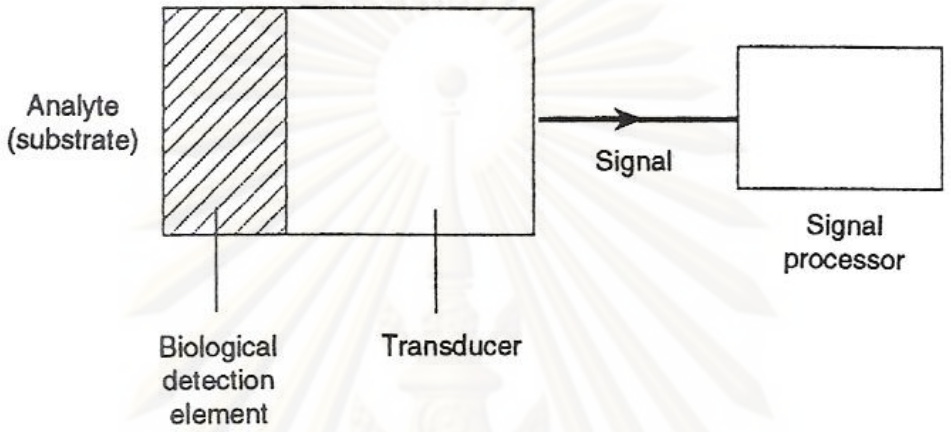

Fig. 2.1 Schematic layout of a biosensor (Eggins, 1999).

2.1.1 A current response of an electrochemical system

Determination of the current response in an eletroanalytical experiments can be considered with a simple redox reaction (Eq. 2.1):

$$O + ne^- \rightleftharpoons R \qquad (2.1)$$

From this equation, O and R display as oxidized and reduced forms of the redox couple, respectively, and n is the number of electrons transferred in this reaction. Equation (2.2) is the Nernst equation which can be used to solve the potential of the electrochemical system at the electrode surface under equilibrium condition:

$$E = E^0 + \frac{2.3RT}{nF} log \frac{C_O(0,t)}{C_R(0,t)} \qquad (2.2)$$

Where E^0 is the standard potential of the redox reaction, R is the universal gas constant (8.314 J K^{-1} mol^{-1}), T is the Kelvin temperature, and F is the Faraday constant (96,487 coulombs). The reaction rate and the current of the electrode can be governed by several processes (e.g. mass transfer, electron transfer, catalytic, surface adsorption processes, and etc.). The slowest of such process will determine the reaction rate or that called the rate-limiting step. However, the mass transfer and the electron transfer limited reactions are only represented in the following.

1) Mass transport-Controlled reactions

The mass transport is a controlled reaction when this process is a slowest process. Generally, mass transport can occurs with three patterns involves *diffusion* (the movement by concentration gradient), *convection* (the movement with physical force or density gradient), and *migration* (the movement of charged particles in an electrical filed). The Nernst-Planck equation can be used to describe the mass flux to the electrode:

$$J(x,t) = -D\frac{\partial C(x,t)}{\partial x} - \frac{zFDC}{RT}\frac{\partial \emptyset(x,t)}{\partial x} + C(x,t)V(x,t) \qquad (2.3)$$

Where D is the diffusion coefficient (cm^2s^{-1}); $\partial C(x,t)/\partial x$ and $\partial \emptyset(x,t)/\partial x$ are the concentration and potential gradients at x-axis and time t, respectively; z and C (mol cm^{-3}) are the charge and the concentration, respectively, V(x, t) is the hydrodynamic velocity (in direction x and time t). In this equation, on the right side, the first term is the diffusion rate. The second and the third terms represent the migration and the convection of the solution, respectively. For the simple equation, the solution must be added with excess inert salt (or supporting electrolyte) or unstirred the solution, the mass flux will be only controlled by diffusion (the Fick's first law).

In the diffusion controlled reaction, a current of planar electrode from a controlled potential experiment can be described with the Cottrell equation (Eq. 2.4). This equation is derived from the Fick's first law and the Fick's second law (the change in concentration with times relates to the change in flux with position):

$$i(t) = \frac{nFAD_O C_O(b)}{(\pi D_O t)^{1/2}} \qquad (2.4)$$

Where A is the electrode area (cm^2), r is the distance from the center of the electrode, and $(\pi D_o t)^{1/2}$ is a diffusion layer thickness (δ). Moreover, for the spherical electrode, the equation (2.5) can describe such current:

$$i(t) = \frac{nFAD_O C_O(b)}{(\pi D_O t)^{1/2}} + \frac{nFAD_O C_O}{r} \qquad (2.5)$$

The first term of the equation (2.5) is a time dependent term and dominates at short time. At long time, the second term (a spherical correction term) will be more dominate than the first term, becoming time independent current. This equation can also explain a microelectrode's current.

2) Electron transfer – Controlled reactions

When the electron transfer process is a slowest process, the reaction will be controlled by the rate of electron transfer. The Bulter-Volmer equation is used to describe a net current of the reaction where the net current is the difference between forward (reduction) and backward (oxidation) currents of the reaction:

$$i = i_0\{exp(-\propto nF\eta/RT) - exp[(1-\propto)nF\eta/RT]\} \qquad (2.6)$$

Where i_0 is the exchange current or the current under equilibrium state ($E=E_{eq}$), η is the overpotential or the overvoltage which must be used in non-spontaneous cell reaction, and α is the transfer coefficient, generally, this value closes to 0.5. While the value of i_0 is given by:

$$i_0 = i_c = i_a = nFAk^0C \qquad (2.7)$$

Where i_c and i_a are cathodic (reduction) and anodic (oxidation) currents, respectively, and k^0 is the standard heterogeneous rate constant (cm s^{-1}). The value of k^0 depends on the particular reactant and the electrode material used.

2.1.2 Electrochemical method

1) Cyclic voltammetry

Cyclic voltammetry is a popular technique for study the charge transfer from electrochemical cell. The current at a working electrode is monitoried when the potential between a working electrode and a reference electrode is varied. The resulting plot of current versus potential is known as a voltammogram (Fig. 2.2).

Assume that only an oxidized form (O) is present at the initial state. Determining for a forward scan, a current is higher as well as increasing the potential in negative way due to the reduction of O is more increased. For this situation, the concentration of a reduced form (R) near the electrode surface is higher than concentration of O and becomes highest at the peak of the voltammogram. The peak current at the cathodic peak potential ($E_{p,c}$) is called a cathodic (reduction) peak current ($i_{p,c}$). At the switching potential or reverse scanning, R molecules are reduced back to O molecules. The peak on this side will usually have a similar shape to the cathodic peak and it is called an anodic (oxidation) peak current ($i_{p,a}$). The potential at the anodic peak current is an anodic peak potential ($E_{p,a}$).

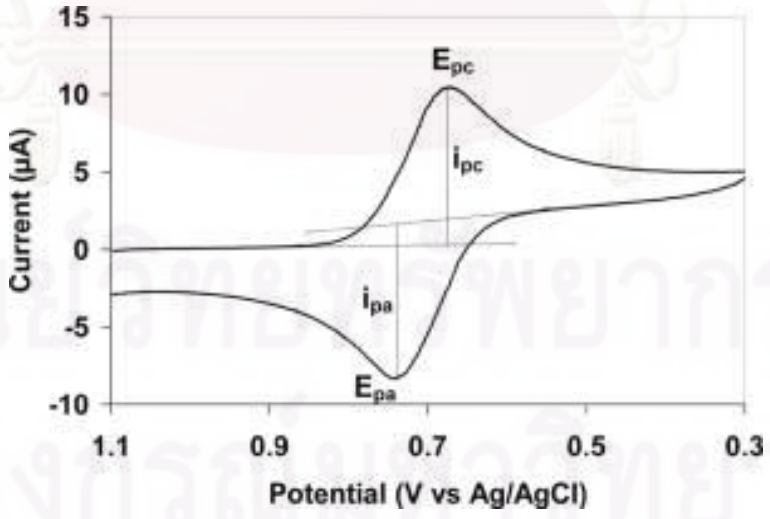

Fig. 2.2 Cyclic voltammogram with four main parameters
(http://upload.wikimedia.org/wikipedia/en/4/4c/Cyclovoltammogram.jpg)

Additionally, the standard potential (E^0) and the number of electrons transferred (n) can be determined from cathodic and anodic peak potentials:

$$E^0 = \frac{E_{p,c}+E_{p,a}}{2} \quad (2.8)$$

$$\Delta E_p = E_{p,a} - E_{p,c} = \frac{0.059}{n} \quad (2.9)$$

Where ΔE_p is the difference in cathodic and anodic peak potential and the values of 0.059 V is a ΔE_p of a fast one electron process. Moreover, data from the cyclic voltammogram can be used to impart the controlled process in the electrochemical system. When the current is controlled with diffusion process, the forward peak current will be linear proportional with the square root of the scan rate.

2) Amperometry

The amperometry technique is a controlled potential of the working electrode experiment and the current responses from this technique are monitored as a function of time. Amperometry is applied to explain about the diffusion controlled reaction. Thus, the current responses are directly proportion to the concentration of the substrate according to the Cottrell equation (eq. 2.4):

$$i(t) = \frac{nFAD_O C_O}{(\pi D_O t)^{1/2}} \quad (2.4)$$

From this equation, *n, A*, D_O or C_O can be determined. However, a disadvantage of amperometry is observed when the electrode surface has impurities that show the lack of reproducibility of this technique. A simple current-time profile for amperometry is shown in the Fig. 2.3.

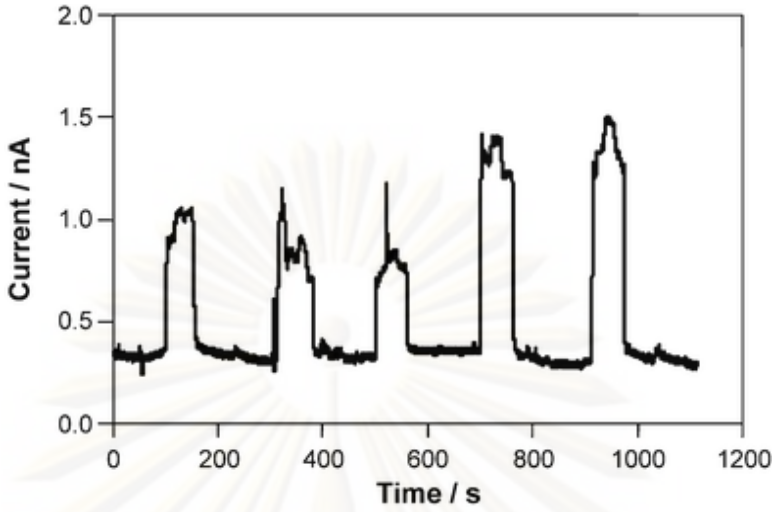

Fig. 2.3 Current-time for constant potential amperometry (www.rsc.org/ej/AN/2007/b611920d/b611920d-f5.gif)

2.1.3 Performance Factors

Now, biosensors are applied in many fields for detection of analytical substances. Thus, fabrications of biosensors are also increased as shown in several researches. However, each biosensor is fabricated by different methods and cause different performance. Thus, methods for determining the biosensor performance factors are necessary. Five important factors are defined to use in measuring of biosensor's performance.

1) Selectivity

The selectivity is a range of analytical substances that responses to the sensor. A broad range of substances refers to low selectivity sensor. On the other hand, a narrow range refers to a high selectivity sensor.

2) Range and Detection Limit

The concentration range is the range of substance's concentration that can be measured. The lowest measurable concentration is called a detection limit. The detection limit (point L) can be found by a plot of the relationship between electrical

potential and analytic substance's concentration (Fig. 2.4). The detection limit is normally more than 10^{-5} M (0.01 mM).

3) Response time

The response time is the time to allow the system to come equilibrium. This response time can be varied for each biosensor; however, the typical value is less than 5-10 minutes.

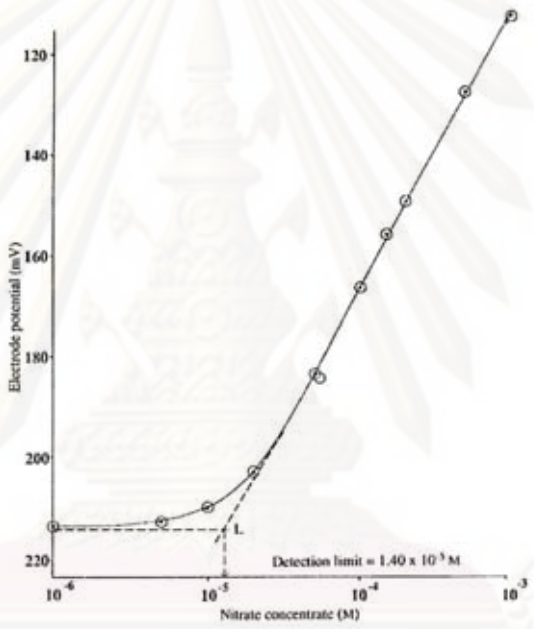

Fig. 2.4 Method of determining the detection limit (Eggins, 1999).

4) Reproducibility

The reproducibility is the ability of a reproduction of a biosensor to give a similar result. The result is meaningless if the error of the experiment cannot be defined. Repetition of numbers of experiment must be performed followed by a standard deviation in order to compare the result from new experiment to a standard value. The expected reproducibility of the biosensor for the repeated experiment should be within ±5 to 10 %.

5) Life time

The lifetime of biosensor are defined in three types; (1) the lifetime of the biosensor in use as known as reusability, (2) the lifetime of the biosensor in storage and (3) the lifetime of the biological material stored separately.

2.2 Microelectrode array

In recent years, there is a new kind of electrodes which its mass diffusion behavior is different from a common electrode. With a small size of radius (less than 50 μm), these electrodes are called microelectrode. Mass transport from bulk solution towards the microelectrode appears as spherical or hemispherical diffusion profiles. These diffusion profiles can make the mass transport of small-size electrodes better than the mass transport of conventional electrodes. The diffusion profiles of general electrodes are planar profiles. However, individual microelectrodes give small responses. One approach for overcoming this problem is to use many microelectrodes together in the form of an array to allow a cumulative and so larger response to be measured. Nevertheless, the overlapped diffusion profiles of each individual microelectrode in an array sometimes may occur and that make the profile become planar diffusion profiles.

Microelectrodes offer several advantages over macro electrodes which results from greater mass diffusion of microelectrodes. Advantages of the small-size electrodes are a reduced ohmic potential drop, a low detection limit, a fast establishment of steady state responses, and a reduced time constant. In addition, a signal to noise ratio (S/N ratio) of microelectrodes is also higher than S/N ratio of macro electrodes which have a similar surface area. The miniature electrodes can moreover, often used in resistance media due to the low operational currents typically encounters (Myler et al., 2004) and in restricted volumes for applications in chemistry and biology fields.

2.2.1 Diffusion at microelectrode arrays

The current response of the unique microelectrode can be calculated from the equation that similar with the equation (2.5) due to the mass transport of microelectrode is a spherical diffusional field like spherical electrode:

$$i(t) = \frac{nFAD_O C^{\infty}}{(\pi D_O t)^{1/2}} + \frac{nFAD_O C^{\infty}}{r_s} \qquad (2.10)$$

Where C^{∞} is the concentration as a function of distance r and time 0 and r_s is radius of a spherical electrode. When the duration of the experiment is short, the diffusion layer thickness is very small with respect to the radius of the electrode, so the current is related only with the Cottrell equation (the first term). Under these conditions, the diffusion profile of the microelectrode behaves like planar of planar macroelectrode and the peak shape of voltammogram will be observed. At long times, the second term more dominates the current than the first. At these long times, spherical diffusion profile is observed on the unique microelectrode. The current of the microelectrode in this experiment approaches to steady state and the shape of the cyclic volammogram will be sigmoidal shape.

In the case of microelectrode arrays, the current of them can be estimated like the unique microelectrode. However, the difference between the unique microelectrode and the microelectrode arrays are the long times experiment. At short times, planar diffusion is observed at each electrode (Fig 2.5a). The current monitored at the array is also given by the Cottrell equation:

$$(D_O t)^2 << r, \qquad i = \frac{nFS^{el} D_O C^*}{(\pi D_O t)^{1/2}} \qquad (2.11)$$

Where C^*, and S^{el} are bulk concentration (mol/cm^3), and the total active area, respectively. In this case, the electrodes behave independently and the array performs like a simple current amplifier but this amplification is small (Zoski, 2009).

At longer times, the diffusion layer of each microelectrodes become larger than the electrode dimensions which depend on the distance, d, separating two active

microelectrodes. Moreover, the steady-state or quasi-steady-state diffusion is observed at each element depending on their shape when d is much larger than the microelectrode dimension and the size of the diffusion layers (Fig 2.5b). The current of the electrode is:

$$r << (D_O t)^2 << d, \qquad i = \frac{nFS^{el} D_O C^*}{\delta(r)} \qquad (2.12)$$

Where $\delta(r)$ is a proportionality factor which depends on the microelectrode shape. However, when the distance (d) is not sufficient long compared with the electrode dimension, the overlap of individual spherical diffusion layers is appeared (Fig 2.5c). In this condition, the array behaves like a conventional planar electrode and having an area equal to the total areas of the array, S^{array}, including the total active area and insulating zones ($S^{array} = S^{el} + S^{insul}$). The current in this case corresponds to:

$$d << (D_O t)^2 << L, \qquad i = \frac{nFS^{arrayl} D_O C^*}{(\pi D_O t)^{1/2}} \qquad (2.13)$$

Where L is the distance as shown in Fig. 2.5c.

ศูนย์วิทยทรัพยากร
จุฬาลงกรณ์มหาวิทยาลัย

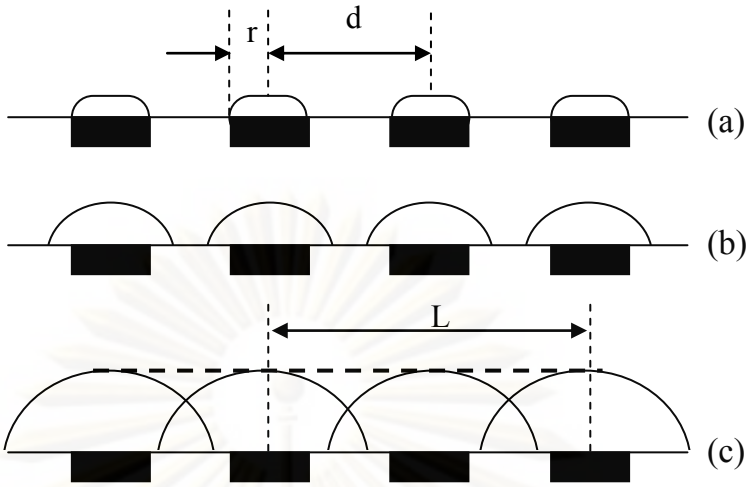

Fig. 2.5 Schematic representation of diffusion layers of concentration profiles developing at arrays of electrodes at different times of the electrochemical perturbation: (a) planar diffusion at short times, (b) hemispherical or cylindrical diffusion at intermediate times, and (c) planar diffusion and overlap of individual diffusion layers at long times (Zoski, 2009).

2.2.2 Classification of microelectrode arrays

The array fabrication means can limit the outlines of the electrodes in array that make the different form of an array. Microelectrode arrays can be classified according to the design of the array as shown in the following.

1) Random microelectrode arrays: An arrangement of individual microelectrodes in an array shows disordered form, dissimilar dimension and shape. Major advantage of this arrangement is the ease of fabrication, however, they also have a main disadvantage that is ill-defined geometries between conducting surfaces which can lead to an overlapping of diffusion profiles. A scheme of the random microelectrode array is shown in Fig. 2.6a.

2) Ordered microelectrode arrays: Individual microelectrode in an array regularly spaced with respect to another. Each electrode in the array has a similar dimension and shape. These arrays are well-defined geometries and the overlapped

diffusion layers are difficult to occur. However, ordered microelectrode arrays are difficult to fabrication for high quality approach. A scheme of the ordered microelectrode array is shown in Fig. 2.6b.

3) Three-dimensional microelectrode arrays: A structure of these arrays is cylindrical structure. This geometry has found wide application in biosensing and in recording electrical neural signals from nervous systems. Moreover, this configuration of the electrode can be used to develop the permeation into the tissue slice. A Fig. of this microelectrode array is shown in Fig. 2.6c.

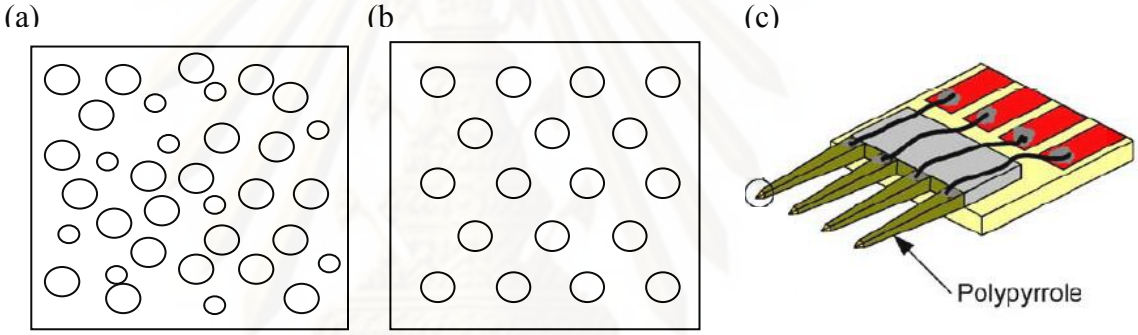

Fig. 2.6 (a) random array scheme, (b) ordered array scheme, and (c) Three-dimensional arrays from etching method (Zoski, 2009; Lee et al., 2006).

2.3 Horseradish peroxidase (HRP)

Peroxidases are hemoproteins in the class of EC 1.11.1.7 and contain iron (III) protoporphyrin IX (ferriprotoporphyrin IX) as the prosthetic group. There are a group of oxidoreductases that catalyze the reduction of peroxides such as hydrogen peroxide (H_2O_2) and the oxidation of a variety of organic and inorganic compounds (Hamid et al., 2009; Songa et al., 2009). Peroxidases have been found in plant, animal and a number of microorganisms, i.e. cytochrome c peroxidase (CCP), chloroperoxidase, lactoperoxides, and etc (Ruzgas et al., 1996).

Horseradish peroxidase (HRP) is a member of the plant heme-peroxidase and it is extracted from horseradish roots. HRP is the most commonly used enzyme for practical analytical applications, mainly because it retains its activity over a broad range of pH and temperature (Ruzgas et al., 1996; Songa et al., 2009). The mechanism of HRP when the electron donors, mediators, are involved can be represented by the follow equations (Ruzgas et al., 1996; Rosatto et al., 1999).

$$HRP\ (Fe^{3+}) + H_2O_2 \longrightarrow HRP\ (Fe^{5+}) + H_2O \quad (1)$$

$$HRP\ (Fe^{5+}) + AH_2 \longrightarrow HRP\ (Fe^{4+}) + AH^* \quad (2)$$

$$HRP\ (Fe^{4+}) + AH_2 \longrightarrow HRP\ (Fe^{3+}) + AH^* + H_2O \quad (3)$$

In the first reaction (1), a native peroxidase, HRP(Fe^{3+}), is two-electron oxidized by H_2O_2 (or organic hydroperoxides) and becomes HRP(Fe^{5+}). The next reaction (2) represents a reduction of HRP(Fe^{5+}) by the first electron donor, (AH_2), and HRP(Fe^{4+}) is formed. Then, the native peroxidase is achieved from the one-electron reduction of HRP(Fe^{4+}) by second electron donor in the final reaction (3). In each step, the electron donor species (such as aromatic amines and phenolic compounds) are oxidized to free radicals, AH*(Ruzgas et al., 1996; Rosatto et al., 1999). In many cases, the electrochemical reduction of the enzyme on the electrode is slow, in which case, a mediator is used instead for a fast reaction with the oxidized peroxidase. The mechanism is shown in Fig. 2.7.

Nevertheless, HRP(Fe^{5+}) can be reduced and becomes HRP(Fe^{3+}) directly from an electrode as shows in Fig. 2.8. Direct electron transfer between an electrode and an enzyme is very important for the fundamental studies (the kinetics and thermodynamics of biological redox processes), and the construction of biosensors (Xu et al., 2006, Zhao et al., 2008). However, the limited sensitivity of an enzyme electrode is occurred by a background current of the direct electron transfer from peroxide.

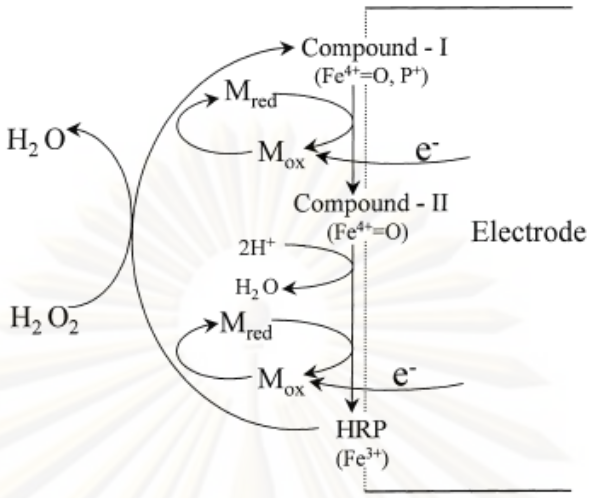

Fig. 2.7 Mechanism of mediated bioelectrocatalytic reduction of hydrogenperoxide at peroxidase-modified electrodes. M_{ox} and M_{red} are the oxidised and reduced forms of the mediator, respectively (Rosatto et al., 1999).

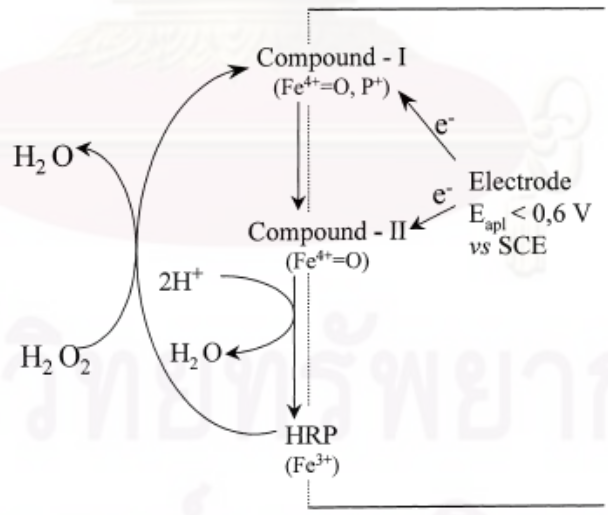

Figure 2.8 Mechanism of the direct bioelectrocatalytic reduction of hydrogenperoxide at peroxidase-modified electrodes (Rosatto et al., 1999).

2.4 Enzyme immobilization

Enzyme immobilization is a restriction of enzyme mobility in a fixed space. An enzyme immobilization provides several important advantages, such as easy to purify and recover an enzyme, easy to prevent an enzyme from severely surrounding condition (such as shear forces, high temperature), and high performance and storage stability. Sometimes, a better environment for an enzyme activity may be provided from the enzyme immobilization. There are many methods for immobilization of enzyme. Methods of enzyme immobilization are classified in two major categories.

2.4.1 Immobilization by binding

1) Physical adsorption

A physical adsorption is an attachment of enzymes on a surface of supporting materials by weak physical forces. Examples of the physical bonding are Vander Waals, ionic bonding, and hydrogen bonding. A physical adsorption is very simple, easy for preparation, and inexpensive. Moreover, an enzyme inactivated problem is difficult to occur. The disadvantage of this method is the ease of an enzyme losing from the support.

2) Covalent binding

A covalent binding is the retention of enzyme on support surfaces by covalent bonding. The enzyme molecules bind to the supporting materials with their functional groups, for example, amino, carboxyl, hydroxyl, and sulfohydryl groups. Additional, functional groups of the supporting material can be activated by chemical reagents, such as glutaraldehyde, cyanogen bromide, and carbodiimide. Strong forces of the covalent bonding can give a durable immobilization of an enzyme on the material. Nevertheless, an appearance of some covalent bonding at active sites of an enzyme may be leads to the inactivated enzyme problem.

3) Cross linking

This method is a connecting of enzyme molecules together by adding chemical reagents or flocculating reagents. In the chemical reagent adding, a covalent

bonding of an enzyme can connects with functional groups of the chemical reagent to forming large polymer networks. These networks are not water soluble. The chemical reagent is called cross linking agent, such as glutaraldehyde, carbodiimide, and etc.

For the flocculating reagent adding is a physical method for a flocculation of enzyme molecules. Examples of this reagent are polyamines, polyethyleneimine, polystyrene, and sulfonates. Cross linking method can prevent leakage of enzyme because strong covalent binding. On the other hand, cross linking may cause significant changes in the active site of an enzyme, and also severe diffusion limitations may result.

2.4.2 Immobilization by entrapment

In this method, an enzyme is physical enclosed in small spaces of a matrix or a porous membrane. The matrix or the membrane can protect the leakage of enzyme but they cannot fix the motion of enzyme molecules. Nonetheless, the pore size of an enzyme support must be higher than enzyme molecule size for the permeation of enzyme molecules to the support pores. The matrices for an enzyme entrapment are usually polymeric materials such as agar, K-carrageenin, calcium alginate, collagen, and etc (Shuler and Kargi). However, some solid matrices can also be used for entrapment such as porous ceramic, activated carbon and diatomaceous earth. Four matrix forms are particles, membranes, tubes, and fibers which are usually entrapped an enzyme.

Furthermore, an enzyme can also be encapsulated in a microscopic hollow sphere as well known as microencapsulation. For keeping the enzymes inside the sphere, the pore diameter of sphere must be smaller than an enzyme molecule diameter. An advantage of this method is the less degenerated enzyme problem, but the problem of this method is the low mass transfer. Fig. 2.9 shows the schemes of adsorption, covalent bonding, cross-linking and encapsulation methods of an enzyme immobilization, respectively.

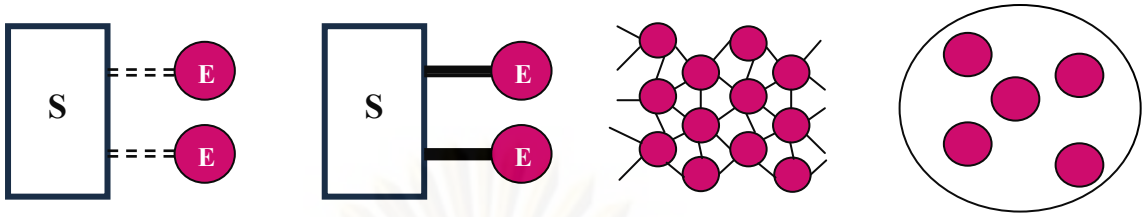

Fig. 2.9 Schemes of adsorption, covalent bonding, cross-linking and encapsulation methods of an enzyme immobilization, respectively (Blanch and Clark, 1997).

2.5 Conducting polymer for fabrication of biosensor

Generally, polymers are known to have good insulating properties but some polymers have electrical conductivity properties, as well known as conducting polymers. Conducting polymers are also known as "synthetic metals" that have electronic properties (magnetic, conducting and optical) similar to metals, but retaining the properties of conventional organic polymers (Vidal et al., 2003). The significant properties of conducting polymers are useful for many applications such as applied in rechargeable batteries, sensors, diodes, catalysts, and etc. Conducting polymers are conjugated (have alternating single and double bonds), having extended delocalized [π]-bonds along the polymer backbone. It is the [π]-orbital delocalization (single-double bond alternation) that facilitates the electron mobility and charge transport within the conducting polymer chain (Mohamoud, 2009). By contrast, traditional polymers, such as polyethylene, polyphenol, and polypropylene, are essentially made up of [$\sum$]-bonds where all valence electrons are bound in fully saturated chemical bonds and as a result there are no mobile electrons that can participate actively in electron transport. Conducting polymers can be grouped into six main families: aniline, pyrrole, thiophene, phenylvinylene, acetylene, and phenylene (and their derivatives) (Mohamoud, 2009).

In recent years, the entrapments of enzymes in conducting polymer films with electrochemical polymerization method are more attractive because they can be easily prepared in one-step process. The quantities of enzyme molecules entrapped in polymer film can be controlled due to controlling of the film thickness by an electric

charge passed during electropolymerization. Furthermore, there are no chemical reagents for enzyme entrapment and these polymers can also improve the electron transfer of electrode as mediator (Benedetto, 1996, Cosnier, 1999, and Thanachasai et al., 2002).

2.5.1 Polypyrrole (PPY)

Pyrrole is a heterocyclic aromatic organic compound, a five-membered ring with the molecular formula C_4H_5N (Fig. 2.10) and molecular weight is 67.09 g/mol. Substituted derivatives are also called pyrroles. Pyrrole has very low basicity compared to conventional amines and some other aromatic compounds. This decreased basicity is attributed to the delocalization of the lone pair of electrons of the nitrogen atom in the aromatic ring.

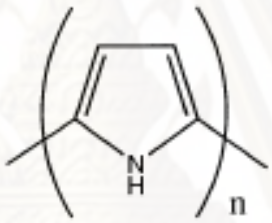

Fig. 2.10 Polypyrrole molecule (Cosnier, 1999).

In the fabrication of HRP based biosensors, many conducting polymers are used to immobilize an enzyme molecule. For example, aniline was used to fabricate the HRP based biosensor in some research (Chen et al., 2008, and Wang et al., 2009). Polypyrrole and its derivatives were used to entrap horseradish peroxidase (HRP) (Razola et al., 2002, Korkut et al., 2008). Although there are various kinds of conducting polymers, polypyrrole and its derivatives are most widely used for entrapping enzyme because of their advantages.

There are several advantages of polypyrrole (PPY) for enzyme entrapment. First, PPY can be easily electrodeposited onto an electrode surface from aqueous solutions, which are compatible with most biological elements (Li et al., 2007). Moreover, pyrrole has a high electrical conductive property, low cost, and stable at ambient conditions (Ekanayake, 2008).

2.5.2 Electrochemical polymerization of conducting polymer

Two methods are most often used for the preparation of conducting polymers from their respective monomer solutions that are an electrochemical polymerization and a chemical polymerization. However, the chemical synthesis does not describe in this research due to the electrochemical synthesis is commonly preferred. Generally, an electrochemical polymerization of monomeric species results in polymer films immobilized on electrode surfaces. The electrochemically deposited polymeric materials can be well suited for fabrications of surface-modified electrodes. In addition, electrochemical preparation of the polymers is both cost and time-effective. It is also the preferred method for the full control of thickness, composition, film compactness, and surface morphology of polymer film (Mohamoud, 2009).

In general, the mechanism of conducting polymer electropolymerization can be described as a cascade of $E(CE)_n$ reaction. An electron transfer reaction is substituted with E and a chemical reaction is substituted with C. The electropolyrnerization reaction for a molecule can be summarized by reactions (4)-(7):

$$RH_2 \xrightarrow{-e^-} RH_2^{+\cdot} \quad (4)$$

$$2RH_2^{+\cdot} \longrightarrow [H_2R\text{-}RH_2]^{2+} \xrightarrow{-2H^+} HR\text{-}RH \quad (5)$$

$$HR\text{-}RH \xrightarrow{-e^-} [HR\text{-}RH]^{+\cdot} \xrightarrow{RH_2^{+\cdot}} [HR\text{-}RH\text{-}RH_2]^{2+} \xrightarrow{-2H^+} HR\text{-}R\text{-}RH \quad (6)$$

$$(X+2)\ RH_2 \longrightarrow HR\text{-}(R)_x\text{-}RH + (2X+2)H^+ + (2X+2)e^- \quad (7)$$

Reactions (4)-(6) represent the step by step electropolyrnerization reaction of a monomer RH_2. The first reaction (4), molecule of a monomer is electrooxidized to a radical cation form, $RH_2^{+\cdot}$, at an electrode surface. The second reaction (5) represents a dimerization reaction of two radical cations which then losses two protions to form the neutral dimer. Further reaction (6) is a subsequence electrooxidization and trimerization. While reaction (7) is an overall electropolymerization reaction.

CHAPTER III

LITERATURE REVIEWS

Presently, the enzyme based biosensors are used in varied fields such as pharmaceutical, food, industrial, and environment analysis. The developments of these biosensors are shown in many researches. In this chapter, there are two major sections which describe fabrication techniques of microelectrode arrays, and horseradish peroxidase (HRP) based biosensor.

3.1 Fabrication techniques of microelectrode arrays

Microelectrode arrays can be prepared by different methods such as template approaches, lithographic techniques, etching method, and mechanical method. In the following section, many literatures on fabrication of microelectrode arrays with varied technique are presented.

1) Template approaches

This method involves the synthesis of desired material within the cylindrical and monodisperse pores of a membrane or other porous materials. The desired materials used are such as metal, polymer, protein, semiconductor, carbon nanowire, and etc. An example of the fabrication of microelectrode arrays using this method appears in the research of Yang et al (2004) who fabricated neural microelectrode arrays. In this study, they electrochemically deposited microporous conducting film of poly (3,4-ethylenediozythiophene) (PEDOT) and polypyrrole (PPY) onto electrode sites of neural probes by using different sized polystyrene (PS) latex spheres as templates. The PS latex spheres were allowed to sediment on the probes. The thickness of the templates could be controlled by changing the amount of PS latex spheres suspension deposited. Then PEDOT and PPY doped with lithium perchlorate ($LiClO_4$) were electropolymerized on these electrode sites. The PS templates were removed from the electrode after the electrochemical deposition was completed. The surface morphology of the films was found to vary with the particle size of PS latex

spheres and coating thickness. The microporous conducting polymer films with different pore sizes electrodeposited on the electrode sites have high regularity in pore size. Fig. 3.1 shows the feature of probe before and after removed PS template.

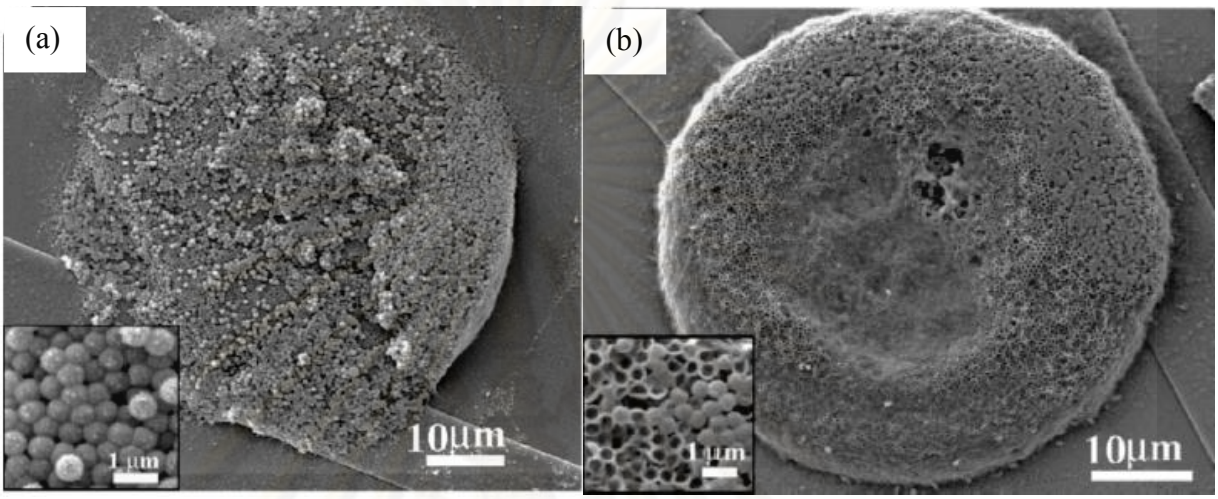

Fig. 3.1 SEM micrographs of (a) PEDOT doped with $LiClO_4$ grown through a polystyrene latex sphere template on the electrode site before removal of polystyrene template (inset showing the high magnification); (b) A microporous film of PEDOT doped with $LiClO_4$ after partially removal of polystyrene template (inset showing the template was removed partly) (Yang et al, 2004).

2) Lithographic techniques

This method is effective for fabrication of microelectrode arrays because of high reproducibility and controllability. In general, lithography is a technique that transfers a copy of a master pattern onto the desired solid's surface. Revzin et al. (2002) co-immobilized variety of enzymes (glucose oxidase, lactate oxidase, and pyruvate oxidase) on photolithographically fabricated gold microelectrode arrays. Silicon dioxide on silica wafers were used as rigid and flexible insulating substrate for electrode manufacturing. Subsequently, gold microelectrode arrays were fabricated by using combinations of photolithographic techniques and metal depositions. The steps of photolithographically fabrication are shown in Fig. 3.2.

Additionally, Burmeister et al. (2003) produced a ceramic-based multisite microelectrode array to measure cholines in vivo in brain tissues. Reverse photolithography was used to pattern 64 microelectrodes including recording sites, connecting lines, and bonding pads onto a ceramic substrate. The connecting lines were insulated with polyimide with an additional photolithographic step. The microelectrodes were wire bonded to a printed circuit board holder that was connected to their equipment for testing. Finally, the wire bonding and printed circuit board were insulated with epoxy. After that, the recording sites of microelectrode were coated with choline oxidase enzyme by cross linking method.

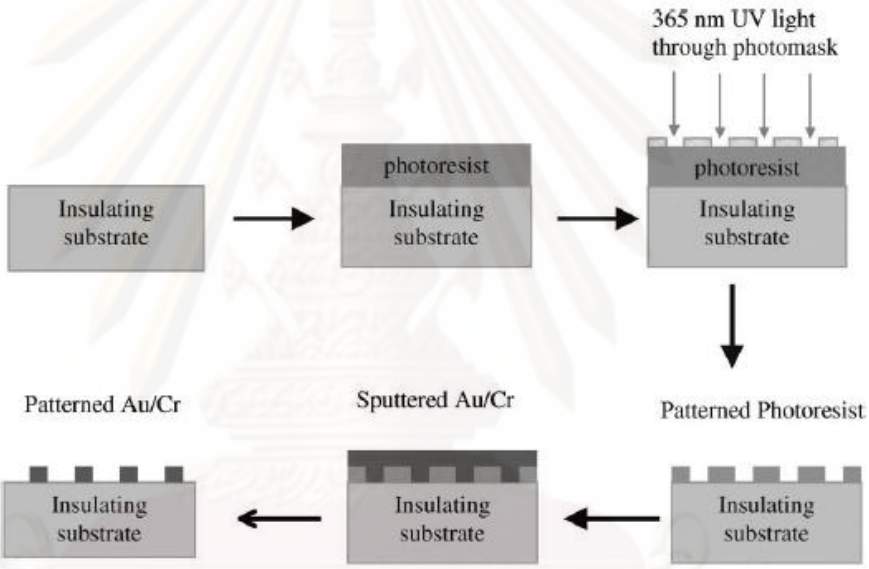

Fig. 3.2 Schematic of the electrode array fabrication process. A clean insulating substrate was coated with photoresist, then patterned photolithographically and developed. The patterned substrate was then metalized and lift-off used to create the electrode array (Revzin et al., 2002).

3) Etching method

Etching is a method of removing and/or adding a material for the construction of electrode arrays. The subtractive etching has several approaches such as wet etching, electrochemical etching, photo-electrochemical etching, plasma etching, laser machining, and etc. For example, Lee et al. (2006) studied the fabrication of four-glass probe microelectrode arrays by using a modified two-step, HF-based meniscus

etching process. The first etch-step serves to reduce the size of probes and to produce and initial taper of the probe shafts. At the end of this step, glass probes reduce to approximately 20 μm square at the tip. The second etch-step sharpens the tips to approximately 200 nm using the self-terminating meniscus etching method. For the self-terminating meniscus etching method, glass probes are immersed in to HF- based etchant. Then, an organic layer is added on the top of the etchant. The etchant wets the probe's surfaces and gradually reduces their dimensions. This process is self-terminating. These microelectrode arrays exhibited a substantially faster response time on the order of seconds rather than minutes, as compared to the commercial planar-electrodes.

4) Mechanical method

This method is the most inexpensive method and the ease for fabrication. Examples of this method are wire techniques, sandwich techniques, formation of composition, and sonochemical fabrication. However, disadvantage of this method is the limit of reproducibility. A major limitation is that a careful polishing technique has to be employed. Moreover, a careful design is essential to ensure that the diffusion layers at each microelectrode do not interfere with others. In the follow section, some literatures are represented, especially in the sonochemical fabrication research.

In wire techniques, Schwarz et al. (2000) produced microelectrode arrays for examination ferrocene under flow-through conditions with flow-injection analysis. The electrodes (gold wires, platinum wires and carbon fibers) were embedded in an epoxy resin which is resistant against acetonitrile and methanol. This microelectrodes show particularly good analytical sensitivities and fast response. Fig. 3.3 shown the schematic of this microelectrode.

ศูนย์วิทยทรัพยากร
จุฬาลงกรณ์มหาวิทยาลัย

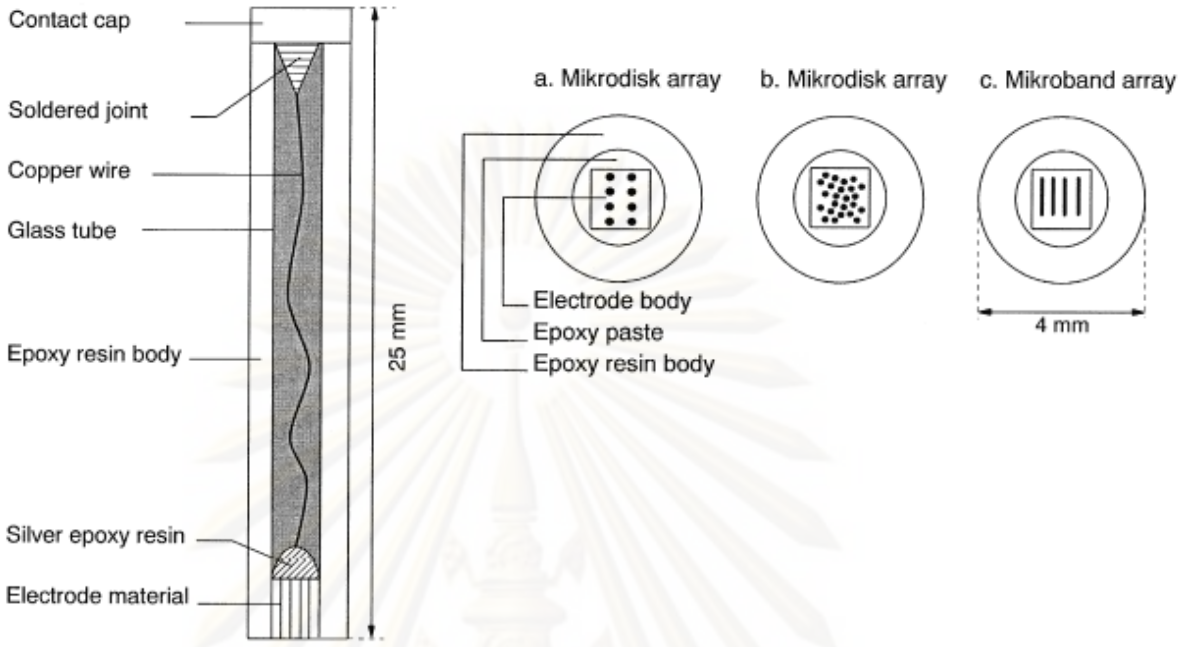

Fig. 3.3. Schematic of structure of microelectrode arrays (Schwarz et al., 2000).

In the sonochemical fabrication, Barton et al. (2004) is a first group which studied the sonochemical fabrication of microelectrode arrays. A gold-coated glass slides were electrochemically polymerized with 1,2-diaminobenzene dihydrochloride to form the thin insulating film. These electrodes were then immersed in a beaker containing distilled water and sonicated for arrays forming. A sonochemical ablation of thin insulating polymer films at electrode surfaces may expose localized areas. These areas can act as localized microelectrodes and collectively as an array of microelectrode with electrode element populations of up to $2x10^5$ cm^{-2}. After that, they entrapped glucose oxidase (GOx) within polyaniline on the microelectrode arrays. These biosensors enhanced the sensitivities and lowered the limits of detection. These results were received because the hemispherical diffusion profiles of the microelectrode arrays. However, it loses the signal linearity at high glucose concentration (>10mM).

Myler et al. (2005) produced the microelectrode array biosensor with a similar technique of Barton's research. But alcohol oxidase was immoblized for determination of ethanol. The results when compared with planar electrode results,

showed alcohol oxidase microelectrode system that enhanced sensitivity. In addition, Pritchard et al. (2004) sonochemically fabricated microelectrode biosensor for determination of pesticides. They immobilized acethylcholinesterase (AChE) with polyaniline on the screen-printed (SPEs) carbon ink doped with cobalt phthalocyanine (CoPC) electrode. Paraoxon, pesticide, was determined at low detection limit, down to the concentration of $1x10^{-17}$M. This result could not be achieved from common planar electrodes because of the diffusion profiles of microelectrode arrays were hemispherical geometries.

Moreover, there are two researches which studied of antibodies immobilization on sonochemically fabricated microelectrode arrays. Barton et al. (2008) developed immunosensors for the prostate cancer marker prostate specific antigen (PSA) with fabrication of antibodies for prostate specific antigen (APSA) based a microelectrode array. This research was developed from researches of sonochemical microelectrode array which described before. In this research, two methods were utilized to immobilize APSA. The first involved entrapment of APSA during polyaniline electropolymerization. The second utilized a polyaniline array as a substrate to immobilize APSA using a classical avidin-biotin affinity approach. Sensors fabricated using an affinity approach exhibited detection limits 1000 times lower than sensors fabricated by the entrapment method.

Further research, Barton et al. (2009) developed immunosensors for the cardiac drug dioxin and bovine serum albumin (BSA) with two methods to compare the behavior of sensors. First method, they immobilized anti-digoxin on a thin planar film of polyaniline using a classical avidin-biotin affinity approach. For the second, anti-BSA was entrapped within polyaniline on microelectrode arrays like earlier works. Both the use of microelectrode arrays and affinity binding protocols showed large enhancements in sensitivity over planar electrodes containing entrapped antibodies.

Researches of enzyme based microelectrode arrays within biosensor are shown in the table 3.1. Although there are many researches of microelectrode arrays, however, there are few researches that using a glassy carbon as a working electrode.

Furthermore, there are no researches of sonochemical microelectrode arrays fabrication with the glassy carbon electrode. Thus, it is very attractive to fabricate microelectrode arrays with a glassy carbon electrode because this electrode has many advantages such as its excellent mechanical and electrical properties, wide potential window, chemical inertness, and relatively reproducible performance. In this research, a sonochemical technique will be used to fabricate microelectrode arrays because this technique is very easy for fabrication and inexpensive.

ศูนย์วิทยทรัพยากร
จุฬาลงกรณ์มหาวิทยาลัย

Table 3.1 Researches of microelectrode arrays for enzyme based biosensors from different fabrication methods.

Fabrication method	**Microelectrode arrays**	**Enzyme/ Substrate**	**Detection limit** (M)	**Linear range (M)**	**Sensitivity**	**Response time**	**Researchers**
Lithographic techniques	Gold	GOx Glucose Lactate oxidase / Lactate Pyruvate oxidase / Pyruvate	-	$0\text{-}2.0\times10^{-2}$ $0\text{-}1.0\times10^{-2}$ $0\text{-}2.0\times10^{-3}$	0.26 0.24 0.133 $\mu AmM^{-1}\,cm^{-2}$	<20s.	Revzin et al. (2002)
	Gold nanoparticles modified gold ultramicro-electrode arrays	HRP / Catechol	5.0×10^{-5}	1.0×10^{-4} - 4.0×10^{-4}	228.6 $\mu AmM^{-1}\,cm^{-2}$	-	Orozco et al. (2009)
Etching method	Carbon fiber	GOx / Glucose	-	$0\text{-}2.0\times10^{-3}$	35 $nAmM^{-1}$	10s.	Netchiporouk et al. (1995)
	Gold	GOx/ Glucose	-	$0\text{-}5.0\times10^{-2}$	470 $nAmM^{-1}\,cm^{-2}$	-	Kim et al. (2002)
	Gold	GOx / Glucose	1.0×10^{-4}	1.0×10^{-4} - 1.0×10^{-2}	396.4 $\mu AmM^{-1}cm^{-2}$	-	Liu et al. (2005)
Mechanical method	Platinum	GOx / Glucose (Wire technique)	1.0×10^{-7}	1.0×10^{-7} - 6.0×10^{-2}	-	-	Zhang et al. (2000)
	Platinum	Tryrocinase / Phenol (Wire technique)	1.0×10^{-9}	-	-	-	Zhang et al. (2001)
	Gold	GOx / Glucose (Sandwich technique)	-	8.0×10^{-4} - 3.0×10^{-2}	3.4 $nAmM^{-1}$	<8-10s.	Pan et al. (2003)

Mechanical method (Sonochemi-cal fabrication)	Gold	GOx / Glucose	-	$0\text{-}4.0\times10^{-2}$	-	-	Barton et al. (2004)
	Gold (Modified with polysiloxane film)	GOx / Glucose	-	$0\text{-}6.0\times10^{-2}$	-	-	Myler et al. (2004)
	Carbon/ CoPC SPEs	AChE / Paraoxon	Down to $1x10^{-17}$	$1x10^{-17}$-$1x10^{-8}$	-	-	Pritchard et al. (2004)
	Gold	Alcohol oxidase/ Ethanol	-	-	-	-	Myler et al. (2005)
	Carbon/ CoPC SPEs	AChE / Dichlorvos, / Parathion / Azinphos	$\sim1x10^{-17}$ $\sim1x10^{-16}$ $\sim1x10^{-16}$	-	-	-	Law and Higson (2005)
	Screen-printed carbon	APSA/PSA	$1x10^{-9}$ (Entrap Mtd.) $1x10^{-12}$ (Affinity Mtd)	$1x10^{-9}$-$2x10^{-7}$ (Entrap Mtd.) $1x10^{-12}$-$1x10^{-10}$ (Affinity Mtd)	-	-	Barton et al. (2008)
	Screen-printed carbon	Anti-digoxin/ digoxin Anti-BSA/ BSA	$1x10^{-10}$ (for digoxin) $1.5x10^{-9}$ (for BSA)	$0\text{-}1.5x10^{-9}$ (for digoxin) $1x10^{-9}$-$3x10^{-7}$ (for BSA)	-	-	Barton et al. (2009)

3.2 Horseradish peroxidase (HRP) biosensor

Phenols and their derivative compounds are the major classes of pollutants. They are found in the waste waters from variety of industries such as oil, paint, resins and plastics, textiles, pharmaceutical industries, and etc. Horseradish peroxidase (HRP) based biosensor can be applied for detection of these toxins. In the following literatures, the immobilization methods for fabrication of HRP based biosensor and the electrochemically polymerization of conducting polymer are detailed.

3.2.1 Immobilization methods for fabrication of HRP based biosensor

There are many methods for immobilization of enzymes on the electrode such as physical adsorption, covalent bounding, cross linking, entrapment and sol-gel. In addition, immobilization methods can affect the properties of immobilized enzyme such as, activity, stability, deactivation, and regeneration. The following part presents research of amperometric biosensors with immobilized horseradish peroxidase (HRP) using several techniques.

1) Physical adsorption

This immobilization is an attachment of enzymes onto the surfaces of supporting materials by weak physical forces. This method is advantages for ease of preparation. For example, Gao et al. (2007) fabricated hydrogen peroxide biosensor based on the immobilization of HRP onto the nano-Au layer on modified glassy carbon electrode (GCE). This electrode was modified with composite membrane between thionine (Thi) and p-aminobenzene sulfonic acid (p-ABSA). They used self-assembly technology to adsorb HRP on a modified electrode. This studied biosensor exhibited good accuracy and high sensitivity and maintained more than about 70% of the initial response after storage for more than 1 month. Yang et al. (2009) adsorbed HRP on the glassy carbon electrode which was modified with Au nanoelectrode ensembles (Au NEEs), mutiwalled carbon nanotube (MWNTs), and chitosan (CHIT) film. This biosensor displayed rapid response, expanded linear response range and

retained 98.2% of the initial response after 25 days. Moreover, Chen et al. (2009) used ion adsorption technique to fabricate HRP based biosensor. They constructed the HRP on a composite matrix of multiwall carbon nanotubes (MWNTs) and core–shell organosilica@chitosan crosslinked nanospheres on glassy carbon electrode (GCE). The HRP was immobilized onto positively charged organosilica@chitosan nanospheres of the composite materials by electrostatic procedure. This biosensor exhibited a rapid response to H_2O_2 and possessed a good stability and reproducibility. The biosensor response only decreased 14% after a storage period of 1 month. However, desorption of an enzyme resulting from changes in temperature, pH, ionic strength or even the mere presence of substrate, is often observed, because of the weak bonds involved.

2) Covalent binding

Enzyme molecules bind to support with functional groups between enzymes and a matrix (by covalent binding). Kong et al. (2003) fabricated hydrogen peroxide biosensor. The HRP was immobilized by covalent bonding between amino group of the HRP and carboxylic acid group of 5,2':5',2''-terthiophene-3'-carboxylic acid polymer (TCAP) which is present on a glassy carbon (GCE). The results showed an excellent specific response to the reduction of H_2O_2 without the aid of an electron transfer mediator. The linear range was determined from 3.0×10^{-4}-1.5×10^{-3} M with a good linear relation.

Moreover, Li et al. (2009) covalently immobilized HRP into hybrid biocompatible material through chitosan-incorporated sol gel process. The epoxide ring and trimethoxy anchor groups of a γ-glycidoxypropyltrimethoxysiloxane (GPTMS) were applied as a bi-functional cross-linker. The fast amperometric response for detection of hydrogen peroxide and high reproducibility were achieved from this biosensor. The catalytic current response could maintain about 81% of its original response after 2 months. Nonetheless, the applications of this technique are limited by two characteristics; (1) the binding reaction must be performed under

conditions that do not cause loss of enzymatic activity and (2) the active site of the enzyme must be unaffected by the reagents used.

3) Cross linking

Cross linking is a linking of enzymes using cross linking agents. The examples of cross linking agents are glutaraldehyde, polyazetidine prepolymer. Qian et al. (2006) studied amperometric biosensor based on cross-linking HRP by glutaraldehyde with multiwall carbon nanotubes/chitosan (MWNTs/chitosan) composite film coated on a glassy carbon electrode. The amperometric experiments showed excellent electrocatalytical activity of the biosensor for H_2O_2 detection. Moreover, this biosensor had a good repeatability and stability. Frasconi et al. (2009) built HRP and/or glucose oxidase (GOx) based biosensor and use polyazetidine prepolymer (PAP) as a cross linking agent. The usage of PAP shows a good permeability for classical electrochemical mediators and offers a biocompatible micro-environment for restrictive enzyme. Immobilization by using PAP as cross linking agent resulted in a good stability and reproducibility of the enzymatic–polymeric film. Nevertheless, cross linking may cause significant changes in the active site of enzymes, and also severe diffusion limitations may result.

4) Entrapment

This technique is an enclosing the enzyme in a small spaces of matrix or membrane. For example, Wang et al. (2000) immobilized horseradish peroxidase (HRP) in sol–gel/hydrogel composite film for the detection of hydrogen peroxide. From the result, the response time of the biosensor was about 10 sec; the linear range was up to 3.4 mM with a detection limit of 5×10^{-7} M. The sensor also exhibited high sensitivity and good long-term stability. Chen et al. (2008) entrapped HRP in hybrid materials, colloidal carbon microspheres (CMS) and chitosan (CHIT), which modified on glassy carbon electrode. With the help of CMS, nice electrochemical response of HRP was obtained.

Researches of HRP based amperometric biosensors for different immobilization techniques shown in table 3.2. In this research, HRP will be immobilized with entrapment method because a matrix that uses to entrap is able to protect an enzyme from leaking and severe surrounding conditions. Moreover, this method little effects with an enzyme activity. The matrix that will be used to entrap HRP is a polypyrrole, a conducting polymer, due to there are no chemical reagents using for enzyme entrapment. Especially, conducting polymers can also improve the electron transfer of electrode. Researches of HRP-polypyrrole co-immobilization biosensors are represented in the follow section.

ศูนย์วิทยทรัพยากร
จุฬาลงกรณ์มหาวิทยาลัย

Table 3.2 Research of HRP based on amperometric biosensors with different immobilization methods.

Immobilization method	**Modified electrode**	**Analytical performance**					**Researcher**
		Detection limit (M)	**Linear range** (M)	**Stability**	**sensitivity**	**Response time**	
Physical adsorption	HRP/GCE for phenolic compounds detection	$5x10^{-7}$ (for 2-amino-4-chlorophenol)	-	-	85 $nA\mu M^{-1} cm^{-2}$	-	Ruzgas et al. (1995)
	HRP on nano-Au / Thi / poly(p-ABSA)-modified GCE for H_2O_2 detection	$6.4x10^{-7}$	2.6×10^{-6} - 8.8×10^{-3}	retained 70% after more than 1 month	-	8s.	Gao et al. (2007)
	HRP on GCE modified with zinc oxide nanoflowers for H_2O_2 detection	5.0×10^{-7}	9.9×10^{-7} - 2.9×10^{-3}	retained 90% after 20 days	-	<5s.	Bai et al. (2008)

Physical adsorption	HRP/ Au NEEs / MWNTs / CHIT / GCE for H_2O_2 detection	1.02×10^{-7}	2.08×10^{-7} - 7.6×10^{-3}	retained 98.2% after 25 days	-	<5s.	Yang et al. (2009)
	HRP /organosilica@chitosan /MWNTs / GCE for H_2O_2 detection	2.5×10^{-7}	7.0×10^{-7} - 2.8×10^{-3}	retained 86% after than 1 month	49.8 $\mu A m M^{-1} cm^{-2}$	6s.	Chen et al. (2009)
Covalent binding	HRP / TCAP / GCE for H_2O_2 detection	2.0×10^{-4}	3.0×10^{-4} - 1.5×10^{-3}	Retained over 90% after 3weeks	-	-	Kong et al. (2003)
	HRP / CHIT / GPTMS / GCE for H_2O_2 detection	8.1×10^{-8}	2.0×10^{-7} - 4.6×10^{-5}	retained 81% after 2 months	84.3 $\mu A m M^{-1}$	-	Li et al. (2009)
Cross linking	HRP/ silica-titanium / cross linked with glutaraldehyde in carbon SPE for phenol detection	-	10×10^{-6} - 50×10^{-6}	-	-	3s	Rosatto et al. (1999)

Cross linking	HRP cross linked with glutaraldehyde on GCE for nitric oxide detection	2.0×10^{-6}	2.7×10^{-6} - 1.1×10^{-5}	-	-	-	Casero et al. (2000)
	HRP/SiO_2-Nb_2O_5/ cross linked with glutaraldehyde in carbon SPE for phenol detection	$5\ x10^{-7}$	$5\ x10^{-6}$ – $25\ x10^{-6}$	-	3.2 $nA\mu M^{-1}$	-	Rosatto et al. (2002)
	HRP+DNA/silica-titanium cross linked with glutaraldehyde in carbon SPE for polyphenolic compound detection	$0.7\ x10^{-6}$	$1\ x10^{-6}$ – $50\ x10^{-6}$	-	181 $nA\mu M^{-1}$ cm^{-2}	-	Mello et al. (2003)
	HRP / MWNTs / CHIT / cross linked with glutaraldehyde on GCE for H_2O_2 detection	$1.03x10^{-5}$	1.67 x 10^{-5}- $7.4\ x\ 10^{-4}$	retained 90% after 20 days	4.995 μAmM^{-1}	-	Qian et al. (2006)

Cross linking	HRP cross linked with glutaraldehyde on PANI–polyvinyl sulfonate (PVA) / GCE for H_2O_2 detection	3.0×10^{-5}	1.0×10^{-4} - 2.0×10^{-3}	-	1.9 μAmM^{-1}	5s.	Ndangili et al. (2009)
	HRP cross linked with poly(PAP) on GCE for H_2O_2 and glucose detection	-	1.0×10^{-5} - 1.0×10^{-3}	retained 80-85% after 10 days	26.2 μAmM^{-1}	-	Frasconi et al. (2009)
Entrapment	HRP/silk fibroin composite membrane / GCE for H_2O_2 detection	1.0×10^{-7}	0- 4.0×10^{-3}	retained 85% after 2 month	-	30s.	Liu et al. (1995)
	HRP /poly(*m*-aminoanilinomethyl-ferrocene)/ GCE for H_2O_2 detection	8.0×10^{-8}	8.0×10^{-8} - 1.5×10^{-5}	retained 90% after 10 days	34 $nA\mu M^{-1}$	-	Mulchandani and Pan (1999)
	HRP in sol–gel/hydrogel composite film for H_2O_2 detection	5.0×10^{-7}	0- 3.4×10^{-3}	retained 92% after 110 days	15 μAmM^{-1}	10s.	Wang et al. (2000)

Entrapment	HRP -sol–gel thin layer/ nafion-methylene Green modified GCE for H_2O_2 detection	1.0×10^{-7}	5.0×10^{-7} - 1.6×10^{-3}	Retained 91% after 1weeks	13.5 μAmM^{-1}	20s.	Wang and Dong (2000)
	HRP/didodecyldimethylammonium bromide (DDAB)/ GCE for H_2O_2 detection	1.0×10^{-3}	1.0×10^{-3} - 4.0×10^{-3}	-	-	5s.	Tang et al.(2003)
	Tyrosinase+HRP/agar-agar gel/Pt for phenol detection	-	-	-	0.326 mA/M	-	Stanca et al. (2003)
	HRP/Chi-BMIM•BF_4/GCE for H_2O_2 detection	2.5×10^{-7}	7.5×10^{-7} - 1.35×10^{-6}	retained 95% after 1 month	0.184 AM^{-1} cm^{-2}	-	Lu et al. (2006)
	HRP / CMS / CHIT / GCE for H_2O_2 detection	$9.3x10^{-7}$	0- 2.5×10^{-3}	retained 90% after 25 days	120.17 μAmM^{-1} cm^{-2}	<5s.	Chen et al. (2008)

ศูนย์วิทยทรัพยากร
จุฬาลงกรณ์มหาวิทยาลัย

	HRP/PPY+CNT/ Au for phenol and its derivatives detection	3.52×10^{-6} (for phenol)	16×10^{-6} – 44×10^{-6}	retained 70% after 1 month	1 $nA\mu M^{-1}$	2s	Korkut et al. (2008)
Entrapment	Poly-thionine nanowires–HRP–nano-Au-modified GCE for H_2O_2 detection	3.0×10^{-7}	5.0×10^{-7} - 1.3×10^{-2}	retained 82% after 1 month	168 $\mu A m M^{-1} cm^{-2}$	<5s.	Shi et al. (2008)
	HRP/PPY/PVF/ GCE for phenol and its derivatives detection	2.3×10^{-7} (for phenol)	0.5×10^{-6} – 10×10^{-6}	retained 60% after 2 month	25.93 $nA\mu M^{-1}$	5 min	Sulak et al., 2009
	HRP/PPY/GCE for phenol and its derivatives detection	3×10^{-7} (for phenol)	2×10^{-6} – 12×10^{-6}	retained 80% after 40 days	90 $nA\mu M^{-1}$	-	Korkut et al. (2009)
	HRP-methylene blue/CHIT/Au modified TiO_2 nanotube arrays for phenol and its derivatives detection	1.95×10^{-7}	8×10^{-7} – 1.3×10^{-4}	retained 92% after 45 days	0.19 $\mu A \mu M^{-1}$	5s	Kafi and Chen (2009)

3.2.2 Electrochemically polymerization of conducting polymer for HRP biosensor fabrication.

Conducting polymers have been extensively studied during the last 20 years in view of their potential application. In the recent years, this type of polymer can be used to construct the biosensor. A possibility of a polymer film formation directly on a metal surface in the electropolymerization process is a large advantage, thus such films are obtained mostly by the polymerization of appropriate monomers (Pournaghi-Azar et al., 2007). Although, there are many kinds of conducting polymer, a polypyrrole (PPY) is widely used to fabricate biosensors. Many advantages of the polypyrrole can attract researchers to use it for enzyme entrapment such as high stability at ambient conditions, high conductivity, well-controlled film (thickness, location, and area). The polypyrrole is also easily formed from aqueous buffered solutions under mildly oxidative conditions which are compatible to enzymes, antibodies and nucleic acid. For these reasons, there is interesting to use the polypyrrole as a matrix to entrap HRP in this research.

3.2.2.1 HRP-pyrrole co-immobilization on biosensor

There are many researches about horseradish peroxidase (HRP) biosensor that immobilize an enzyme into pyrrole and its derivative film. Tatsuma et al. (1992) immobilized HRP within polypyrrole onto a SnO_2 electrode for H_2O_2 determination. They found that PPY functioned not only as an enzyme support but also as a part of the electrode material. Tian et al. (2001) electrodeposited HRP/PPY membrane on the surface of ferrocenecarboxylic acid mediated sol-gel derived composite carbon electrode. Their biosensor gave response to hydrogen peroxide in a few seconds with detection limit of 5.0×10^{-5}M. The biosensor exhibited a good stability. Razola et al. (2002) also constructed H_2O_2 biosensor by HRP-pyrrole electropolymerization onto platinum electrode. The biosensor allowed the determination of H_2O_2 in the concentration range comprised between 4.9×10^{-7} and 6.3×10^{-4} M.

In addition, Lomillo et al. (2003) electropolymerized HRP and pyrrole onto a platinum electrode for fabrication of rifampicin biosensor. Li et al. (2007) entrapped HRP within PPY film onto screen printed carbon paste electrode (SPE). The biosensor shows a linear amperometric response to H_2O_2 from 0.1 to 2.0 mM, with a sensitivity of 33.24 μA mM^{-1} cm^{-2}. Korkut et al. (2008) developed HRP immobilized within pyrrole onto gold electrode by using carbonnanotube (CNT). The HRP was incorporated into the CNT/PPY nanocomposite matrix in one-step electropolymerization process. They used their biosensor for eighteen phenol derivatives detection.

Moreover, HRP entrapment in a copolymer film can be observed in some research. Thanachasai et al. (2002, 2003) used poly{pyrrole-co-[4-(3-pyrrolyl)butanesulfonate]} (Py-Ps) as copolymer to entrap HRP on SnO_2 electrode. Sulak et al. (2009) constructed phenol biosensor by HRP entrapment within polypyrrole electropolymerized film an using polyvinylferrocene (PVF) as a mediator. Korkut et al. (2009) fabricated various HRP co-immobilized polypyrrole electrodes for phenol and its derivatives detection. Moreover, they used a newly synthesized poly(glycidyl methacrylate-co-3-thienylmethylmethacrylate) [poly(GMA-co- MTM)] to modify a working electrode before entrapped HRP. This research group compared six methods of fabrication biosensor. A gold electrode was used as a working electrode in five methods and a glassy carbon electrode was used in another method. The result showed the Poly(GMA-co-MTM)/polypyrrole/HRP coated glassy carbon electrode displayed significantly higher performance for the same composite film configuration comparing to the gold-based working electrode. This electrode exhibited a fast response less than 3 s, a high sensitivity (90 nAμ$M^{-1}$for phenol), a long-term stability (retained about 80% of initial activity after 40 days) and a low detection limit ranging between 0.3 μM for phenol.

Researches of HRP-incorporated polypyrrole film electrode and their electro-polymerization conditions represented in table 3.3.

Table 3.3 Researches of an enzyme entrapment within polypyrrole film by electropolymerization for fabrication HRP biosensor and their electropolymerization conditions.

Modified electrode	Pyrrole concentration	HRP concentration (g/l)	Electrolyte	Condition for electropolymerization	Detection	Researcher
HRP/PPY/ SnO_2	0.05M	0.6	0.06M KCl	+0.8 to 0.9V	H_2O_2	Tatsuma et al., 1992
HRP/PPY/ Composite carbon	0.25M	3	0.1M PBS	0.06mA/cm^2	H_2O_2	Tian et al., 2001
HRP/PPY/ Pt	0.05M	0.48 (228 U/mg)	0.1M LiClO4	0 to 1V at 10mV/s	H_2O_2	Razola et al, 2002
HRP/Py-Ps / SnO_2	0.05M PPY+ 0.01M modified PPY	0.6	0.06M KCl	5mC/cm^2 0.1mA/cm^2	H_2O_2	Thanachasai et al., 2002
HRP/PPY/ Pt	0.05M	12.1μM	0.1M LiClO4	0 to 1V at 10mV/s	H_2O_2	Lomillo et al., 2003

HRP/Py-Ps / SnO_2	0.05M PPY+ 0.01M modified PPY	0.6	0.06M KCl	Gal. 5mC/cm^2 0.1mA/cm^2	H_2O_2	Thanachasai et al., 2003
HRP/PPY/ SPE	0.075M	0.8 (300 U/mg)	0.2M PBS +0.075M LiClO4	1V, 50mC/cm^2	H_2O_2	Li et al.,2007
HRP/PPY+CNT/ Au	0.01M	0.3	50mM citrate buffer	0 to 1.2V, 4min	phenol	Korkut et al., 2008
HRP/PPY/PVF/ GCE	0.01M	0.3	100mM citrate buffer	0 to 1V at 100mV/s	phenol	Sulak et al., 2009
HRP/PPY/GCE	0.01M	0.6	50mM citrate buffer+0.6 g/l SDS	-1.2 to 1.2V at100mV/s, 4min	phenol	Korkut et al. (2009)

ศูนย์วิทยทรัพยากร
จุฬาลงกรณ์มหาวิทยาลัย

3.2.2.2 Condition of electrochemical polymerization

There are some operating conditions of electropolymerization which influence to biosensor response, i.e. a scan rate, monomer, electrolyte and enzyme concentrations, and a number of scan cycles etc. *The scan rate* and *the number of cycles* are critical parameters since the film thickness, as well as the internal organization of the polymer, depend directly on the time scale. A thicker film can obstruct the electron transfer which lowers the sensitivity to analyze and prolongs response time. *The electrolyte concentration* should be high enough to facilitate the charge transfer in solution. *The monomer concentration* is an important factor which may influence with the polymer development. *The amount of enzyme* immobilized into the polymeric matrix is a critical parameter for the sensitivity, reproducibility, and stability of the biosensor. For these reasons, a study of electropolymerization condition of the conduction polymer is necessary to improve the response of biosensors.

Nowadays, there has a little research that study conditions of electropolymerization of HRP based amperometric biosensor. Firstly, Moreno et al. (2001) fabricated a peroxidase biosensor by immobilization of the enzyme during the electropolymerization of *N*-methylpyrrole. The polymerization potential, the concentration of monomer and enzyme in the polymerization solution, and the pH and concentration of the phosphate buffer solution were optimized. The effect of the electropolymerization potential was evaluated in the range of 0.70 and 0.95V. The best potential was 0.85V. The study of monomer concentrations shown that the concentrations between 0.2 and 0.4 mol/l were no influences on the biosensor's sensitivity. Concentrations lower than 0.2 mol/ l prolonged the polymerization time, and concentrations higher than 0.4mol/l caused solubility problems. The HRP concentrations were studied in the range of 20 and 120U/ml and the sensitivity increased with the enzyme content, up to 80 U/ml. Moreover, the effect of pH and phosphate supporting electrolyte concentration of buffer solution were studied in range of 7.0-9.5 and 0.1-0.3 mol/l, respectively. An increase in sensitivity was observed with a pH up to 8.5 which indicated that an increase in the net enzyme

charge gave rise to a higher amount of immobilized enzyme. However, no significant variation was observed when changing the phosphate concentration.

Razola et al. (2002) studied many conditions of polypyrrole (PPY) electropolymerization (such as scan rate, electrolyte concentration, monomer concentration, enzyme concentration, and number of cycles) to fabricate the HRP based biosensor for hydrogen peroxide detection. For the scan rate studied, the various scan rates, 1, 5, 10, 20 and 50 mV/s, was studied The result shown that the signal increased when used the scan rate at 5 or 10 mV/s. In the Electrolyte concentration studied in ranges of 0.01, 0.05, 0.075, 0.3 and 0.5 M, higher responses were observed in concentration range between 0.075 and 0.2 M. After that, the following pyrrole concentrations 0.01, 0.05, 0.1, 0.3 and 0.5 M were studied. From the results, lower monomer concentrations did not allow sufficient polymer formation and HRP entrapment onto the electrode surface to give a response in the hydrogen peroxide concentration studied. However, higher monomer concentrations generated insensitive polymer films. Different concentrations of HRP in the polymerization solution were studied, namely, 0.10, 0.29, 0.48, 0.96 and 1.80 g/l. The biosensor response improved by raising the concentration of HRP from 0.10 till 0.48 g/l. For the study of the cycle number, the biosensor response became higher with a maximum for three cycles, and then the response decreased again.

Tian et al. (2001) used a galvanostatic method for pyrrole electro-polymerization. They studied effect of electrodeposition charge, an enzyme concentration to the response of their biosensor. The biosensor exhibited an optimum response at 6.79mCcm^{-2} of electrodeposition charge and 3.0 to 3.5M HRP. Thanachasai et al. (2003) fabricated HRP-carrying poly{pyrrole-co-[4-(3-pyrrolyl)butanesulfonate]} (Py-Ps) on SnO_2 electrode. They researched effects of fabrication parameters such as the electropolymerization charge, the deposition current density, and the monomer solution pH on the HRP loading and biosensor response. The results suggest that the amount of entrapped HRP increases almost linearly with the total charge passed, and strongly depends on the monomer solution pH. In addition, Gao et al. (2007) used poly (p-aminobenzene sulfonic acid, (p-

ABSA)) for fabrication of hydrogen peroxide biosensor. They studied the effects of the number of scan cycles in the current response of the biosensor. They found that the peak current decreased when more than 10 of cycle number were applied. Li et al. (2007) used polypyrrole to entrap HRP on screen print electrode. They optimized polymer electropolymerization operational parameters such as pyrrole concentration, density of charge deposit, electropolymerization potential, electrolyte and enzyme concentration. Optimized pyrrole concentration, the density of charge deposit, potential were 0.075M, 50mCcm^{-2}, and 1.0V, respectively. The electrolyte and enzyme concentration were optimized at 0.075M and 0.8mg/ml, respectively. Finally, Sulak et al. (2009) studied effect of HRP concentration within composite polymeric matrix of PPY and PVF on the response of the biosensor. The results shown that excess amount of enzyme (more than 2 mg/ml) could not be entrapped due to the supporting capacity of the formed polymeric matrix under electropolymerization conditions.

In the present work, HRP based microelectrode biosensors are fabricated with sonochemically technique because the high sensitivity and the lower detection limit are achieved from the microelectrode biosensor and this fabrication technique is very easy to proceed and inexpensive. Additionally, the polypyrrole electropolymerization operational parameters will be studied because these factors may be affected with the biosensor response and performance.

ศูนย์วิทยทรัพยากร
จุฬาลงกรณ์มหาวิทยาลัย

CHAPTER IV

MATERIALS AND METHODS

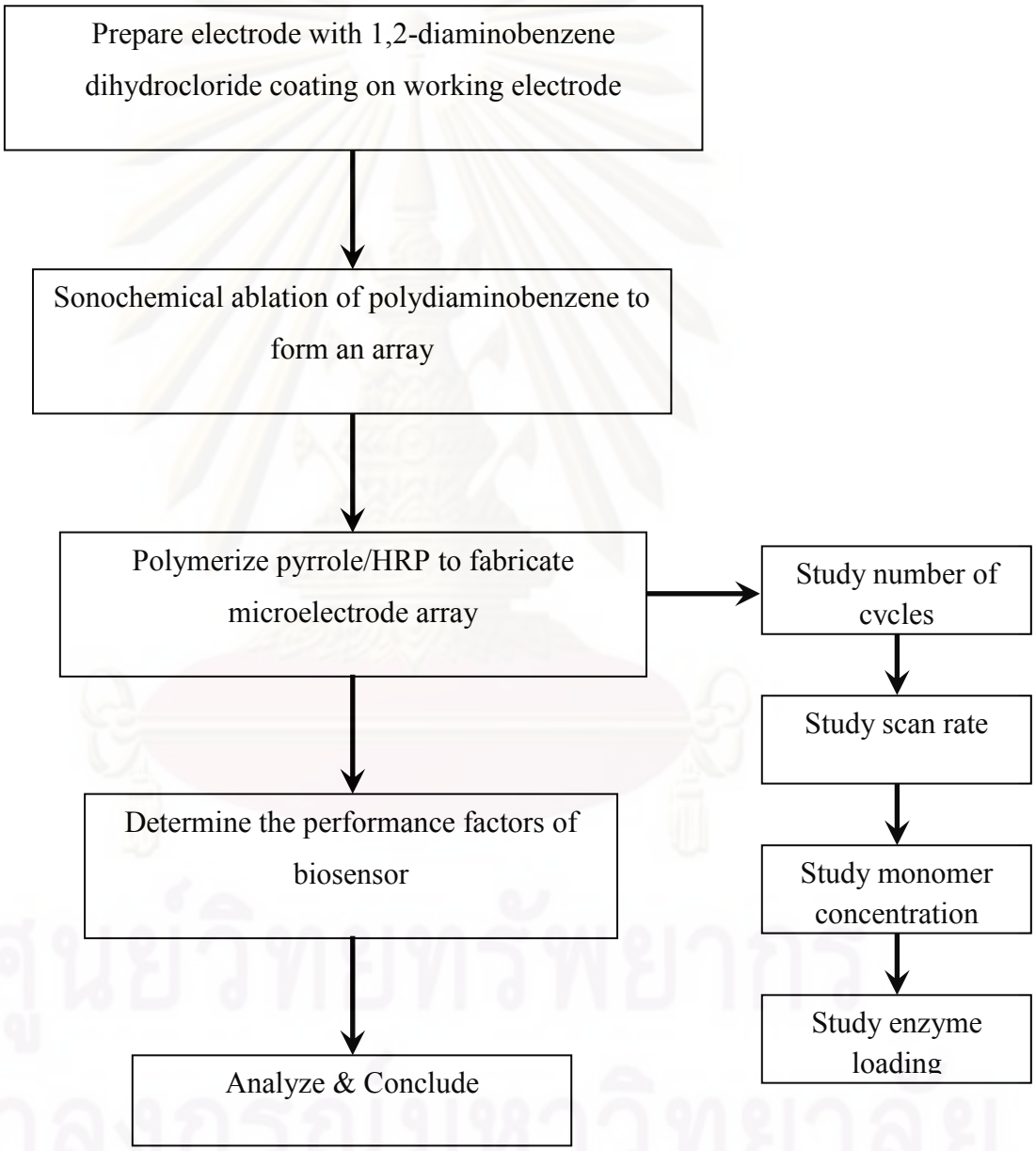

Fig. 4.1 The experimental chart of this work.

4.1 Materials

1. 1,2-Diaminobenzene dihydrochloride (o-Phenylenediamine dihydrochloride, 99% $C_6H_{10}Cl_2N_2$,), available from Fluka Analytical, Switzerland.
2. Disodium hydrogen orthophosphate (Na_2 HPO_4), available from Fisher Scientific.
3. Horseradish peroxidase (131 U/mg HRP, EC 1.11.1.7), available from Toyobo, Japan.
4. Hydrogen peroxide (30% H_2O_2), available from E.Merck, Darmstadt.
5. Phenol (C_6H_5OH), available from Carlo Erba Regent Co.
6. Potassium ferrocyanide (99% $K_4Fe(CN)_6$), available from RANKEM, RFCL limited, New Delhi.
7. Potassium sulfate (K_2SO_4), available from Fisher Scientific, Mumbai, India.
8. Pyrrole (98% C_4H_5N), available from SIGMA-ALDRICH, Steinheim, Germany.
9. Sodium chloride (NaCl), available from Asia Pacific Spacialty Chemical limited, Australia.
10. Sodium dihydrogen orthophosphate (NaH_2PO_4), available from Fisher Scientific

* All chemicals were used without further purification.

4.2 Apparatus

Electrochemical measurements of cyclic voltammetry and amperometry were performed with an Autolab potentiostat (Metrohm, model PGSTAT30) with nova software version 1.5. The electrochemical cell consisted of a three-electrode system with a glassy carbon electrode (GCE) as the working electrode, a platinum wire as the counter electrode, and a silver/silver chloride (Ag/AgCl) electrode as the reference electrode. Before each experiment, the glassy carbon electrode (GCE) was first polished with 0.3 μm alumina slurry and polishing cloth for 5 minutes and rinsed with distilled water. Repeat the polishing with 0.05 μm alumina slurry for 5 minutes and rinses. Then, the electrode was sonicated using ultrasonic cleaner (CREST, model D (30 kHz), Malaysia) in absolute ethanol for 5 minutes and distilled water 5 minutes, respectively. After these pretreatment, the electrode was dried in air.

4.3 Preparation of buffer solution

The stock of phosphate buffer (PBS, pH 7.4) of disodium hydrogen orthophosphate, 5.28×10^{-2} M, sodium dihydrogen orthophosphate, 1.3×10^{-2} M, and sodium chloride, 5.1×10^{-3} M was prepared using distilled water and stored under 4ºc.

4.4 Electrode preparation

5 mM of 1,2-diaminobenzene dihydrocloride was prepared in phosphate buffer solution pH 7.4 and purged the oxygen in solution with nitrogen gas for 5 min. Then GCE was electropolymerised with this monomer solution by potentially cycling of the working electrode between 0 and +1.0 V versus Ag/AgCl at a scan rate of 20 mV/s for 50 cycles. The electrochemical polymerization of 1,2-diaminobenzene dihydrocloride was a self limiting process because polydiaminobenzene was an non-conducting polymer (Myler et al., 1997). The prepared working electrode was then rinsed with dionised water to remove unreacted monomer from the electrode surface after dry at room temperature for 2 hours.

Sonochemical ablation of polydiaminobenzene modified insulated GCE was performed by holding the electrode upright in a 250ml beaker containing 150ml of distilled water which was then subsequently positioned into the ultrasonic bath. The electrode was then sonicated for 25 min at a frequency of 30 kHz at a center of the sonicate tank (measured with a ruler).

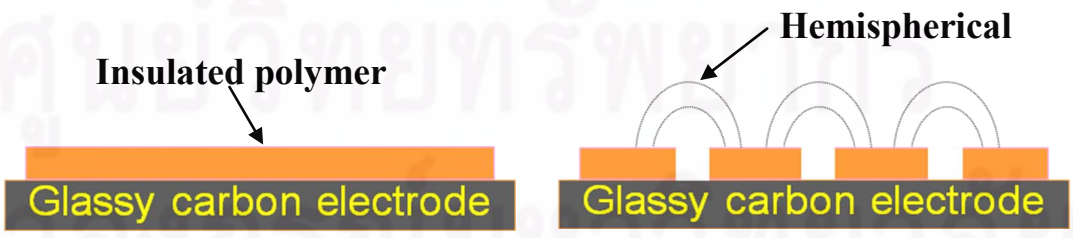

Fig. 4.2 Schematics of polymer insulated electrode and microelectrode array, respectively (Barton et al., 2004).

4.5 Polymerization and enzyme immobilization of microelectrode arrays

Before electropolymerization, the solution of HRP-PPY must be purged oxygen with nitrogen gas for 5 min. The experiments were performed under 25ºC.

4.5.1 Number of scan cycles study (10, 15, 20, 25, and 30 cycles).

The immobilization of HRP was preceded in this step. The polymerization medium contained 5ml of phosphate buffer (PBS, pH 7.4), including 0.05M pyrrole and 250 unit /ml HRP. This solution was polymerized onto sonicated polydiaminobenzene coated GCE by potentially cycling between 0 and +1.0 V versus Ag/AgCl with 10 mV/s by various for five scan cycles. Immediately following polymerisation, the working electrode was submerged in pH 7.4 phosphate buffer at 4ºC to prevent enzyme denaturizing and store at 4ºC prior to use.

4.5.2 Scan rate study (5, 10, 20, 30, and 50 mV/s).

These experiments were similar with scan rate study but vary the scan rate from 5, 20, 30, and 50 mV/s and use the optimum cycle from item 4.5.1.

4.5.3 Pyrrole concentration study (0.03, 0.05, 0.07, and 0.09 M).

These experiments were similar with item 4.5.1 and 4.5.2 but use their optimum condition and vary pyrrole concentration between 0.03, 0.07, and 0.09 M in PBS (pH 7.4).

4.5.4 HRP concentration study (150, 250, 350, and 450 unit/ml).

These experiments varied HRP concentration from 150, 350, and 450 unit/ml in PBS pH 7.4 and used optimum conditions from item 4.5.1-4.5.3.

จุฬาลงกรณ์มหาวิทยาลัย

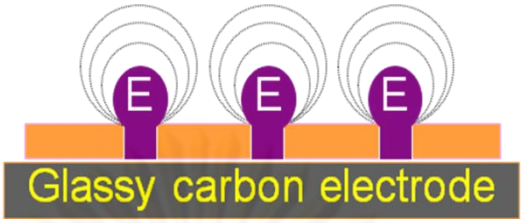

Fig. 4.3 Schematic of sonochemically fabricated polypyrrole/HRP microelectrode array (Barton et al., 2004).

4.6 Cyclic voltammetric and Amperometric phenol sensor

The cyclic voltammogram responses of bare electrode and polydiamino-benzene modified GCE were measure in 10mM ferri/ferrocyanide. This solution was prepared by adding $K_4Fe(CN)_6$ in 0.1M potassium sulfate and purged oxygen with nitrogen gas for 5 min before to use. Cyclic voltammogram (CV) was measured at scan rate 20 mV/s between -1.0V and 1.0 V at 25ºC.

The current response of HRP modified microelectrode biosensor to phenol was measured with an amperometry technique at a fixed potential (-0.05V). The solution of 50µM H_2O_2/ 50 µM phenol in PBS was used as a substrate solution. However, this solution should be separately prepared which the solution of H_2O_2 in PBS must be prepared for day by day while the solution of phenol in PBS can be prepared like a stock solution and stored at 4ºC prior to use. Before the measurement these solutions were mixed at required.

4.7 Performance factor of microelectrode biosensor

4.7.1 Calibration curve

The calibration curve of phenol was used to analyze three performance factors were linear ranges, sensitivity, and detection limit of the biosensor. The amperometric current responses (at -0.05V) of biosensor which fabricated under optimum electropolymerization conditions were measured in various phenol concentrations (from 10^{-7} to10^{-3} M) in 50µM H_2O_2 /PBS (pH 7.4) at 25ºC .

4.7.2 Repeatability

The amperomatric response (at -0.05V) of an optimum conditions fabricated biosensor was measure in 50μM H_2O_2/ 50 μM phenol/ PBS (pH 7.4) at 25ºC for ten times in one day.

4.7.3 Reproducibility

The small modified glassy carbon electrodes were used in this experiment. A glassy carbon rod was cut with the length of 6mm. and polished with sand papers (No.400, 600, 1200, and 1400, respectively) and alumina powder (0.3 and 0.05μM, respectively) until received a smooth electrode surface. Small GCEs were coated with epoxy resin around the sidewall of them for controlled conductive area and connected to the silver wire with silver paste, respectively. The schematic diagram of the small electrode was shown in Fig. 4.4. These small GCEs must be run the cyclic voltammetry in 10mM ferri/ferrocyanide to test the response similarity of different electrodes before fabrication of microelectrode biosensors. Ten microelectrode biosensors were fabricated under the same process with small modified electrodes. The current responses of these biosensors were measured in 50μM H_2O_2/ 50 μM phenol/ PBS (pH 7.4) at 25ºC with amperometry technique at -0.05V.

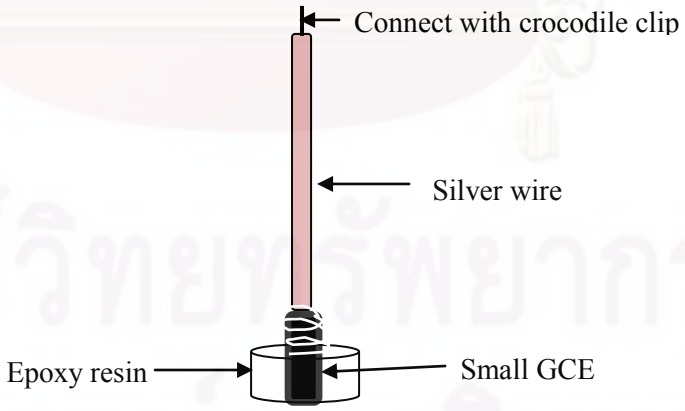

Fig. 4.4 The schematic diagram for small GC electrode connection.

4.7.4 Life time

The amperometric current (at -0.05V) of biosensor which fabricated under optimum electropolymerization conditions was periodically measured with 50µM H_2O_2/ 50 µM phenol/ PBS (pH 7.4) in the period of one month. The biosensor was dipped in PBS (pH 7.4) when was not used and stored under 4ºc.

4.8 Characterization of modified electrode

The surface characterization of microelectrode arrays from each preparing step was performed with Scanning Electron Microscopy (SEM) (JEOL JSM-6480 LV) and Atomic Force Microscope (AFM) (Veeco, model nanoscope IV, mode : tapping Si-probe). Diameters and number of pores on sonicated electrode surfaces were analyzed from AFM images with –A Pro Plus" program.

4.9 Statistical differences

All statistical calculations were performed on the Minitab system for Windows (version 14, USA). P-values of <0.05 was significantly considered.

ศูนย์วิทยทรัพยากร
จุฬาลงกรณ์มหาวิทยาลัย

CHAPTER V

RESULTS AND DISCUSSIONS

5.1 Microelectrode arrays formation

In this research, microelectrode arrays must be firstly prepared on a bare glassy carbon (GCE) electrode before HRP immobilization (fixed-position of electrochemical cells). This could be achieved by a primary formation of an insulated layer of elecropolymerized 1,2-diaminobenzene dihydrochloride, a monomer of a polydiaminobenzene (PPD). The obtained insulated electrode was then sonicated for the fabrication of microelectrode arrays. Fig. 5.1 shows cyclic voltammograms of polydiaminobenzene electropolymerization which is a self-limitting process since PPD is an insulating polymer (Myler et al., 1997). Diminishing peak currents of the coated electrode are observed with increasing coating cycles. The polymer film gradually covered the electroactive surface to almost completion which resulted in minute detection of current responses at higher coationg cycles. This confirmed that GCE was successfully coated with polydiaminobenzene and became insulating.

Microelectrode arrays were then formed via ultrasonic ablation of the insulated PPD layer resulting in revealing of electro-active surface of glassy carbon micro arrays. Superheated vapor bubbles are generally formed while ultrasonicating a specified solvent. The powerful micro-jets of solvent are asymmetrically generated within these bubbles and are expelled from bubbles. These fast micro-jets could destroy a solid surface, thus soft solid surfaces of polymers may be also ablated (Stephanis et al., 1997; Barton et al., 2004). Since microelectrode arrays were, in this case, formed by fixed position ultrasonic ablation, sonication time was therefore played a significant role in determining obtained pore numbers and characters. In this section, optimum sonication time must then be studied for fabrication of suitable microelectrode arrays on the glassy carbon surface which would be analyzed both electrochemically and physically.

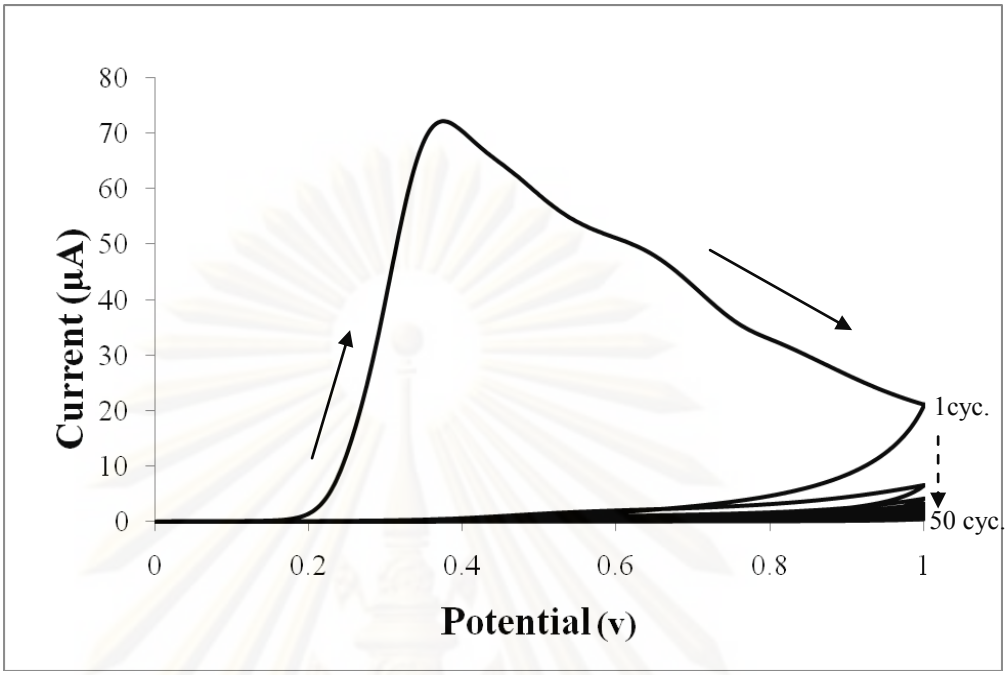

Fig. 5.1 Cyclic voltammogram of polydiaminobenzene dihydrocholride electropoly-merization for 50 cycles at 20mV/s.

5.1.1 Electrochemical analysis

Electrochemical analysis was used to observe the formation of microelectrode arrays after ultrasonication for specified periods of time (10, 20, 25, 30, 50, and 90 mins) on PPD coated GCE. Cyclic voltammograms of bare and modified electrodes are shown in Fig. 5.2 and 5.3. A cyclic voltammogram of bare GCE (Fig. 5.2(i)) shows high peak currents due to its electro conductivity. When the electrode is coated with PPD (PPD/GCE) (Fig. 5.2(ii)), very little current response was observed in cyclic voltammogram, less than 5µA, because GCE was deposited with an insulated polymer, a polydiaminobenzene. For a 10 min sonication (Fig. 5.3(i)), the current is quite similar to non-sonicated PPD coated GCE, thus, pores were not much formed at this time. At a 20 min sonochemical ablation (Fig. 5.3(ii)), cyclic voltammogram shows higher current than the 10 min sonochemical ablation and its shape looked like a sigmoid shape. The sigmoid shape current response represents the characteristic of cyclic voltammrgrams of microelectrodes and microelectrode arrays (Barton et al.,

2004). Generally, the diffusion profiles of each microelectrode become larger than the electrode dimensions with hemispherical or spherical shapes which depends on the distance, d, separating two active microelectrodes. The steady-state diffusion is observed at each element when d is much larger than the microelectrode dimension and the size of the diffusion layers (Zoski, 2009). The rate of mass transport is much greater than that in a planar electrode and the current of the electrode is:

$$r << (D_O t)^2 << d\,, \qquad i = \frac{nFS^{el} D_O C^*}{\delta(r)} \qquad (5.1)$$

Where F is the Faraday constant (96,487 coulombs); n is the number of electrons transferred in a reaction; D_0 is the diffusion coefficient (cm^2s^{-1}); C^* and S^{el} are bulk concentration (mol/cm^3) and the total active area, respectively; $\delta(r)$ is a proportional factor which depends on the microelectrode shape. The current response from the equation 5.1 is time independent which causes the sigmoidal CV at low scan rates (Wang, 2000; Zoski, 2009). Thus, the cyclic voltammogram from our experiments confirmed that microelectrode arrays were formed on the surface of the coated electrode starting at 20min sonication.

Moreover, when PPD/GCE was sonicated for 25 min (Fig. 5.3(iii)), the sigmoid shape of the cyclic voltammogram is still observed with even higher current reponse, however, longer than 25 min sonication, namely, 30, 50, and 90 min (Fig. 5.3(iv), (v), and (vi), respectively), the peak shaped cyclic voltammograms appear. Sonication of PPD/GCE more than 25 min led to the formation of higher numbers of pores which might not be well separated so the overlap of individual spherical diffusion layers appeared before reaching steady state diffusions (Zoski, 2009). Microelectrode arrays under this situation behave like a planar macroelectrode. The current in this case corresponds to:

$$d << (D_O t)^2 << L\,, \qquad i = \frac{nFS^{arrayl} D_O C^*}{(\pi D_O t)^{1/2}} \qquad (5.2)$$

Where S^{array} is the total array area which includes the total active area and insulating zones ($S^{array} = S^{el} + S^{insul}$). The current demonstrated in equation 5.2 is time

dependent as in the case of conventional planar electrodes which results in peaked-shape CV. The results obtained for 30, 50, and 90 minutes sonication obviously illustrate the character of conventional planar electrodes due to the observed peak responses. For this reason, sonication time longer than 25 min should not be applied.

To give a clearer picture of sonicated PPD-coated GCE, physical characterization of the surfaces will be elaborated in the next section.

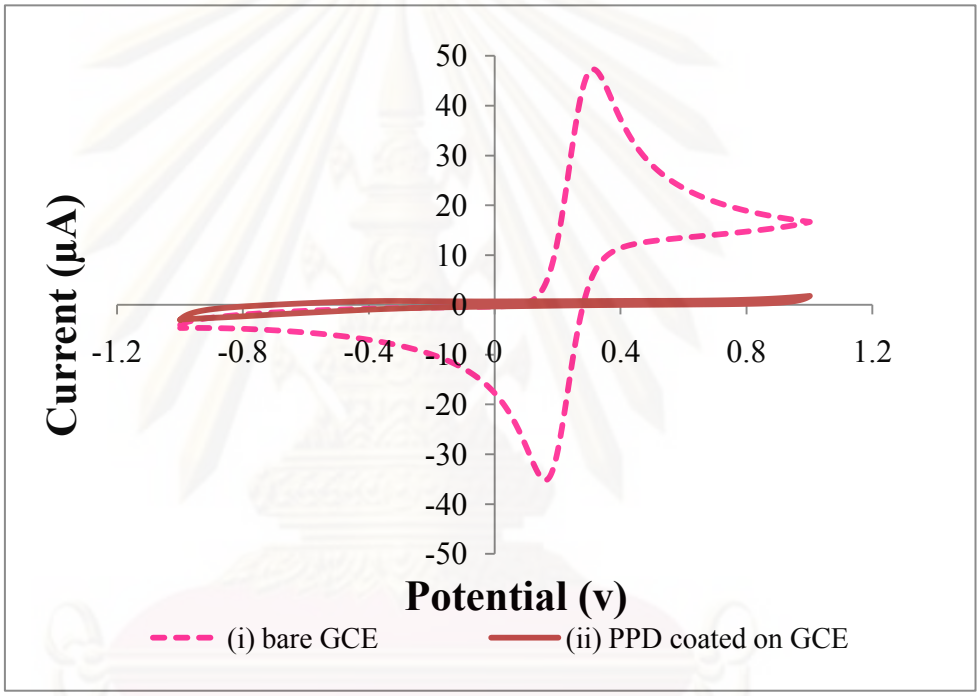

Fig. 5.2 Cyclic voltammograms (vs. Ag/AgCl) in 10mM ferri/ferrocyanide couple solution of (i) bare GCE, (ii) PPD coated GCE, and (iii) a 25 min sonicated PPD/GCE, respectively. Scan rate 20mV/s.

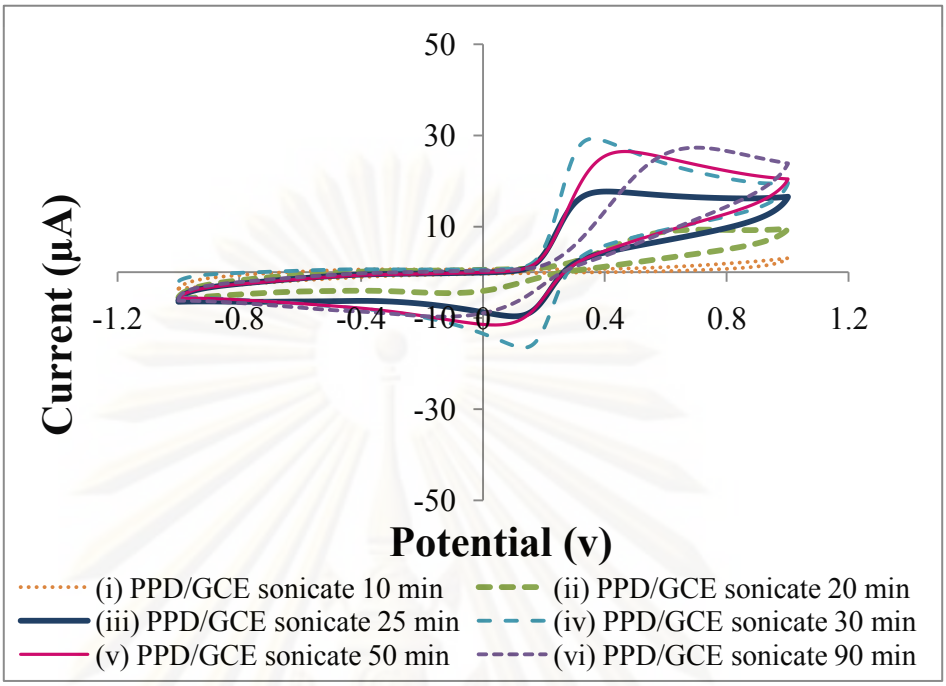

Fig. 5.3 Cyclic voltammograms (vs. Ag/AgCl) in 10mM ferri/ferrocyanide couple solution of (i) 10, (ii) 20, (iii) 25, (iv) 30, (v) 50, and (vi) 90 min sonicated PPD coated GCE, respectively. Scan rate 20mV/s.

5.1.2 Physical characterization

Physical characterization namely; AFM, and SEM, were used to confirm the formation of microelectrode arrays in addtion to those of electrochemical results. Analyses were done both on the bare and modified electrodes for the sake of comparison. In addition, pore numbers and diameters were also analysed for the effect of sonication time on pore formation.

Images from AFM analysis in scale of 3x3µm and SEM images of bare and PPD/GCEs showed in Fig. 5.4. These SEM and AFM images of bare and PPD coated electrodes showed the similar characteristic. The AFM and SEM image of bare glassy carbon electrode (Fig. 5.4a, c) showed a very flat and smooth surface. For the PPD/GCE (Fig. 5.4b, d), a surface of this electrode was very rough compared with the bare GCE. It looked like all of bare GCE surface was covered with ellipsoidal shape

of individual PPD particles and this film coating was quite uniform. This result confirmed that the GCE was already coated with PPD film.

a)

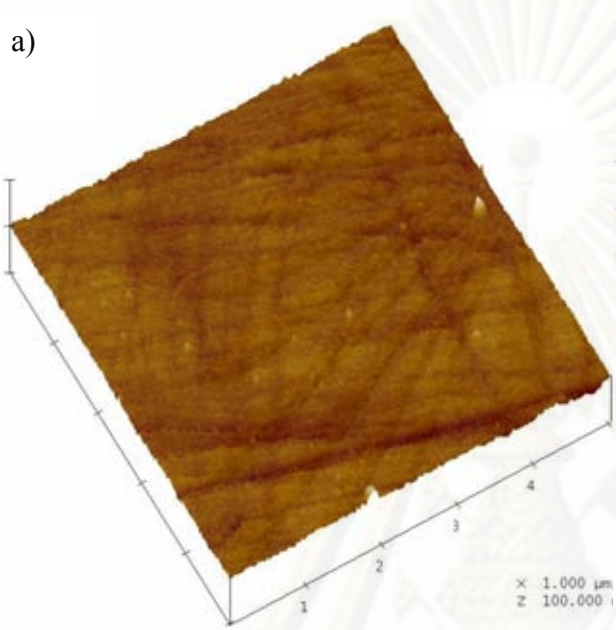

b)

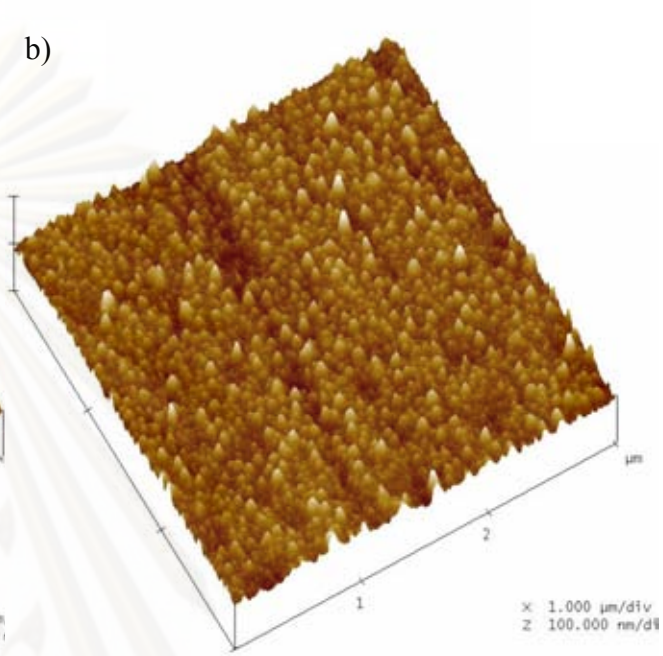

c)

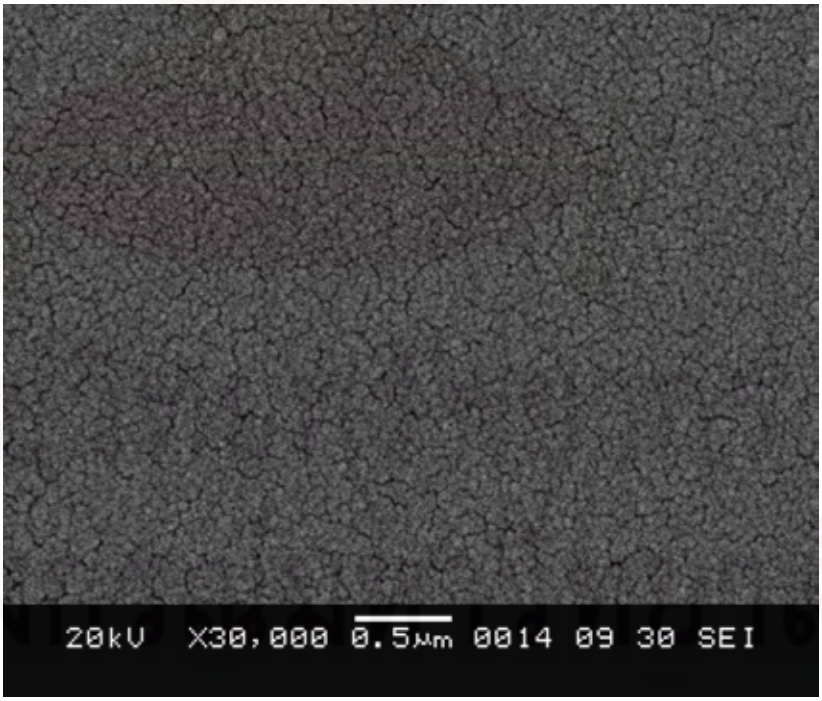

d)

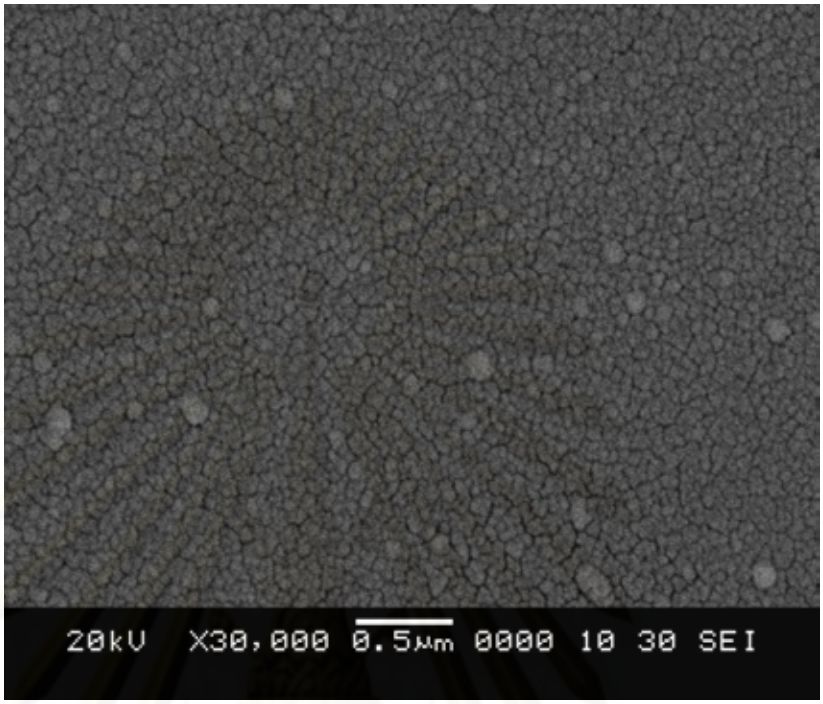

Fig. 5.4 AFM images of (a) bare GCE and (b) PPD coated GCE; and SEM images of (c) bare GCE and (d) PPD coated GCE, respectively.

A film thickness could be estimated by scraping the film with a sharp pin and compared the thickness between scraped and normal film zones (bits of the polymer film were piled beside of the scraped zone: a film edge zone). The film thickness of a 50 cycles PPD coated GCE showed in cross section analysis image of AFM (Fig. 5.5) which was estimated about 15-25 nm. This very thin film is an advantage of an polymer electropolymerization. However, when coating this insulated polymer onto an electrode surface for less or more than 50 cycles, the film thickness were not different from the ranges of 15-25 nm (the results were not shown) due to this electropolymerization is a self-limiting process. More insulating polymer coating was not required because using longer time and no much changing in thickness.

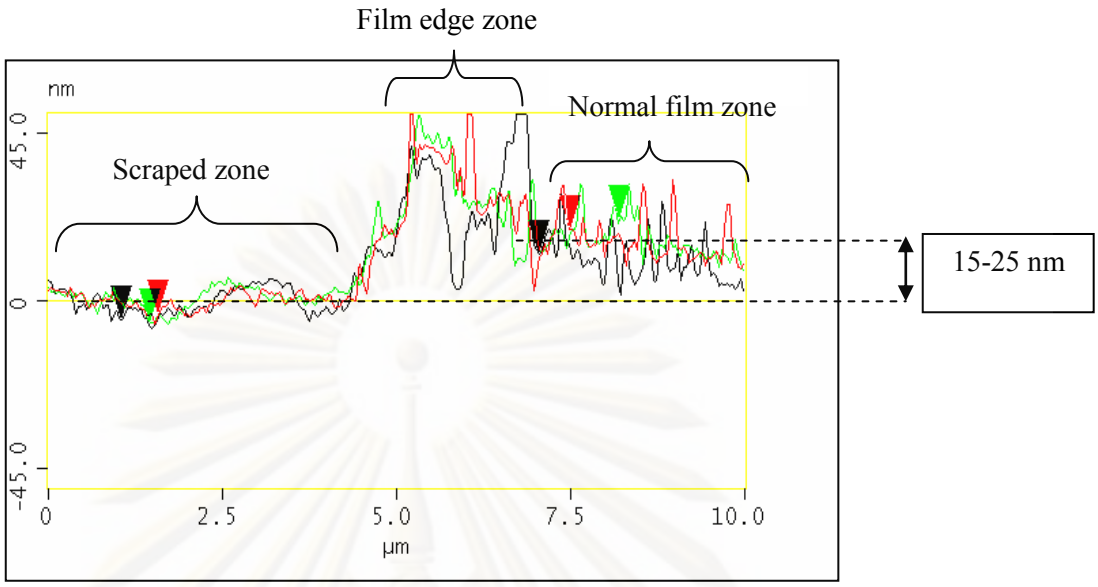

Fig. 5.5 Section analysis from AFM image for the film thickness determination of a 50 cycles PPD coated GCE.

AFM images in scale of 3x3µm and SEM images of sonicated PPD/GCEs at different times showed in Fig. 5.6 and 5.7, respectively. For the AFM image of a 10 min sonicating (Fig 5.6a), the PPD film was more smooth than a non sonicated PPD/ GCE since the sonication could damage the protuberances of the PPD film.

However, the SEM image of the 10 min sonicated electrode (Fig. 5.7a) was different from AFM image, although it is the same electrode. For assumption, the polymer films might be peeled with layer by layer when this coated electrode was sonicated. At the first time, liquid micro-jets might destroy protuberances on an outside of polymer film and became to smooth film, after that the sonication would destroy the smooth polymer film to form a porous surface. From this reason, the sonication at short time was not sufficient for pores formation, thus pores were not appeared on surfaces of 10 min sonicated electrodes. A no pore surface of the 10 min sonicated GCE related with a small current of cyclic voltammogram (Fig. 5.3(i)).

The PPD films were smoother when increasing the sonication time which could see from the Fig. 5.6 and 5.7 b to f due to protuberances of PPD films were longer damaged with ultrasonication. More smooth film when using longer sonication time could also confirm sonication could peel the polymer with layer by layer.

However, scratches on bare GCE surface could effect to the flatness of polymer film surface.

At the 20 min sonicated GCE surface of AFM image (Fig. 5.6b), pores were not also observed on the PPD surface even though the current response from cyclic voltammogram (Fig. 5.3(ii)) was higher than the current responses of PPD/GCE and the 10 min sonicated PPD/GCE. At this time, pores might be formed but they were very small size so they could not to clearly observe. This assumption was cleared by a SEM image of the 20 min sonicated PPD/GCE surface (Fig. 5.7b) that appeared some of very small pores (some pores were shown in circles). These small size of pores were damaged by the first set of liquid micro-jets. These small cavities played a significant role as nucleation sites for further bubble formation. These bubbles could implode at same or around of old cavities and bacame to larger pores (Barton et al., 2004). This assumption was confirmed from the bigger pores that were able to observe from the AFM and SEM images of 25 ,30, 50, and 90 min sonicated electrodes (Fig. 5.6 and 5.7 c to f, respectively). However, some of small pores may not resulted in damaging PPD film to the GCE surface.

Nanopores could be seen on the surface of a 25 min sonicated PPD/GCE from AFM image (Fig. 5.6(c.1)) and the SEM image (Fig. 5.7c) (some pores were shown in circles). The diameter of pores on this surface (Fig 4 (c.2)) ranged between 10-50 nm. The distribution of these pores were in disorder due to an ultrasonic ablation is a random process (Barton et al., 2004). Morever, distances between pores were not closed up which is a good characteristic of microeletrde arrays due to their diffusion profiles are difficult for overlapping. This characteristic caused the sigmoid shape of the cyclic voltammogram from the Fig. 5.3(iii). These images confirmed the success of microelectrode arrays fabricating on the insulated glassy carbon electrode.

However, many closed up pores of 30, 50, and ,especially, 90 min sonicated electrode surfaces from the AFM images Fig. 5.6 (d.1) to (f.1), respectively, matched with their peak shapes of cyclic voltammograms (Fig. 5.3(iv), (v), and (vi), respectively). The distance between two pores was very small so a diffusion profile overlapping would occur (Zoski, 2009). Moreover, microelectrodes (radius r) should

be separate from their nearest neighbour by 10r to avoid the diffusion profile overlapping (Simm et al., 2005). In addition, many pores and the film cracking were more observed when increasing the sonication time (30, 50, and 90min) as showed in Fig. 5.7d to f, respectively. These pores could be clearly observed on the surface of them which were similar with their AFM images. The film cracking could be occurred because this thin film were not durable for damaging of high speed liquid micro-jets when prolonged sonication. Connections between these cracking surfaces might cause the diffusion profiles overlapping of each microelectrode in an array. From these result, the sonication time longer than 25 min should not be selected for microelectrode arrays fabrication due to they would bring to the diffusion profile overlapping problem. Thus, the optimum time for microelectrode arrays fabrication was 25 min that indicated from results of cyclic voltammogram, AFM, and SEM images.

For determination of pores sizes of 30, 50, and 90 min sonicated GCE (Fig. 5.6 (d.2) to (f.2)), many pores diameters from 10 to 100 nm were observed on these sonicated surfaces. Pores size distribution which resulted from 25, 30, 50, and 90 min sonicated film could confirm that the ultrasonic technique is a random microelectrode arrays fabrication. When longer sonication, the numbers of larger pores diameters trended to increase which resulted from a more bubble imploding within the confines of the original pores (as represented above) (Barton et al., 2004). Since the largest pore was observed in the ranges of 90-100 nm, it was believed that these diameter pores no longer acted as nucleation sites (Barton et al., 2004), however, the quantitiies of these largest diameter were very low so this diameter was difficult to occur. Higher numbers of large pores when longer sonication could increase the chance of diffusion profile overlapping.

Additional, pores mean sizes on the PPD films were calculated from equation 5.3.

$$\bar{d} = \frac{1}{N}\sum_{i=1}^{n} d_i n_i \qquad (5.3)$$

Where $\bar{d}$ is average pore diameter; N is total number of pore; d_i is diameter in i ranges; and n_i is number of pores in i ranges. These average pore diameters from

these sonication times also presented in similar ranges about 20-30 nm (table 5.1). These means diameter showed that sonication time in this study did not much effect to mean diamiter of pore. It was believed that these diameter pores acted as general nucleation sites.

Table 5.1 Average diamiter from formular calculation of pores on surface of each sonicated electrodes.

Sonicate time (min)	AVG. diameter (nm)
25	23.467
30	33.366
50	32.423
90	27.369

a)

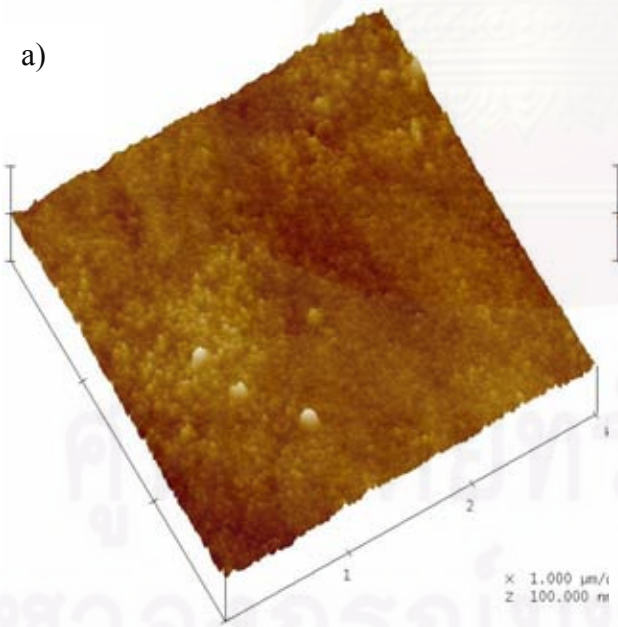

b)

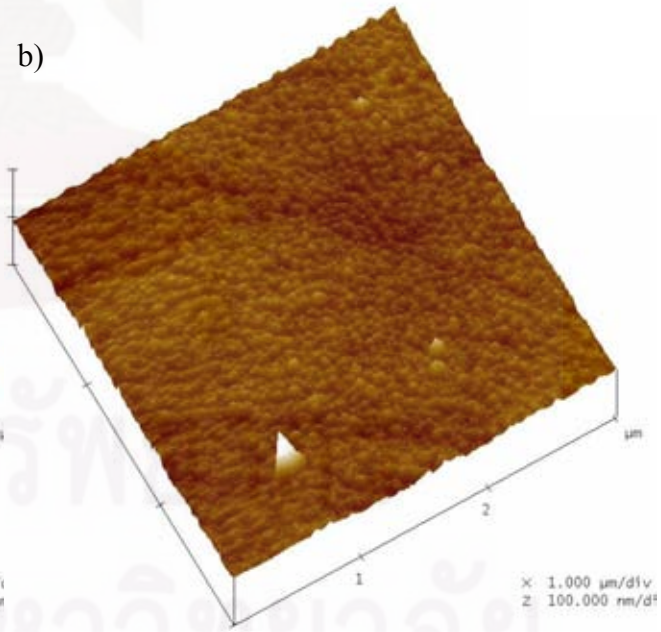

c.1)

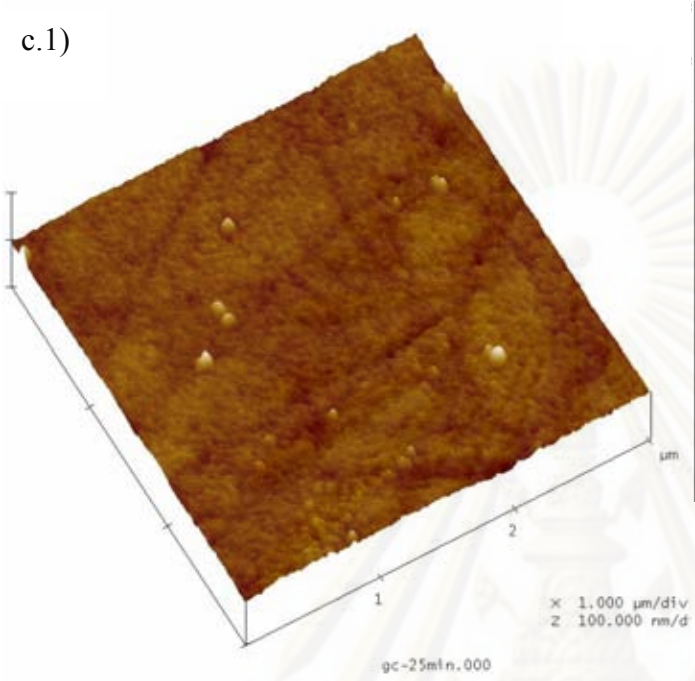
µm
2
1
× 1.000 µm/div
Z 100.000 nm/d
gc-25min.000

c.2)

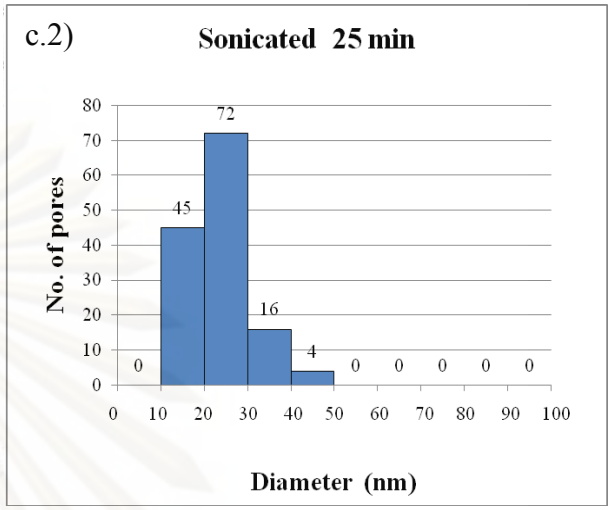
Sonicated 25 min
No. of pores
Diameter (nm)
0
45
72
16
4
0 0 0 0 0
0 10 20 30 40 50 60 70 80 90 100

d.1)

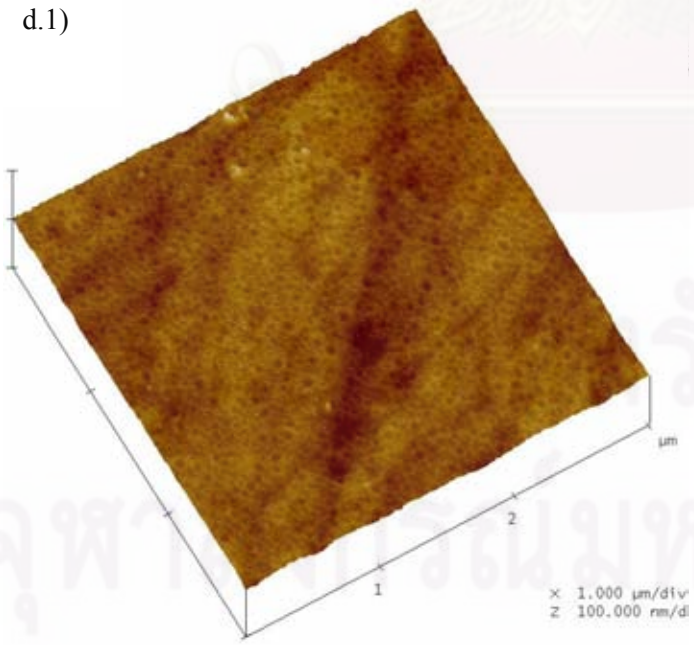
µm
2
1
× 1.000 µm/div
Z 100.000 nm/d

d.2)

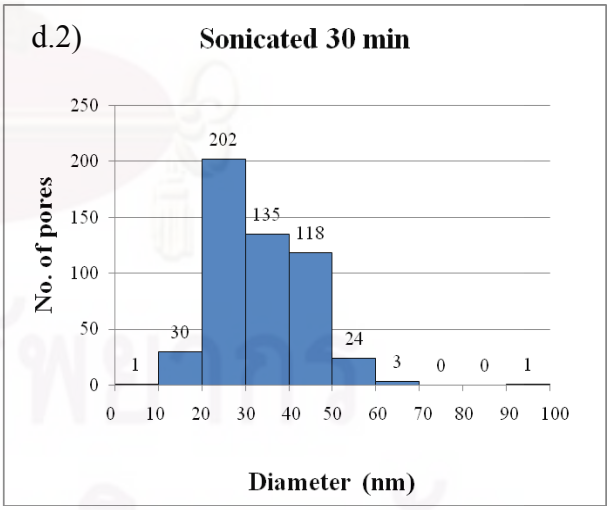
Sonicated 30 min
No. of pores
Diameter (nm)
1
30
202
135
118
24
3
0 0 1
0 10 20 30 40 50 60 70 80 90 100

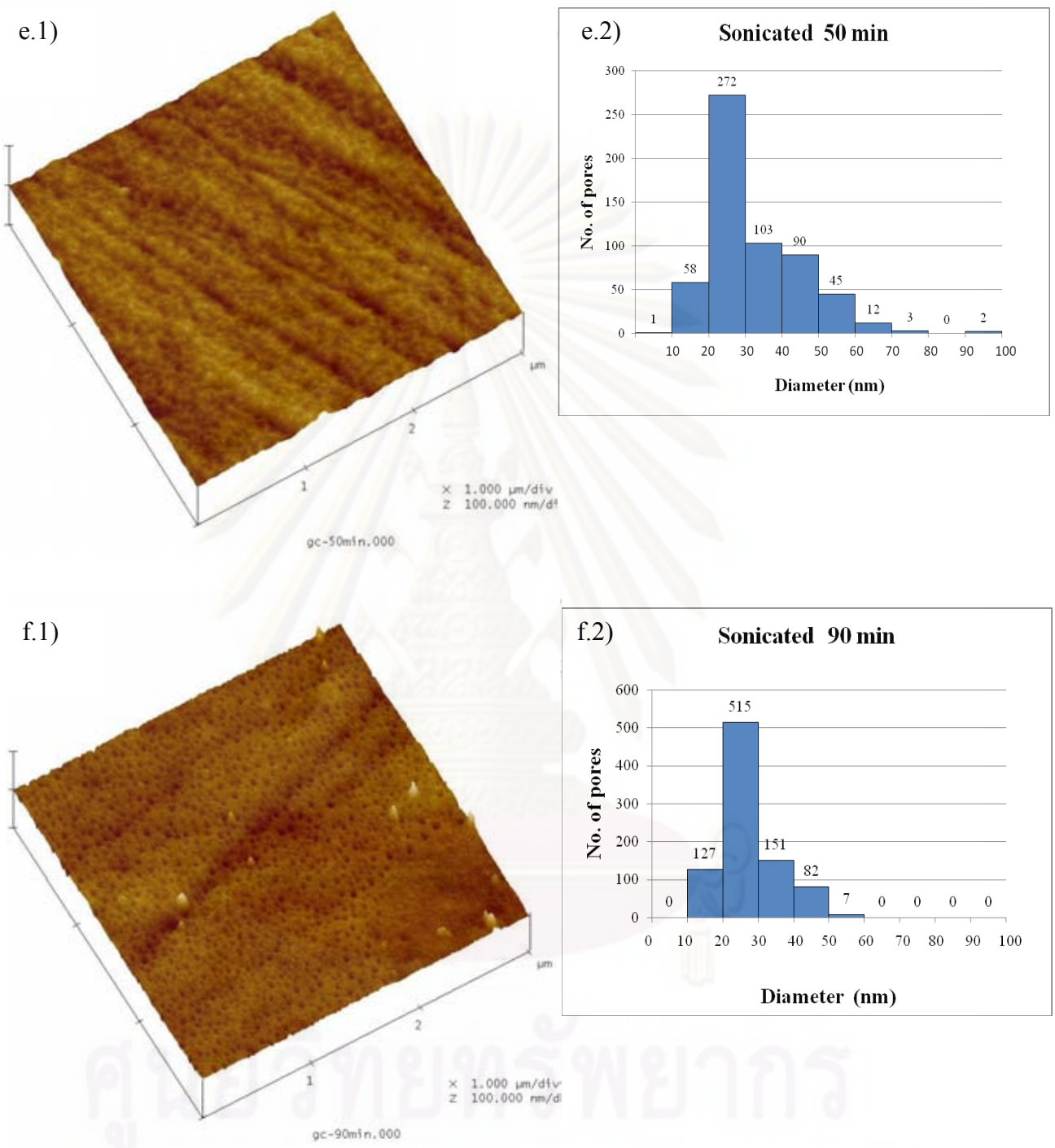

Fig. 5.6 AFM images of sonicated PPD/GCE for (a) 10, (b) 20, (c.1) 25, (d.1) 30, (e.1) 50, and (f.1) 90 min.; (c.2) to (f.2) are distributions of pore's sizes on 3x3µm surfaces of a 25, 30 50, and 90 min sonicated electrodes, respectively.

a)

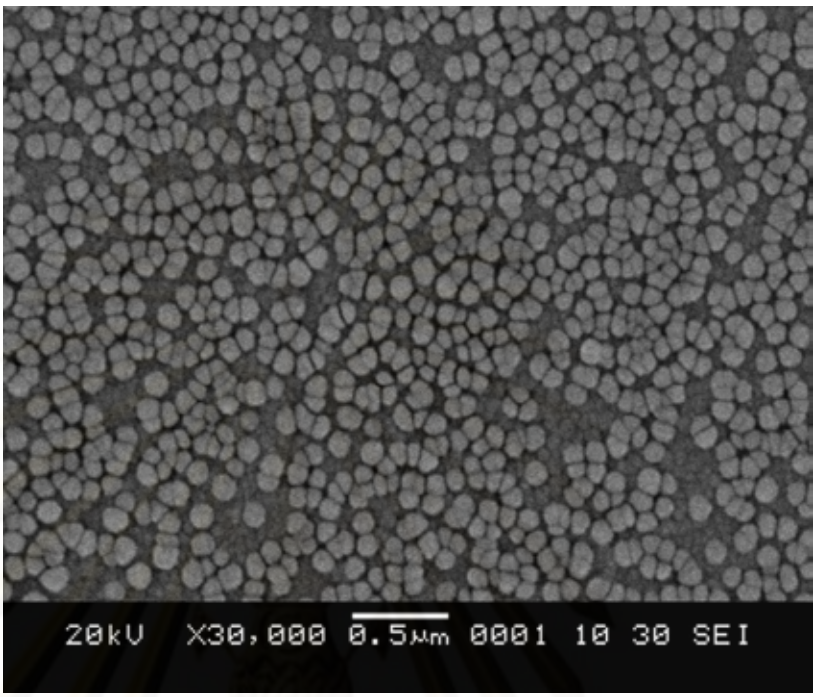
20kV X30,000 0.5µm 0001 10 30 SEI

b)

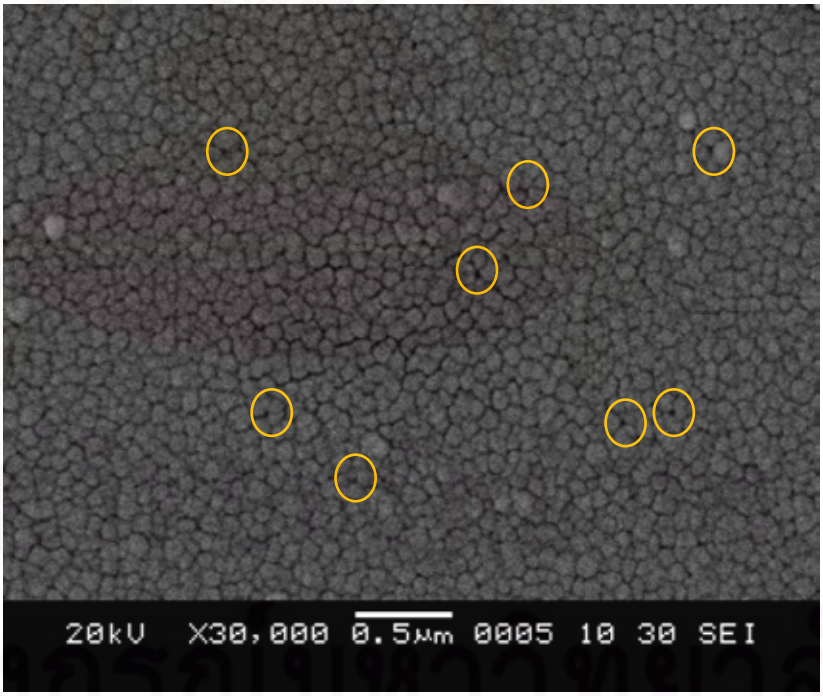
20kV X30,000 0.5µm 0005 10 30 SEI

c)

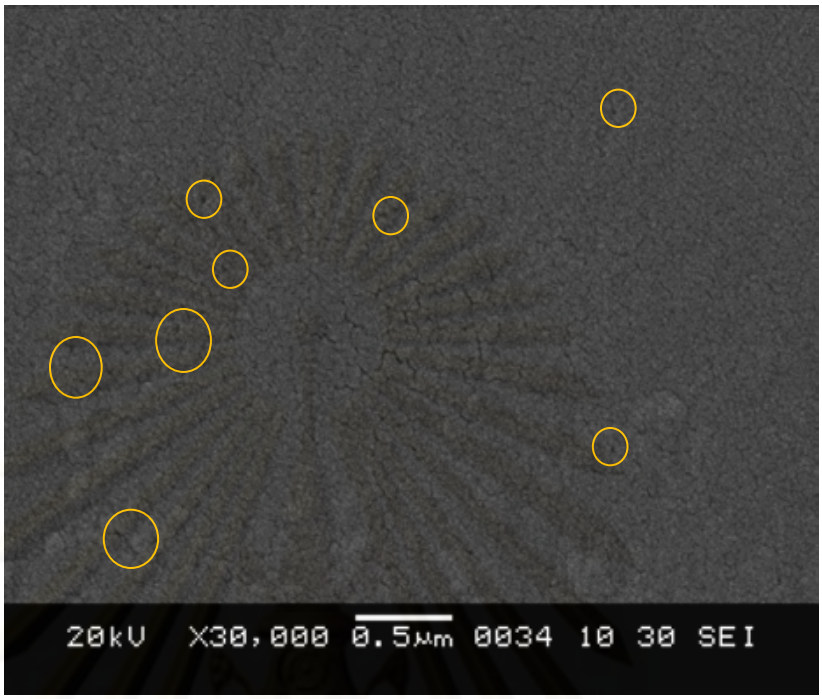
20kU X30,000 0.5µm 0034 10 30 SEI

d)

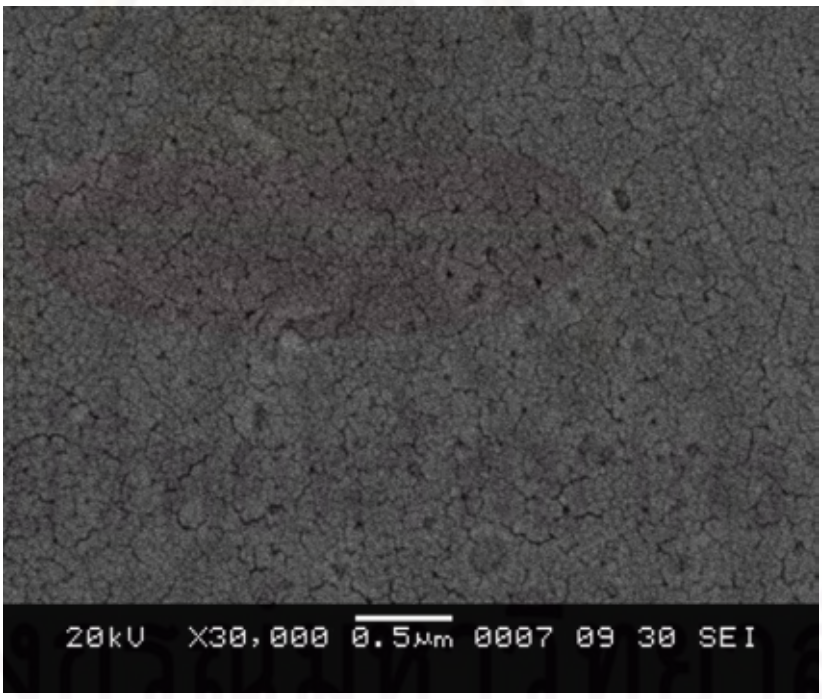
20kU X30,000 0.5µm 0007 09 30 SEI

e)

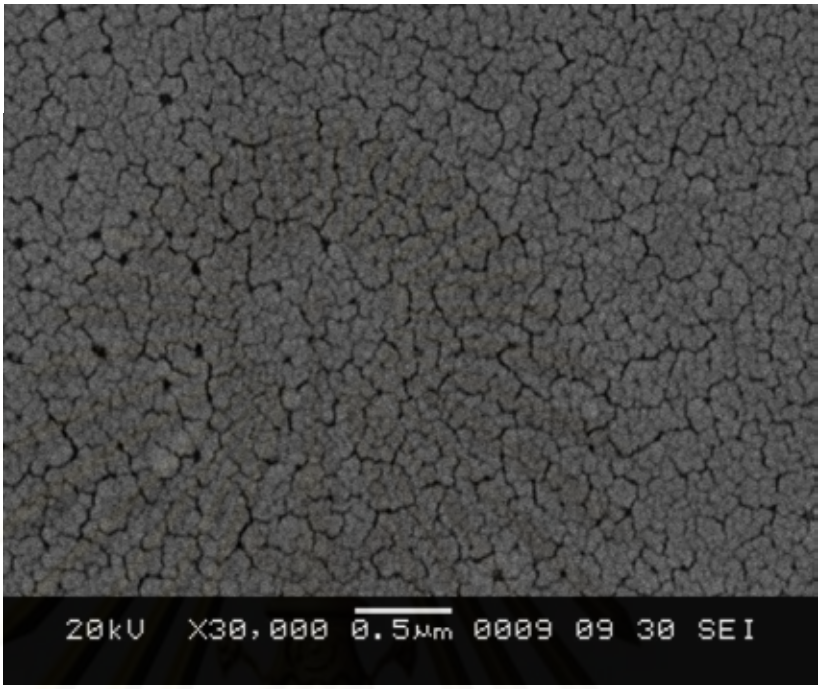

f)

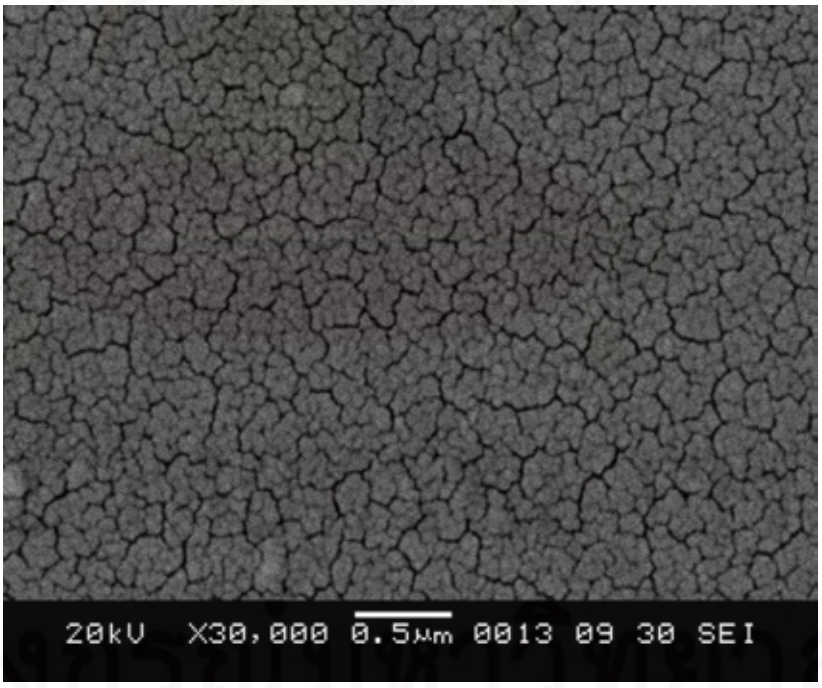

Fig. 5.7 SEM images of sonicated PPD/GCE with (a) 10, (b) 20, (c) 25, (d) 30, (e) 50, and (f) 90 min.

For more understanding, the schematic diagrams of polymer film sonication showed in Fig. 5.8. In Fig. 5.8a, a rough surface of coated electrode was covered with ellipsoidal particle. When sonicate at a short time (such as 5 min), the solvent micro-jets destroyed protuberances on the polymer film (Fig. 5.8b). After that, a 10 min sonication, the film surface was smoother (Fig. 5.8c) and very small pores could be formed on the surface under a 20min sonication (Fig. 5.8d). When longer sonication (such as 25 min) the PPD film became to a smooth film and the pores became to a larger size (Fig. 5.8e). However, at a too long sonication time, pores were more formation in distribution sizes and a film cracking was observed on the film (Fig. 5.8f).

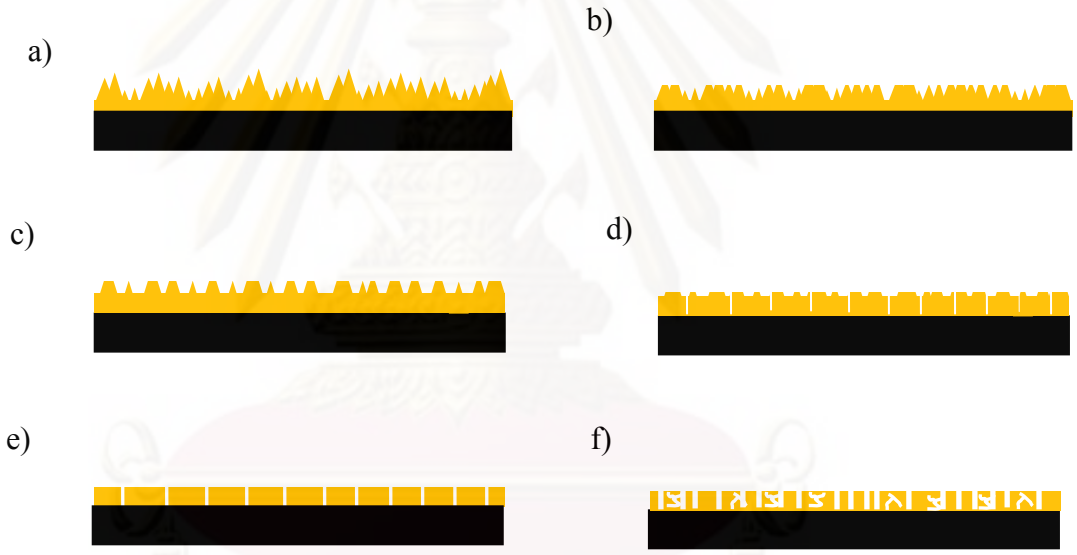

Fig. 5.8 Schematic diagrams of polymer film sonication (black is GCE and orange is PPD film); (a) non-sonicated PPD/GCE, (b) before 10 min sonicated PPD/GCE, (c) a 10 min sonicated PPD/GCE, (d) a 20 min sonicated PPD/GCE, (e) a 25 min sonicated PPD/GCE, (f) 30, 50 and 90 min sonicated PPD/GCE.

Total quantities of pores on surfaces of such coated electrodes were shown Fig. 5.9. Quantities of pores increased when increasing a sonication time. These results could be certainly used to confirm suitable sonication time. When using longer time, the surfaces of polmer films were also longer damaged with an ultrasonic (or micro-jets of solvent) that were represented above. Additional, the surface areas of the film were much damaged from such ultrasonic. Pores were much formed on the polmer surface relating with sonication time. For this reason, high sonication times should avoid because their many pores surface might bring the diffusion profile overlapping problems. For latter experiments, our microelectrode arrays would be fabricated with a 25 min sonication time.

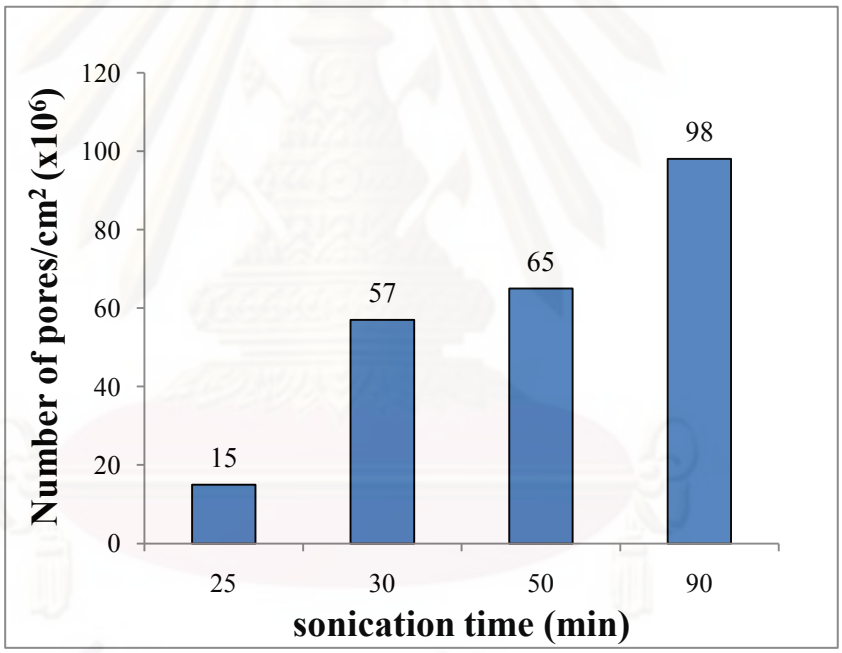

Fig. 5.9 Total number of pores on surface of sonicated electrodes at 25, 30, 50, and 90 min sonication times, respectively.

5.1.3 Microelectrode arrays: comparisons with other researches

In this section, comparisons of the microelectrode arrays fabricated in this work and other works (Barton et al., 2004; Myler et al., 2004; Pritchard et al., 2004; Myler et al., 2005; Law and Higson et al., 2005; Barton et al, 2008; Barton et al., 2009) using the same sonochemical method are discussed. Only pore physical characteristics such as sonication time, pore diameters, and pore densities are of interests at the moment and are elaborated as follows:

1) Sonication time

First, sonication times of minute time scale were used in this study in contrast to others which used very short times of second time scale. This different might be due to the different electrode surfaces applied which was found to influence electropolymerized polymer film characters (Kupila and Kankare, 1995). The different of electrode means deferents of adsorption and chemisorption properties, homogeneity, and smoothness. Previous researches using screen-print electrode as a working electrode which have more rough surface than GCE. The smooth and compact polymer film might be received on GCE, therefore, the soncation time used in this research was much longer than previous researches. The compact film might also are more difficult to damage, thus relatively very small pores were achieved in this work.

2) Pore diameter

Relatively small microelectrodes (10-100 nm) were observed in this research, however, a micron size of microelectrodes in previous researches were observed (while microelectrode diameters of other researches were 10μm (wire technique; Schwarz et al., 2000), 6 μm (etching method; Kim et al., 2002)). This difference scale of diameter might came from a smooth and compact PPD film on surface of GCE that cause difficulty in sonochemical ablation.

In additional, the microelectrodes of previous researches were clearly of two difference sizes (less than 1 micron and 3-4 microns) while the microelectrodes in this research did not clearly show bimodal sizes. This result might be effect from the nano size of this research microelectrode which acted as a nucleation site of a bubble.

When the nucleation site was very small, the bubbles generated in these sites were also small, hence, the power of liquid micro-jets were less than the micro-jets from a larger bubble. The low power of micro-jets was not sufficient for enlargement of pores. For this reason, the microelectrodes from this research were very small and of monodal sizes. Moreover, the ultrasonication device could also affect pores formation. However, too small mircroelectrodes are not satisfactorily required because they can increase solution resistance (Zoski, 2009) according to the follow equation:

$$R = \frac{1}{4Kr_0} \qquad (5.4)$$

Where R is the cell resistance (Ω), K is the conductivity of the solution (S/cm), and r_0 is the electrode radius (cm).

3) Pores population density

For this point, microelectrode population in this arrays were 1.5×10^7 pores/cm^2 while previous researches were 2×10^5 pores/cm^2. The more microelectrodes were observed on surface of PPD/GCE because using longer sonication time than previous researches.

5.2 HRP-PPY biosensor

The mechanism of HRP when the electron donors, mediators, are involved can be represented again by the follow equations (Ruzgas et al., 1996; Rosatto et al., 1999).

$$HRP\ (Fe^{3+}) + H_2O_2 \longrightarrow HRP\ (Fe^{5+}) + H_2O \qquad (5.5)$$

$$HRP\ (Fe^{5+}) + AH_2 \longrightarrow HRP\ (Fe^{4+}) + AH^* \qquad (5.6)$$

$$HRP\ (Fe^{4+}) + AH_2 \longrightarrow HRP\ (Fe^{3+}) + AH^* + H_2O \qquad (5.7)$$

In the first reaction (5.5), a native peroxidase, HRP(Fe^{3+}), is two-electron oxidized by H_2O_2 (or organic hydroperoxides). The next reaction (5.6) represents a

reduction of HRP(Fe^{5+}) by the first electron donor (AH_2), phenol, to form HRP(Fe^{4+}). Then, the native peroxidase is achieved from the one-electron reduction of HRP(Fe^{4+}) by second electron donor in the final reaction (5.7) (Ruzgas et al., 1996; Rosatto et al., 1999). The overall mechanism was shown in Fig. 5.10

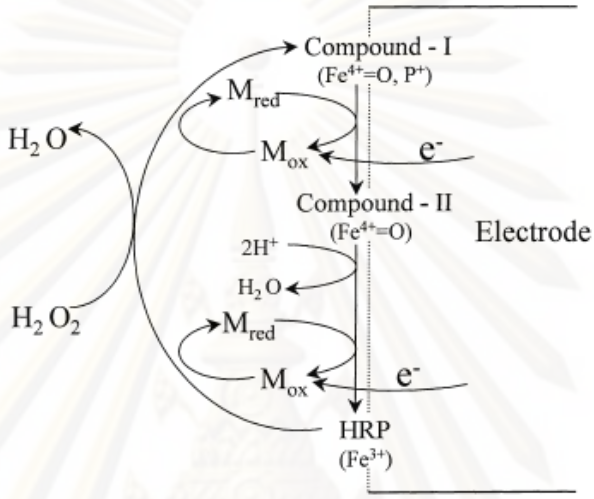

Fig.5.10 Mechanism of mediated bioelectrocatalytic reduction of H_2O_2 at HRP based electrodes where M_{ox} and M_{red} are the oxidised and reduced forms of the phenol, respectively (Rosatto et al., 1999).

5.2.1 Preliminary experiments: HRP/PPy planar electrode

In order to estrablish suitable conditions for HRP/PPy microelectrode arrays for phenol detection, we firstly investigated effects of related compounds, and substrate concentrations on current responses of HRP/PPy planar electrode.

The experiments were carried out by co-deposition of HRP (250 u/ml) and pyrrole (0.05 M) onto GCE by potential cycling between 0-01 V at a scan rate 10 mV/s for 15 cycles. To affirm the catalytic action of HRP, PPy-GCE without HRP was also investigated.

5.2.1.1 Effects of solution types

Effects of solution types on current responses were determined in this section. Current responses of bare and modified electrodes were measured in PBS, 30µM H_2O_2 in PBS, 50µM phenol in PBS, and 30µM H_2O_2 / 50µM phenol in PBS as shown in Fig. 5.11 (using pH 7.4 (Wang et al., 2000)). Current measurements were proceeded using amperometric technique at a potential of -0.05V (Wang et al., 2000; Korkut et al., 2008; Kafi and Chen, 2009) because the enzymes molecules could be inactivated by the formation of HRP(Fe^{6+}) when more negative potential is applied (Rosatto et al., 1999; Rosatto et al., 2002; Mello et al., 2003; Korkut et al., 2009). The results demonstrated that the current responses of the bare GCE in all tested solutions were of similarly low values indicating that both phenol and H_2O_2 were not electro active on the bare GCE. However, after PPy modification, the current responses increased tremendously in all solution types compared to the bare GCE which demonstrated strong conducting characteristic of PPY. Conducting polymer was reported to be able to improve electron transfer like metal properties (Vidal et al., 2003). However, the current responses of PPY/GCE were different in each solutions because the PPY film can be degraded by exposure to H_2O_2 (Umana and Waller, 1986). The current response of the degraded PPY /GCE in the H_2O_2 solution were less than response in PBS. Morover, when using the same biosensor to measure the phenol solution and 30µM H_2O_2/ 50µM phenol in PBS solution, the response were also reduced. Current responses of the HRP-PPY/GCE were also higher than bare GCE responses in all solutions and not much different from PPY/GCE responses except in 30µM H_2O_2 / 50µM phenol / PBS solution. The percentage increase of this HRP biosensor response in 30µM H_2O_2 / 50µM phenol solution were 3542.28% (compared to bare GCE) and 165.33% (compared to PPY/GCE). The current responses of HRP-PPY/GCE in 30µM H_2O_2/PBS or 50µM phenol / PBS solution were small because solution of 30µM H_2O_2/PBS did not contain phenol which is a mediator, on the other hand, solution of 50µM phenol / PBS did not H_2O_2 which was the first substrate for redox reaction. The percentage increase of HRP-PPY/GCE response in 30µM H_2O_2 / 50µM phenol solution were 119.49% (compared with PBS),

60.46% (compared with 30μM H_2O_2/PBS), and 76.48% (compared with 50μM phenol / PBS).

Additionally, for the highest current response of HRP-PPY/GCE in the solution which included both substrates, this result markedly confirmed the activity of HRP for H_2O_2 detection when using phenol as a mediator.

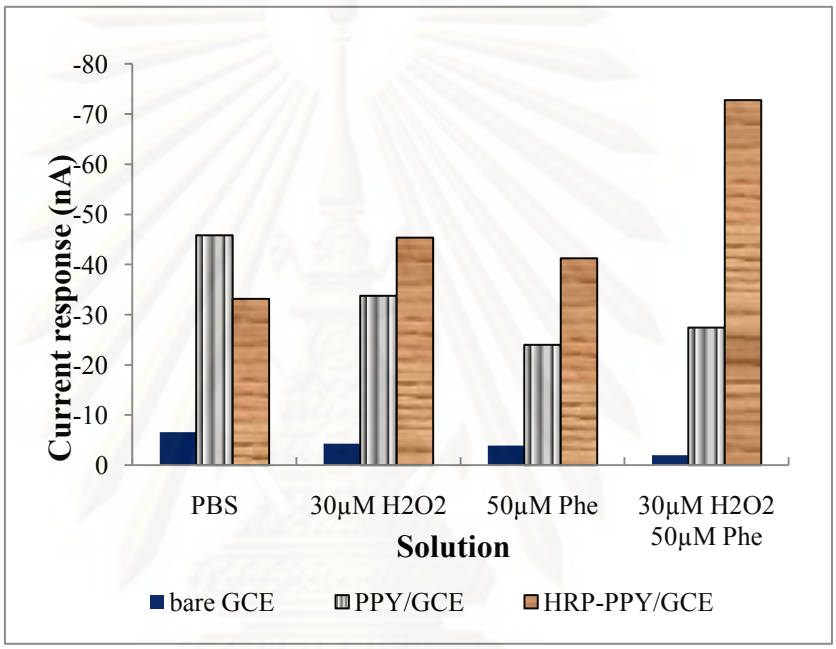

Fig. 5.11 Comparison of current responses between bare GCE, PPY/GCE, and HRP-PPY/GCE in different solution (pH 7.4) at-0.05V.

5.2.1.2 Effects of substrate concentration

In this section, effects of H_2O_2 concentration on response currents were studied at a fixed phenol concentration in oreder to determine suitable H_2O_2 concentration for the HRP catalysed reaction. where H_2O_2 is substrate for HRP. The current responses of different electrodes in different H_2O_2 concentration (mixed in 50μM phenol and PBS solution) is shown in Fig. 5.12. Current responses of bare GCE and PPY/GCE did not show noticable variation with H_2O_2 concentration because HRP was not included thus the reaction rate was too slow for detection. In contrast,

for enzyme based electrode, HRP-PPY/GCE, the current responses were found to increase with H_2O_2 concentration, and was peaked at 50µM H_2O_2. Higher H_2O_2 concentration probably resulted in HRP inactivation as was also reported in other works (Korkut et al., 2008; Kafi and Chen, 2009). Thus solution of 50µM H_2O_2 / 50µM phenol / PBS would be further used for electrochemical analyses in the following experiments.

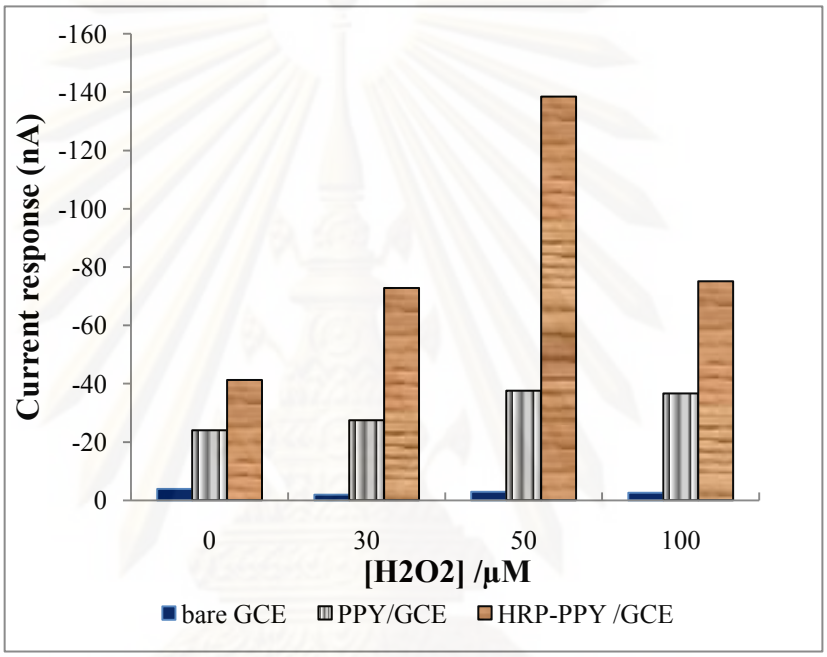

Fig. 5.12 Comparison of current responses between bare GCE, PPY/GCE, and HRP-PPY/GCE with various H_2O_2 concentration in 50µM phenol / PBS solution (pH 7.4) at-0.05V.

5.2.2 HRP-PPY microelectrode arrays for phenol detection

In section 5.1 we discussed microelectrode array formation by ultrasonication. In this section, these microelectrode arrays will be further electropolymerise with pyrrole and HRP to obtain a biosensor for phenol detection. The electropolymerization conditions for fabrication of conducting polymer coated biosensor are generally found to greatly influence electrochemical responses. For instance, the scan rate, number of cycles, and monomer concentration are factors

which affect polymer film thickness and other physical characters and thus governing electron and mass transfer from the solution to enzyme active sites and the electrode surface. In addition, the amount of enzyme entrapped is also governed by these operating parameters.

In the following, therefore, we will discuss effects of scan cycles, scan rate, pyrrole, and HRP concentrations.

5.2.2.1 Electrochemical analysis

For an electrochemistry analysis, an amperometry technique was used to examine responses of fabricated biosensors in 50µM H_2O_2 / 50µM phenol / PBS solutions (pH 7.4) at -0.05V. Firstly, a 25 min sonicated PPD/GCE was electropolymerized with 250U/ml HRP and 0.05M pyrrole with a potential cycling between 0 to 1.0V at 10mV/s. Fig. 5.13 shows the cyclic voltammogram of HRP-PPY electropolymerization. This voltammogram is a characteristic of an irreversible deposition with successive voltammograms progressively showing smaller peak currents (Barton et al., 2004).

The mechanism of conducting polymer electropolymerization can be summarized by reactions (5.8)-(5.11):

$$RH_2 \xrightarrow{-e^-} RH_2^{+\cdot} \qquad (5.8)$$

$$2RH_2^{+\cdot} \longrightarrow [H_2R\text{-}RH_2]^{2+} \xrightarrow{-2H^+} HR\text{-}RH \qquad (5.9)$$

$$HR\text{-}RH \xrightarrow{-e^-} [HR\text{-}RH]^{+\cdot} \xrightarrow{RH_2^{+\cdot}} [HR\text{-}RH\text{-}RH_2]^{2+} \xrightarrow{-2H^+} HR\text{-}R\text{-}RH \qquad (5.10)$$

$$(X+2)\,RH_2 \longrightarrow HR\text{-}(R)_x\text{-}RH + (2X+2)H^+ + (2X+2)e^- \qquad (5.11)$$

In the first reaction (5.8), a monomer molecule is electrooxidized to a radical cation forming $RH_2^{+\cdot}$, at an electrode surface. The second reaction (5.9) represents a dimerization reaction of two radical cations which then loose two protons to form the neutral dimer. Reaction (5.10) is a subsequence electrooxidization and trimerization. While reaction (5.11) is an overall electropolymerization reaction (Waltman et al., 1986).

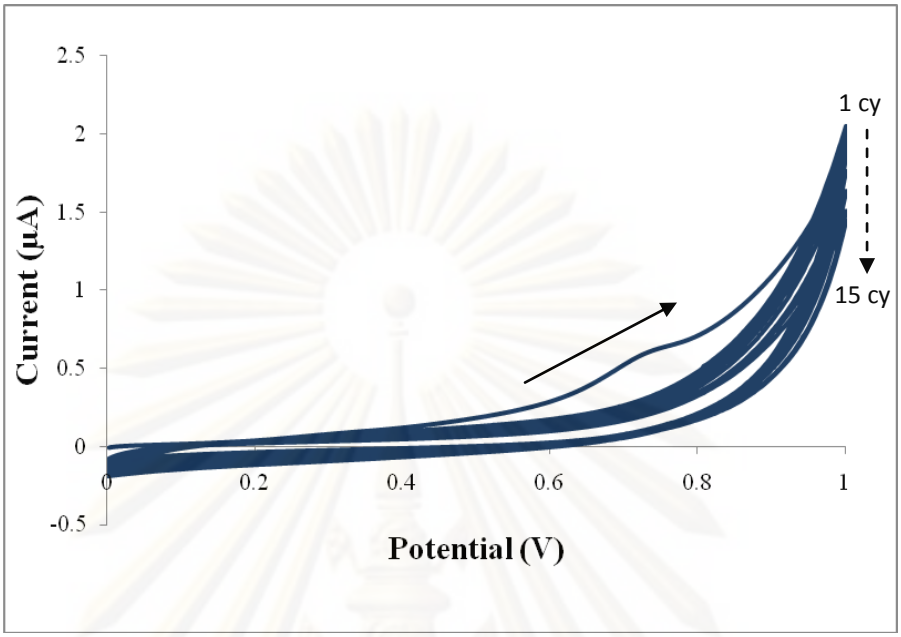

Fig. 5.13 Cyclic voltammogram of polypoyrrole-horseradish peroxidase electropolymerization for 15 cycles at 10mV/s.

1) Study of number of cycles

Number of cycles for electropolymerization is a time scale which directly affects a polymer film thickness (Razola et al., 2002). In this study, a 25 min sonicated PPD/GCEs was brought to electropolymerize with HRP and pyrrole by variation of cycle numbers, which were 10, 15, 20, 25, and 30. Current responses of these biosensors are shown in Fig. 5.14. It is obvious that response currents increases with numbers of electropolymerization cycles up to 20 cycles. For more than 20 cycles, reduced responses are observed. The amount of polymer could enable more enzyme to become entrapped within polymer when increasing the number of scan cycles (Pritchard et al., 2004). The thickness of the film was durable for entrapping the enzyme. However, more cycles of electropolymerization could lead to the thicker film which obstructed the mass and electron transfers (Razola et al., 2002; Chen et al., 2008). The film resistance increases with its thickness. The higher film thickness the longer distance between GCE surface and bulk solution, thus the longer time must be used for diffusion of H_2O_2 and phenol and electron transfer to the electrode surface.

For this reason, the thick film could bring the reduced sensitivity and long response time problems (Gao et al., 2007).

Thus, optimized number of polymerization cycles from this studied was 20 cycles which was used in the next experiments.

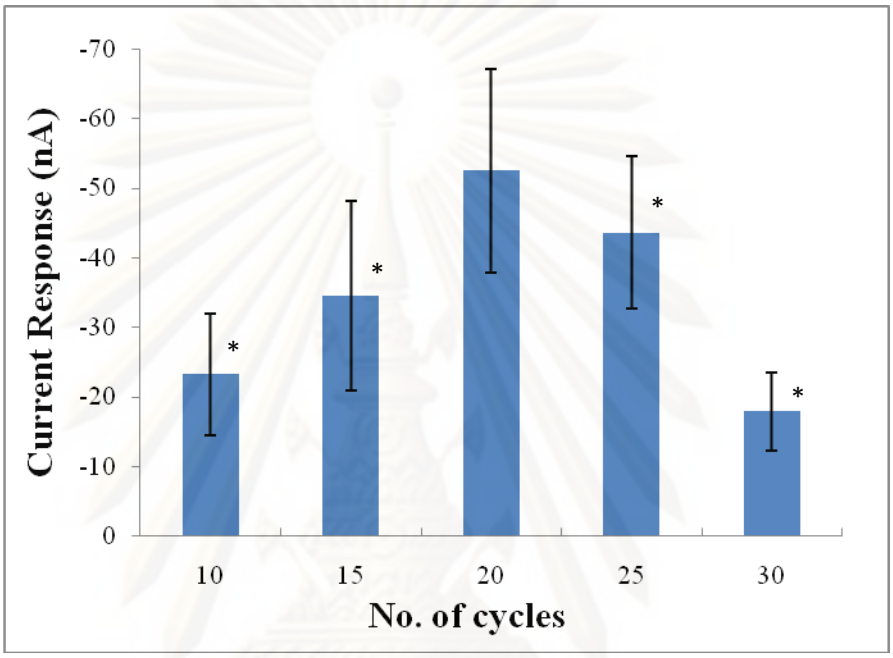

Fig. 5.14 Effect of number of cyles (vs. Ag/AgCl) on the HRP-PPY electropolymerization onto 25 min sonicated PPD/GCE responses to amount of 50µM H_2O_2 and 50µM phenol in PBS at -0.05V. Where * represent the significant difference ($p<0.05$) relative to 10 cycle of PPY-HRP electropoltymerization.

2) Study of scan rate

Polymer film thickness or internal organization of a polymer could also be controlled using a scan rate (Razola et al., 2002). Therefore, scan rates of 5, 10, 20, 30, and 50mV/s were studied and their current responses are shown in Fig. 5.15. The signals are found to increase from the low scan rate of 5 to 10 mV/s, and then the signals reduce at higher scan rates. The electropolymerization under low scan rate might form a compact and smooth film surface (Qu et al., 2005). Slow electropolymerization was received under low scan rate and higher chain polymers were obtained at slow rate (Sarac et al., 2004). Electropolymeriztion at low scan rate

might improve an ability of enzyme entrapment than using high scan rate. For this reason, the high response was received from low scan rate electropolymerizated biosensor. On the other hand, the fast formation of HRP-PPY film might reduce its adhesion to the microelectrode (Ameer and Adeloju, 2009). Thus the electropolymerization with high scan rates was not sufficient for enzyme retention which effected to the current response of biosensors (Razole et al., 2002).

However, the current responses at 10 and 20 mV/s were not statistically different since the P value was higher than 0.05 very much (see from Table A.3). Moreover, using the low scan rate prolongs the electropolymerization time at a fixed polymerization cycle numbers which likely causes lower enzyme activity. From these reasons, the scan rate at 20mV/s was chosen and used in further experiments.

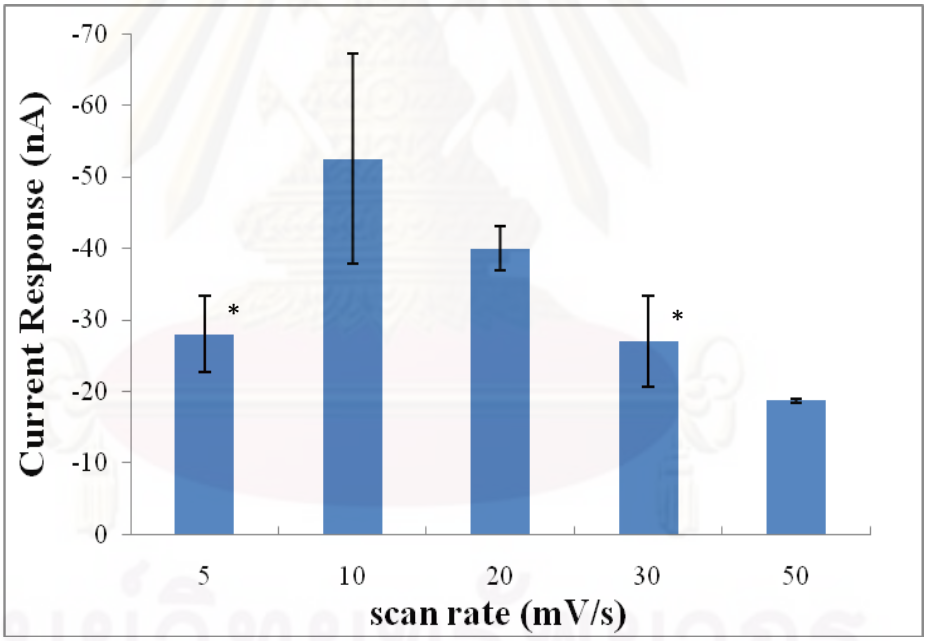

Fig. 5.15 Effect of scan rate (vs. Ag/AgCl) on the HRP-PPY electropolymerization onto 25 min sonicated PPD/GCE responses to amount of 50µM H_2O_2 and 50µM phenol in PBS at -0.05V. Where * represent the significant difference ($p<0.05$) relative to 10 mV/s of PPY-HRP electropoltymerization.

3) Study of pyrrole concentration

Pyrrole concentration is one of the major factors governing electropolymerization. For this reason, varied pyrrole concentrations were studied, namely, 0.03, 0.05, 0.07, and 0.09M. Effect of pyrrole concentrations on current responses is shown in Fig. 5.16. Response current is found highest at 0.05M pyrrole.

When using a lower pyrrole concentration, the film was difficult to grow due to the amount of monomers was insufficient to react in the electropolymerization process (Fortier et al., 1990; Razola et al., 2002). Moreover, thin film was formed when using low pyrrole concentration which was not enough to entrap sufficient amount of enzymes onto electrode surfaces (Razola et al., 2002; Li et al., 2007). The higher concentration of pyrrole referred to the electropolymerized solution having more substrate to react and form polymeric molecules (see from electropolymerization reaction 5.8-5.11). However, the excessive film thickness was received when too much pyrrole concentration was applied (Razola et al., 2002). The optimum pyrrole concentration which was selected for the fabrication of enzyme microelectrode arrays was 0.05M.

ศูนย์วิทยทรัพยากร
จุฬาลงกรณ์มหาวิทยาลัย

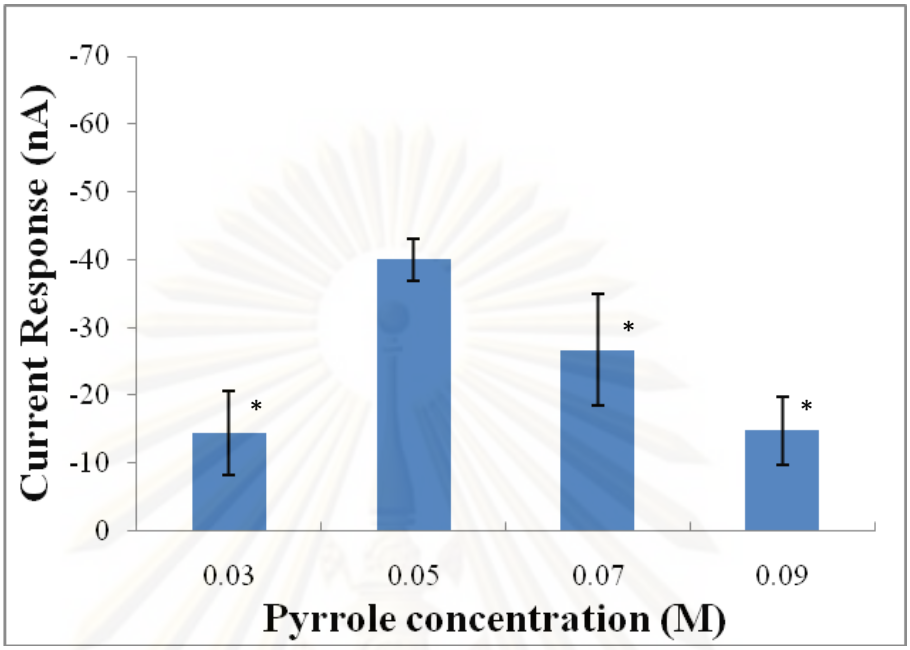

Fig. 5.16 Effect of pyrrole concentration (vs. Ag/AgCl) on the HRP-PPY electropolymerization onto 25 min sonicated PPD/GCE responses to amount of 50µM H_2O_2 and 50µM phenol in PBS at -0.05V. Where * represent the significant difference ($p<0.05$) relative to 0.05M Pyrrole.

4) Study of HRP concentration

Concentration of HRP entrapped in a polymeric matrix is a critical parameter and directly affect current responses and sensitivity of biosensors. The following HRP concentrations of 150, 250, 350, and 450 U/ml were studied. Fig. 5.17 shows that the current responses dramatically increase with HRP concentration up to 250 U/ml. After that, the current responses of biosensors were slightly reduced until 450 U/ml.

At low HRP concentrations caused low reaction rates therefore low current responses were obtained. However, HRP concentrations, could lead to the upper entrap capacity of the polymer film under certain electropolymerization conditions (Sulak et al, 2009). Moreover, poor adhesion and poor PPY polymerization yield might occur when using high enzyme concentration due to molecules of enzyme could obstruct during polymerization process which cause defects in the polymer film and reduced biosensor sensitivity (Tian et al., 2001; Razola et al., 2002). In addition,

for excess enzyme immobilization, entrapped enzymes might agglomerate and their active sites were blocked from the reach of H_2O_2 and phenol molecules. High molecules of HRP in a PPY matrix also obstructed the mass transport. These results leaded to a decreasing of the immobilized enzymes activity. The optimum HRP concentration was determined at 250 U/ml which was used to fabricate enzyme biosensors in this thesis. The suitable electropolymerization conditions are summarized in table 5.2.

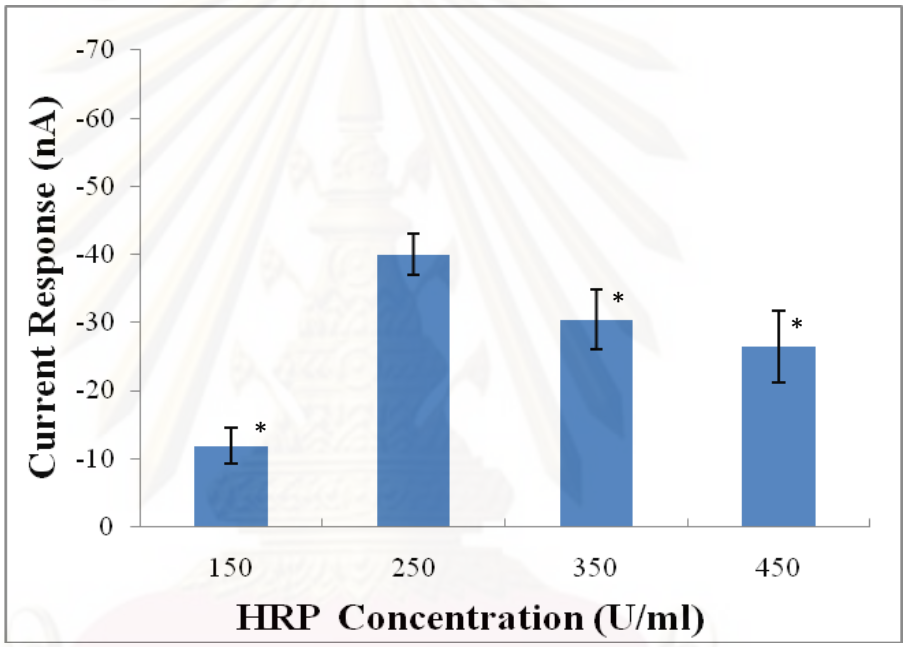

Fig. 5.17 Effect of HRP concentration (vs. Ag/AgCl) on the HRP-PPY electropolymerization onto 25 min sonicated PPD/GCE responses to amount of 50µM H_2O_2 and 50µM phenol in PBS at -0.05V. Where * represent the significant difference ($p<0.05$) relative to 250U/ml HRP.

Table 5.2 Optimum conditions for fabrication of HRP-PPY co-immobilixed on microelectrode arrays.

Conditions	Optimum Values
No. of cycles	20
Scan rate (mV/s)	20
Py conc. (M)	0.05
HRP conc. (U/ml)	250

5.2.2.2 Effect of solution types on current response of biosensor

In this experiment, the optimum conditions of HRP-PPY electropolymerization were used to fabricate a biosensor and studied effect of solution types on its current responses (Fig 5.18). The results shown the current response in PBS and 50µM phenol solution were lower than others since this solution did not have a first substrate, H_2O_2, for react with HRP. The current responses in 50µM H_2O_2 was higher than response in pure solutions since H_2O_2 is the first substrate for redox reaction. However, responses in PBS, 50µM phenol, and 50µM H_2O_2 were lower than the response in 50µM H_2O_2 /50µM phenol/PBS. These currents were background currents of this biosensor.

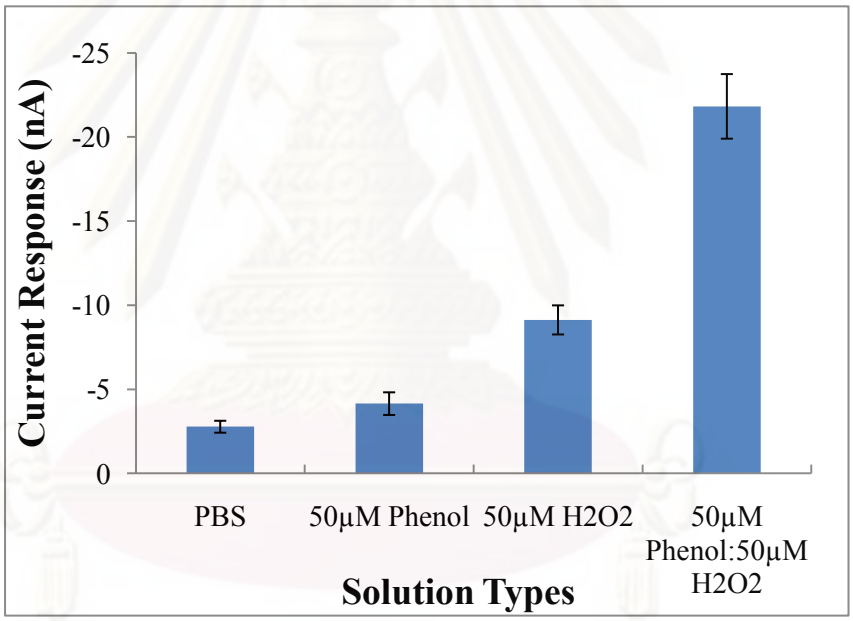

Fig. 5.18 Comparison of amperometry current responses of HRP-PPY/ 25 min sonicated PPD/GCE in different solution (pH 7.4) at-0.05V.

5.2.2.3 Physical characterization

The morphology of electrode surfaces of enzyme biosensors in this study was also studied usig AFM and SEM techniques. In this study, protrusions of HRP-PPY were expected to be observed onto the surface of microelectrode arrays. Due to small cavities of microelectrode arrays, the electropolymerization must be performed at

these limiting conducting surface areas for formation of HRP contained within PPY metrix with the ―mushroom" shape (Barton et al., 2004).

The biosensors for this studied were performed with 250U/ml HRP electro-immobilized in 0.05M PPY film onto microelectrode arrays at 20mV/s for 20 cycles. The AFM images of electrode surfaces are shown in Fig.5.19a and HRP-PPY protrusions are observed as predicted. Moreover, the SEM image of this enzyme biosensor (Fig. 5.19b) still illustrates protrusions (as shown in circles) when compared with the SEM image of microelectrode arrays without HRP (Fig. 5.19c). These protrusion confirmed that the HRP could be immobilized within polypyrrole metrix onto the microelectrode arrays.

From Fig 5.19a and b, two interesting points were observed 1) protrusions of HRP-PPY did not filled in all of microelectrode cavities, and 2) protrusions were formed in several sizes. For the first point, it was explained with PPY film formation behavior and imperfected shaped of microelectrode which could happen in three cases, namely, a recessed protrusion on microelectrode, a too small microelectrode, and an inactive microelectrode. The significant characteristic behavier of PPY film is this polymer can grow on to insulated surface outside conductive μm-structured substrate (Inzelt et al., 2000). For this reason, the polymer-enzyme protrusions were looked like flat film (not looked like ―mushroom") which covered a PPD zone around their microelectrode (Fig 5.20a). The recessed protrusion was the protrusion of HRP-PPY which could form but it was hid within microelectrodes (Fig 5.20b). The protrusion could not be seen from this microelectrode type.

In the second case of the imperfect miroelectrode, the too small microelectrode had very small diamiter which obstruced to mass transfer (Zoski, 2009). This problem effected to polymer formation in the microelectrode which might received a very small protrusion or did not receive in any things. The small protrusion was blended with a microelectrode surround that was very hard to see (Fig 5.20c). For the last case, the inactive microelectrode was a pore that could not explore to the GCE surface (Fig 5.20d). The electropolymerization of HRP-PPY was not proceed at this microelectrode due to no electron transfers between electrode and monomer solution.

For the second interesting point, a small protrusion could be formed from a too small microelectrode (Fig. 5.20c). In addition, a large nushroom occurred from merging of the protrusion at close-up pores (Fig. 5.20e).

a)

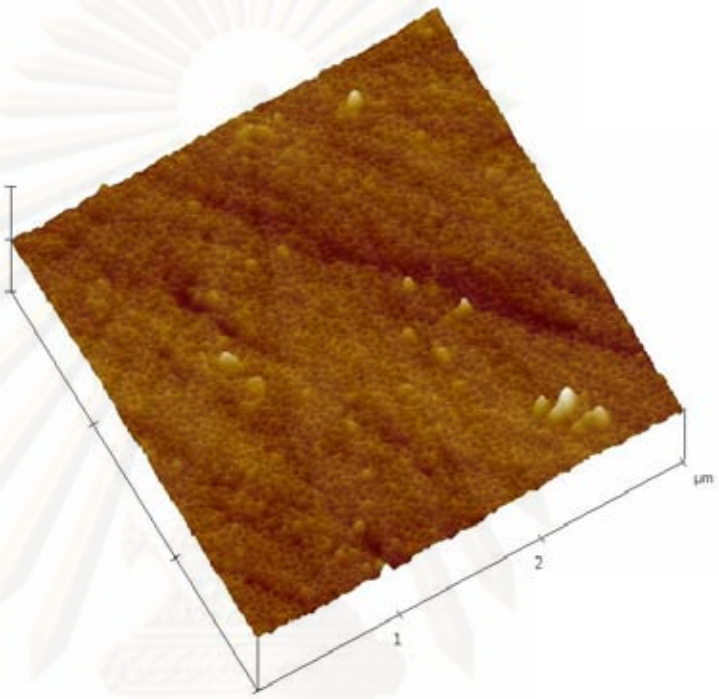

b)

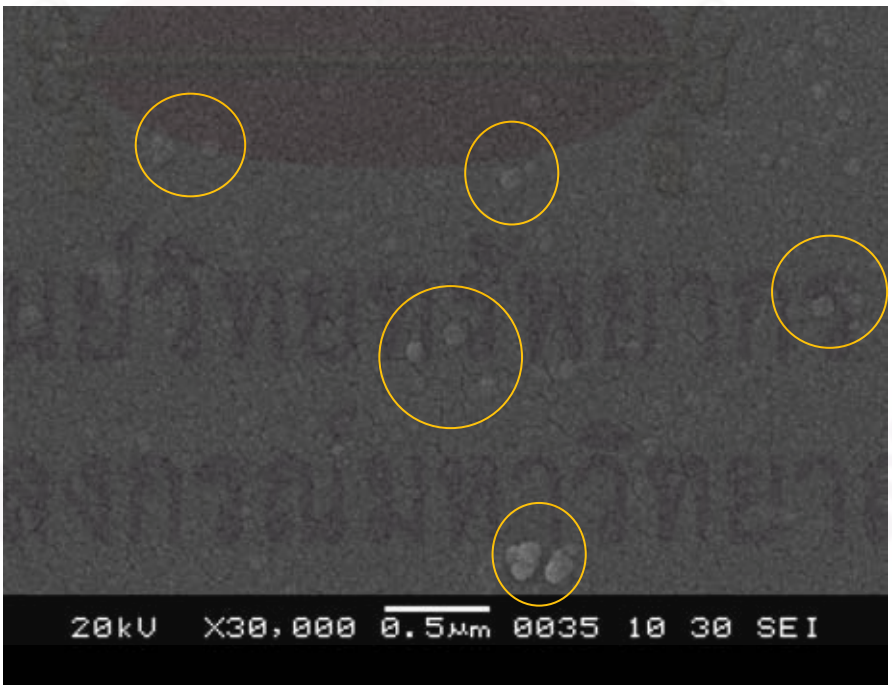

c)

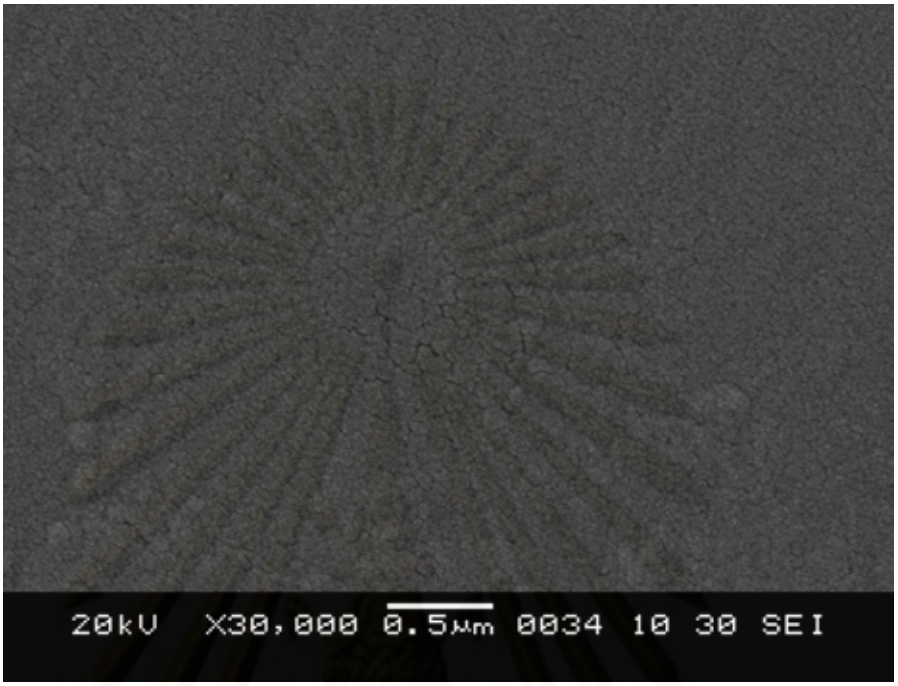

Fig. 5.19 (a) and (b) are AFM and SEM images of HRP-PPY protrusions on arrays of PPD/GCE, respectively; (c) SEM image of 25 min sonicated PPD/GCE without HRP-PPY.

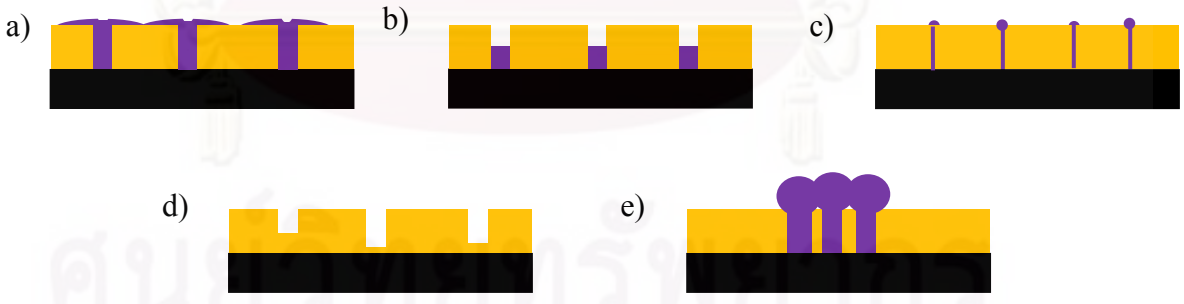

Fig. 5.20 Schematic diagrams of enzyme-polypyrrole protrusion (black is GCE, orange is PPD film, and purple is HRP-PPY protrusion); (a) non-mushroom shape of HRP- PPY protrusion, (b) recessed microelectrode arrays, (c) too small diameter microelectrode arrays, (d) inactive microelectrode arrays (e) merged protrusion.

5.3 Performance factors

5.3.1 Linear range, sensitivity, and detection limit

Linear range, sensitivity, and detection limit can be determined from the calibration curve of phenol. Calibration curve of phenol for concentration ranging from 10^{-7} to10^{-3} M phenol is shown in Fig. 5.21. The phenol solution was prepared in the solution of H_2O_2/ PBS (pH7.4). The concentration of H_2O_2 is one of the other important factors that affected to the response of biosensor (Rosatto et al., 1999; Rosatto et al., 2002; Mello et al., 2003; Korkut et al., 2008; Korkut et al., 2009; Kafi and Chen, 2009). The H_2O_2 concentration was fixed at 50 μM since low H_2O_2 concentration might bring to the low response current of biosensor and more H_2O_2 concetration might effect to PPY film and activity of HRP. However, when using phenol lower than 100 μM, phenol was limiting agent.

Linear range was found in the range of 2-100 μM. The sensitivity of this biosensor was calculated from the slope of the calibration curve which equaled to 0.1053 nA/ μM (R^2=0.993). Moreover, detection limit was calculated according to the follow equation:

$$3S_b/m \qquad (5.5)$$

Where S_b is the standard deviation of the current response at the lowest detectable concentration (n=5) and m is the slope of the linear calibration curve (Sulak et al, 2009). The detection limit of 4.55 μM phenol was obtained.

ศูนย์วิทยทรัพยากร
จุฬาลงกรณ์มหาวิทยาลัย

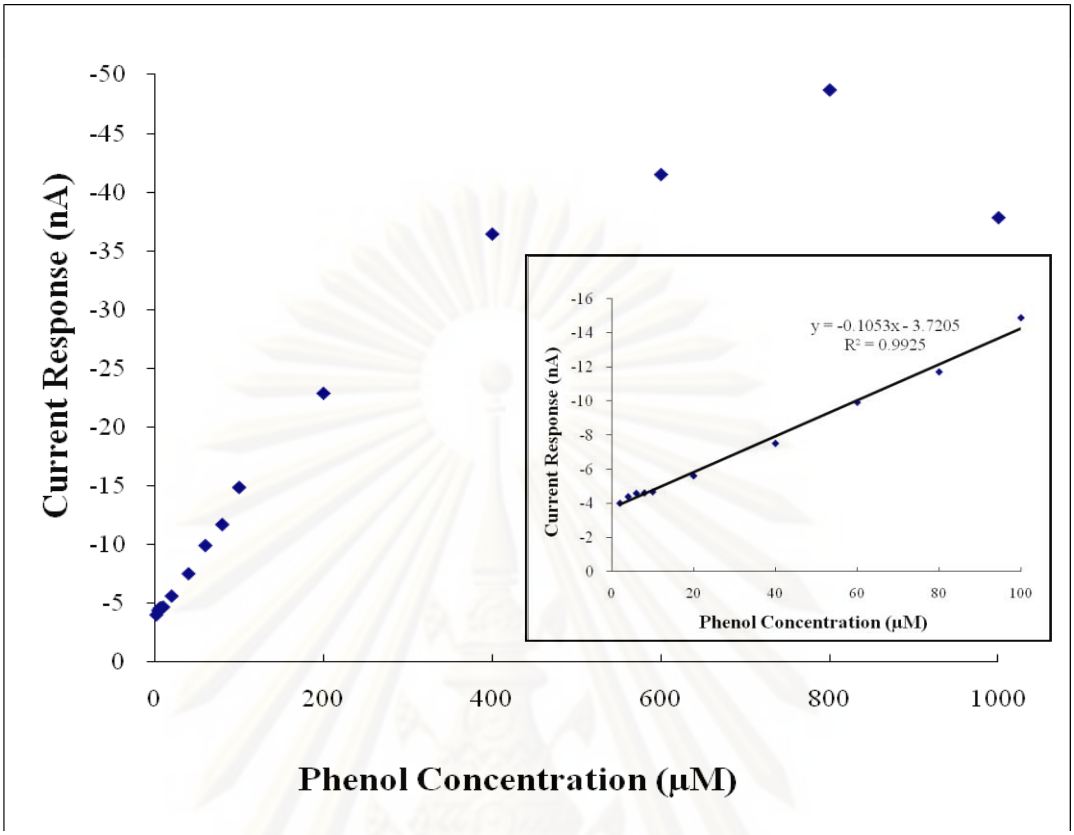

Fig. 5.21 Calibration curve of amperometric phenol response in 50 µM H_2O_2/ PBS solution (pH 7.4) at -0.05V (vs. Ag/AgCl). Inset: the linear part of the calibration curve.

5.3.2 Response Time

Response time is a time when the response current reaches steady state. This response time can be varied for each biosensor. However, the typical value is less than 5-10 minutes (Eggins, 1999). The response time of this biosensor (Fig 5.22) was found within 150 s. This indicated a quite fast diffusion of substrate and reaction products through the composite film.

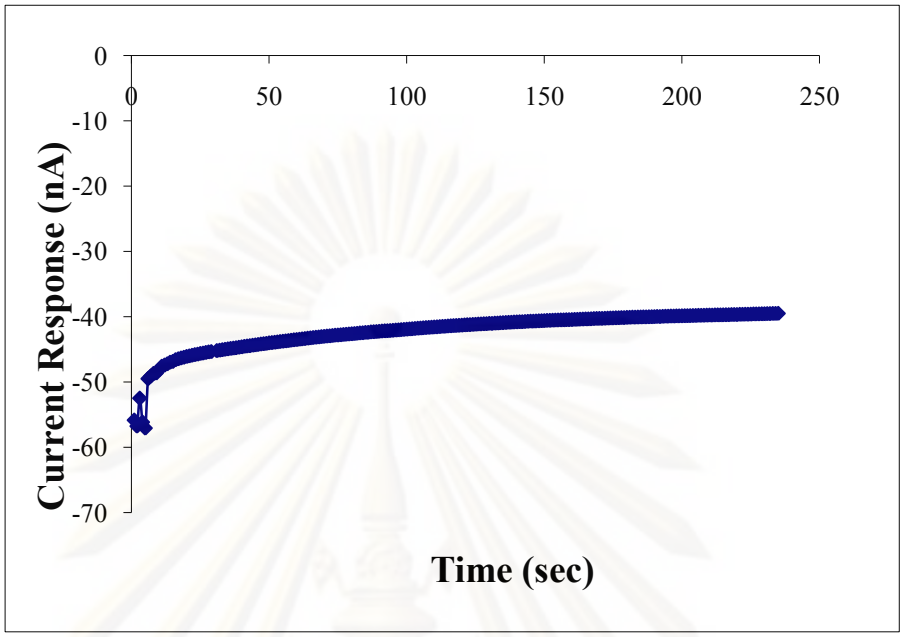

Fig. 5.22 Amperometric current response of biosensor of 50µM phenol/50µM H_2O_2 in PBS solution (pH 7.4) at -0.05V (vs. Ag/AgCl).

5.3.3 Reusability (Repeatability)

The repeatability of the biosensor was evaluated for ten measurements in the 50µM phenol/50µM H_2O_2/PBS solution (pH 7.4) at -0.05V (Fig 5.23). It was found that the amperometric response of the second test was dramatically dropped to 80% of the initial response. After 5 repeated tests, the current response became gradually decrease to 75% of the initial current. At the tenth repeated test, 50% of the initial response was observed. From this study, the current responses of this biosensor at the longer time of measurement were reduced from the first time which effected from the inactivated enzyme. When the biosensor was longer measured, the entrapped enzymes had more a chance to react with the H_2O_2 and became to inactivated enzyme. Moreover, molecules of enzyme could leach out of the PPY film due to PPY film is a porous film and this PPY film could be degraded by H_2O_2 (Umana and Waller, 1986**;** Thanachasai et al., 2002). These reasons resulted to the reduced responses in more assays.

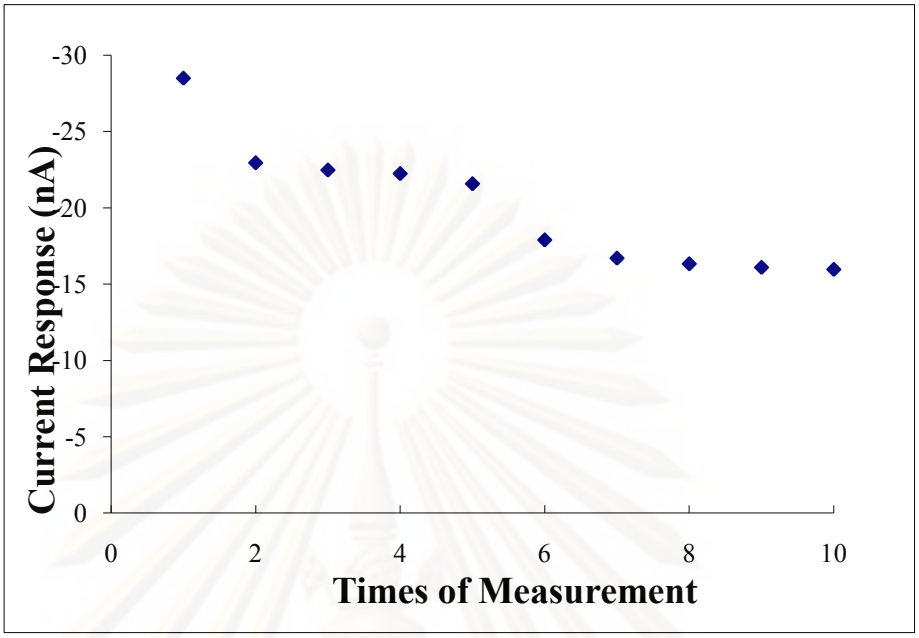

Fig. 5.23 Ten amperometric current responses of a same biosensor in 50μM phenol/50μM H_2O_2 / PBS solution (pH 7.4) at -0.05V (vs. Ag/AgCl).

5.3.4 Reproducibility

Ten biosensors were fabricated in the same way and used to measure the phenol solution for determining reproducibility (Fig 5.24). The reproducibility was presented by a relative standard deviation of the current response of each biosensor in 50μM phenol/50μM H_2O_2/PBS solution (pH 7.4) at -0.05V. The R.S.D. of these current responses was 23.84% (n=10).

The high of R.S.D. was likely to be resulted from the method of microelectrode arrays fabrication. The sonochemical fabrication could form microelectrode arrays with a random arrangement. Moreover, the electrodes which used in this experiment were small GCEs. The error of reproducibility might come from imperfect modification of these small electrodes. For these reasons, the microelectrode arrays formation in new fabrications were different and the responses of these biosensors were also different.

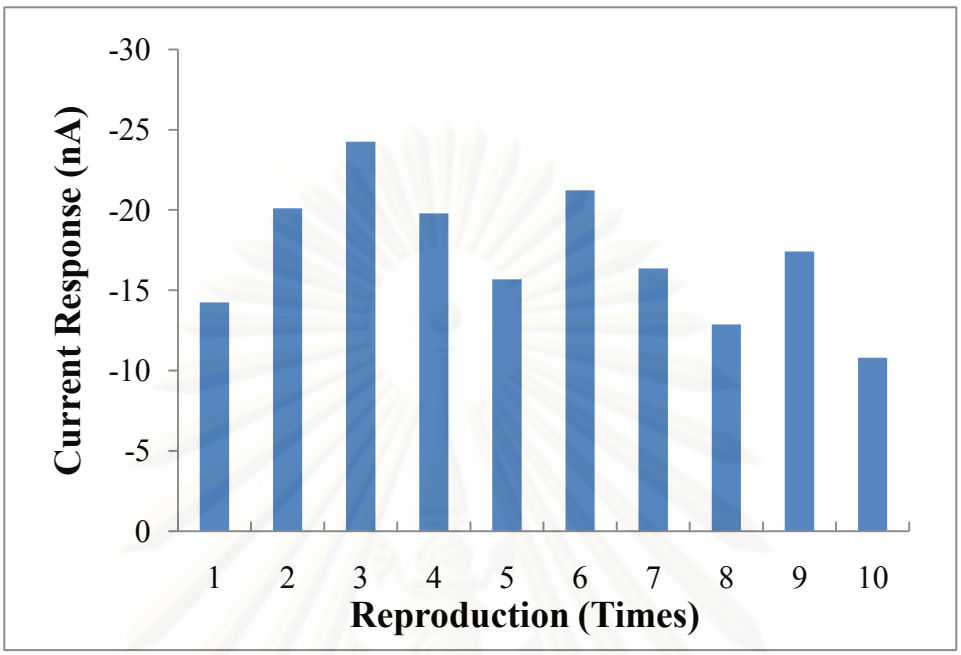

Fig. 5.24 Amperometric current ten biosensors in 50µM phenol/50µM H_2O_2 (pH 7.4) at -0.05V (vs. Ag/AgCl).

5.3.5 Life Time

The result of combined repeat and storage stability study is shown in Fig 5.25. The biosensor was repeated used over a period of 30 days, and kept in PBS (pH 7.4) at 4ºc in between uses. This biosensor lost 54% of its initial response on the second storage day. After 5 and 14 days of storage, the response currents were around 40% and 30% of the initial response, respectively. The current response of this biosensor remained 24.06% of the initial response after storage for one month in 4ºc of PBS. The very low storage stability might come from the leaking out of HRP from PPY membrane because color changing into brown green of solution that used to store the biosensor when tested with H_2O_2. The HRP leaking problem was affected from degradation of PPY film with H_2O_2. Moreover, inactivation of HRP also effected to this performance factor since this biosensor was longer measured in H_2O_2.

In addition, when not using, the enzyme biosensor must be stored in 4ºc of PBS for protection of an enzyme inactivation.

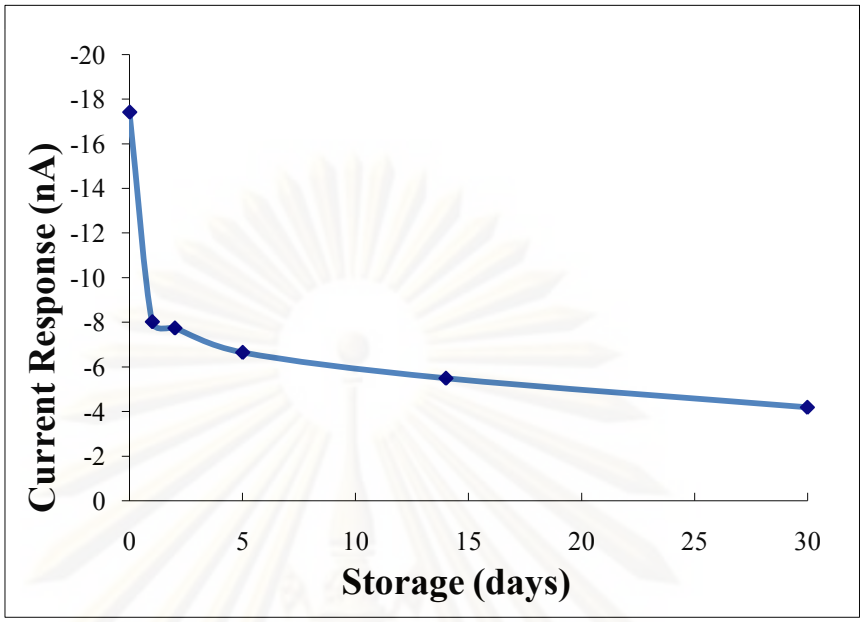

Fig. 5.25 Storage stability of a biosensor in 50μM phenol/50μM H_2O_2 / PBS solution (pH 7.4) at -0.05V (vs. Ag/AgCl).

ศูนย์วิทยทรัพยากร
จุฬาลงกรณ์มหาวิทยาลัย

5.3.6 Comparison of these performance factors to other researches

For this point, some performance factors such as linear ranges, sensitivity, detection limit, and response time were compared to other researches.

Table 5.3 Comparison of performance factors of this research with other researches.

Research	Linear range (µM)	Sensitivity (nA/ µM)	Detection limit (µM)	Response Time (s)	H_2O_2 conc. (µM) and potential (v)
This research biosensor	2-100	0.1053	4.55	150	50 at -0.05V
HRP/ silica-titanium / cross linked with glutaraldehyde in carbon SPE (Rosatto et al., 1999)	10 -50	-	-	3	20 at 0V
HRP/SiO_2-Nb_2O_5/ cross linked with glutaraldehyde in carbon SPE (Rosatto et al., 2002)	5-25	3.2	0.5	-	100 at 0.05V
HRP+DNA/silica-titanium cross linked with glutaraldehyde in carbon SPE (Mello et al., 2003)	1-50	181 cm^{-2}	0.7	30-45	500 at -0.05V
HRP/PPY+CNT/ Au (Korkut et al., 2008)	16-44	1	3.52	2	16 at -0.05V
HRP/PPY/PVF/ GCE (Sulak et al., 2009)	0.5-10	25.93	0.23	300	-0.2V
HRP/PPY/GCE (Korkut et al., 2009)	2-12	90	0.3	3	20 at -0.05V

Low performance factors were observed from this biosensor even though it is microelectrode arrays. This result might come from too small microelectrodes on an array which effected to mass and electron transfer.

ศูนย์วิทยทรัพยากร
จุฬาลงกรณ์มหาวิทยาลัย

CHAPTER VI

CONCLUSIONS AND RECOMMENDATIONS

6.1 Conclusions

Microelectrode arrays were successfully achieved using 25 min sonication time on PPD-coated glassy carbon electrode. Too short sonication time did not result in enough ablated film thus low response currents were observed, while too long sonication time resulted in large electroactive cavities of closed contacts which caused planar electrode behavior.

The optimum conditions of electropolymerization of horseradish peroxidase (HRP) and polypyrrole (PPY) were found as follows:

6.1.1 Number of scan cycles

This parameter effected with the polymer film thickness. When coating for more cycles, the polymer films became to less electroactive. The suitable of number of cycles was 20.

6.1.2 Scan rate

The scan rate of electropolymerization also affected the film thickness and film adhesion. Low scan rate resulted in thin compacted films, however, too high scan rate could reduce film adhesion on the electrode surface. The suitable scan rate determined was 20 mV/s.

6.1.3 Pyrrole concentration

This parameter is major factor influencing film thickness and affect enzyme entrapment. The film was difficult to grow when using low pyrrole concentration but the excessive film thickness was received under too high pyrrole concentration. The best pyrrole concentration was 0.05M.

6.1.4 HRP concentration

An enzyme concentration directly affects the response of biosensors and their sensitivity. Low HRP concentration meant the low response and sensitivity of

biosensor while excess HRP could affect mass transfers of substrates to the enzyme active sites. The optimum concentration of HRP was determined at 250 U/ml.

6.1.5 Performance factors

1) Linear range: The response current of the HRP-PPY microelectrode was linear in the range of 10^{-7} to10^{-3} M phenol.

2) Sensitivity: It was found to be 0.1053 nA/ μM .

3) Detection limit: The value of 4.55 μM phenol was obtained.

4) Response time: A response time was observed within 150 s.

5) Reusability (Repeatability): It was found that the amperometric response of the second test was dramatically dropped to 80% of the initial response. After 5 repeated tests, the current response became gradually decrease to 75% of the initial current. At the tenth repeated test, 50% of the initial response was observed.

6) Reproducibility: The R.S.D. of the ten biosensors current responses was 23.84% (n=10).

7) Storage stability: This biosensor lost 54% of its initial response on the second storage day. After 5 and 14 days of storage, the response currents were around 40% and 30% of the initial response, respectively. The current response of this biosensor remained 24.06% of the initial response after storage with 1 month.

6.2 Recommendations for the future studies

6.2.1 The supporting electrolyte should be added and studied for improve electropolymerization of PPY-HRP on microelectrode arrays. Adding of supporting electrolyte might also improve sensitivity of this microelectrode biosensor.

6.2.2 Other conducting polymer should be studied for improve sensitivity of biosensor.

REFERENCES

Ameer, Q. and Adeloju, S.B. Development of a potentiometric catechol biosensor by entrapment of tyrosinase within polypyrrole film. Sensors and Actuators B 140 (2009): 5–11.

Bai, H.P.; Lu, X.X.; Yang, G.M.; Yang, Y.H. Hydrogen peroxide biosensor based on electrodeposition of zinc oxide nanoflowers onto carbon nanotubes film electrode. Chinese Chemical Letters 19 (2008): 314–318.

Bard, A.J.; and Faulkner, L.R. Electrochemical Methods: Fundamentals and Applications. 2nd Ed. New York: Wiley, 2001.

Barton, A.C.; Collyer, S.D.; Davis, F.; Garifallou, G.Z.; Tsekenisa, G.; Tully, E.; Kennedy, R.O.; Gibson, T.; Millner, P.A.; and Higson, S. P.J. Labeless AC impedimetric antibody-based sensors with pg ml−1 sensitivities for point-of-care biomedical applications. Biosensors and Bioelectronics 24 (2009): 1090–1095.

Barton, A.C.; Collyer, S.D.; Davis, F.; Gornall, D.D.; Law, K. A.; Lawrence, E. C.D.; Mills, D.W.; Myler, S.; Pritchard, J.A.; Thompson, M.; Higson, S. P.J. Sonochemically fabricated microelectrode arrays for biosensors offering widespread applicability: Part I. Biosensors and Bioelectronics 20 (2004): 328–337.

Barton, A. C.; Davis, F.; and Higson, S. P. J. Labeless Immunosensor Assay for Prostate Specific Antigen with Picogram per Milliliter Limits of Detection Based upon an ac Impedance Protocol. Anal. Chem. 80 (2008): 6198–6205.

Benedetto, G.E. De; Palmisano, F.; and Zambonin, P.G. One-step fabrication of a bienzyme glucose sensor based on glucose oxidase and peroxidase immobilized onto a poly(pyrrole) modified glassy carbon electrode. Biosensors & Bioelectronics 11 (1996): 1001-1008.

Blanch,H.W., and Clark, D.S. Biochemical Engineering. U.S.A.: Marcel Dekker, Inc., 1997.

Burmeister, J.J.; Palmer, M.; and Gerhardt, G.A. Ceramic-based multisite microelectrode array for rapid choline measures in brain tissue. Analytica Chimica Acta 481 (2003): 65–74.

Casero, E.; Darder, M.; Pariente, F.; Lorenzo, E. Peroxidase enzyme electrodes as nitric oxide biosensors. Analytica Chimica Acta 403 (2000): 1-9.

Chen, C.C.; and Gu, Y. Enhancing the sensitivity and stability of HRP/PANI/Pt electrode by implanted bovine serum albumin. Biosensors and Bioelectronics 23 (2008): 765–770.

Chen, S.; Yuan, R.; Chai, Y.; Yin, B.; Li, W.; Min, L. Amperometric hydrogen peroxide biosensor based on the immobilization of horseradish peroxidase on core–shell organosilica@chitosan nanospheres and multiwall carbon nanotubes composite. Electrochimica Acta 54 (2009): 3039–3046.

Chen, X.; Li, C.; Liu, Y.; Du, Z.; Xu, S.; Li, L.; Zhang, M.; Wang, T. Electrocatalytic activity of horseradish peroxidase/ chitosan/carbon microsphere microbiocomposites to hydrogen peroxide. Talanta 77 (2008): 37–41.

Cooper, J. M. and Anthony, E.G. C. *Biosensors*. 2nd ed. Oxford, New York, 2004

Cosnier, S. Biomolecule immobilization on electrode surfaces by entrapment or attachment to electrochemically polymerized films. A review. Biosensors & Bioelectronics 14 (1999): 443–456.

Eggins, B.R. Biosensors: An Introduction. England.: Wiley, 1996.

Ekanayake, M. E.M.I.; Preethichandra, D.M.G.; and Kaneto, K. Bi-functional amperometric biosensor for low concentration hydrogen peroxide measurements using polypyrrole immobilizing matrix. Sensors and Actuators B 132 (2008): 166–171.

Fortier, G.; Brassard, E. and Bklanger, D. Optimization of a Polypyrrole Glucose Oxidase Biosensor. Biosensors and Bioelectronics 5 (1990): 473-490.

Frasconi, M.; Favero, G.; Fusco, M.D.; Mazzei, F. Polyazetidine-based immobilization of redox proteins for electron-transfer-based biosensors. Biosensors and Bioelectronics 24 (2009): 1424–1430.

Ganokwan Petchudomsinsuk, Puntarik Anantachoke, and Kongkiat Suriye. A study of biosensor for insecticide detection. Bachelor's Project, Department of Chemical Engineering, Engineering, King Mongkut's University of Technology Thonburi, 2002.

Gao, F.; Yuan, R.; Chai, Y.; Chen, S.; Cao, S.; Tang, M. Amperometric hydrogen peroxide biosensor based on the immobilization of HRP on nano Au/Thi/poly (p-aminobenzene sulfonic acid)-modified glassy carbon electrode. J. Biochem. Biophys. Methods 70 (2007): 407–413.

Hacker, J. IMMOBILIZED ENZYMES [online], 1997. Available from: http://www.rpi.edu/dept/chem-eng/Biotech-Environ/IMMOB/Immob.htm

Hamid, M.; and Rehman, K.U. Potential applications of peroxidases. Food Chemistry 115 (2009): 1177–1186.

Inzelt, G.; Pineri, M.; Schultze, J.W,; Vorotyntsev, M.A. Electron and proton conducting polymer: recent developments and prospects. Electrochimica Acta 45 (2000): 2403-2421.

Kafi, A. K.M. and Chen, A. A novel amperometric biosensor for the detection of nitrophenol. Talanta (2009).

Kim, J. H.; Kim, B. G.; Yoon, J. B.; Yoon, E.; Han, C. H. A new monolithic microbiosensor fro whole blood analysis. Sensoes and Actuators A 95 (2002): 108-113.

Kong, Y. T.; Boopathi, M.; and Shim, Y. B. Direct electrochemistry of horseradish peroxidase bonded on a conducting polymer modified glassy carbon electrode. Biosensors and Bioelectronics 19 (2003): 227-232.

Korkut, S.; Erhan, E.; Yilmaz, F.; Celik, A.; Keskinler, B. Newly synthesized poly(glycidyl methacrylate-co-3-thienylmethylmethacrylate)-based electrode designs for phenol biosensors. Talanta (2009).

Korkut, S.; Keskinler, B.; and Erhan, E. An amperometric biosensor based on multiwalled carbon nanotube-poly(pyrrole)-horseradish peroxidase nanobiocomposite film for determination of phenol derivatives. Talanta 76 (2008): 1147–1152.

Kupila, E.L. and Kankare, J. Influence of electrode pretreatment, counter anions and additives on the electropolymerization of pyrrole in aqueous solutions. Synthetic Metals 74 (1995): 241-249.

Law, K. A.; and Higson, S. P.J. Sonochemically fabricated acetylcholinesterase micro-electrode arrays within a flow injection analyser for the determination of organophosphate pesticides. Biosensors and Bioelectronics 20 (2005): 1914–1924.

Lee, J. H.; Jang, A.; Bhadri, P.R.; Myers, R.R.; Timmons, W.; Beyette, F.R., Jr.; Bishop, P.L.; Papautsky, I. Fabrication of microelectrode arrays for in situ sensing of oxidation reduction potentials. Sensors and Actuators B 115 (2006): 220–226.

Li, F.; Chen, W.; Tang, C.; Zhang, S. Development of hydrogen peroxide biosensor based on in situ covalent immobilization of horseradish peroxidase by one-pot polysaccharide-incorporated sol–gel process. Talanta 77 (2009): 1304–1308.

Li, G.; Wang, Y.; and Xu, H. A Hydrogen Peroxide Sensor Prepared by Electropolymerization of Pyrrole Based on Screen-Printed Carbon Paste Electrodes. Sensors 7 (2007): 239-250.

Liu, J.; Bian, C.; Han, J.; Chen, S.; Xia, S. A silicon-based bulk micromachined amperometric microelectrode biosensor with consecutive platinization and polymerization of pyrrole. Sensors and Actuators B 106 (2005): 591–601.

Liu, Y.; Liu, H.; Qian, J.; Deng, J.; Yu, T. Regenerated silk fibroin membrane as immobilization matrix for peroxidase and fabrication of a sensor for hydrogen peroxide utilizing methylene blue as electron shuttle. Analytica Chimica Acta 316 (1995): 65-72.

Lomillo, A. M.A.; Kauffmann, J.M.; and Martinez, A. M.J. HRP-based biosensor for monitoring rifampicin. Biosensors and Bioelectronics 18 (2003): 1165-1171.

Lu, X.; Zhang, Q.; Zhang, L.; Li, J. Direct electron transfer of horseradish peroxidase biosensor based on chitosan and room temperature ionic. Electrochemistry Communications 8 (2006): 874–878.

Luo, X.; Killard, A. J.; Morrin, A.; Smyth, M. R. Enhancement of a conducting polymer-based biosensor using carbon nanotube-doped polyaniline. Analytica Chimica Acta 575 (2006): 39–44.

Mello, L. D.; Sotomayor, M. D. P. T.; and Kubota, L. T. HRP-based amperometric biosensor for the polyphenols determination in vegetables extract. Sensors and Actuators B 96 (2003): 636–645.

Mohamoud, M.A. Conducting polymers: smart materials with nanotechnology applications: polymers have traditionally been thought of as nonconductors of electricity. Plastics Engineering. Business library [Online], Nov, 2008. Available from: http://findarticles.com/p/articles/mi_hb6619/is_10_64/ai_n30952198/?tag=content;col1[2009, May 17].

Moreno, E. G.; Ruiz, M.A.; Barbas, C., Pingarron, J.M. Determination of organic peroxides in reversed micelles with a poly-*N*-methylpyrrole horseradish peroxidase amperometric biosensor. Analytica Chimica Acta 448 (2001): 9–17.

Mulchandani, A.; and Pan, S. Ferrocene-Conjugated *m* Phenylenediamine Conducting Polymer-Incorporated Peroxidase Biosensors. Analytical Biochemistry 267 (1999)**:** 141–147.

Myler, S.; Collyer, S.D.; Davis, F.; Gornall, D.D.; Higson, S. P.J. Sonochemically fabricated microelectrode arrays for biosensors Part III. AC impedimetric study of aerobic and anaerobic response of alcohol oxidase within polyaniline. Biosensors and Bioelectronics 21 (2005): 666–671.

Myler, S.; Davis, F.; Collyer, S. D.; Higson, S. P.J. Sonochemically fabricated microelectrode arrays for biosensors—part II Modification with a polysiloxane coating. Biosensors and Bioelectronics 20 (2004): 408–412.

Myler, S.; Eaton, S.; and Higson, S. P.J. Poly (o-phenylenediamine) ultra-thin-film composite membranes for enzyme electrodes. Analytica Chimica Acta 357 (1997): 55-61.

Ndangili, P. M.; Waryo, T. T.; Muchindu, M.; Baker, P. G.L.; Ngila, C. J.; Iwuoha, E. I. Ferrocenium hexafluorophosphate-induced nanofibrillarity of polyaniline–polyvinyl sulfonate electropolymer and application in an amperometric enzyme biosensor. Electrochimica Acta (2009).

Netchiporouk, L.I.; Shulga, A. A.; Renault, N. J.; Martelet, C.; Olier, R.; Cespuglio, R. Properties of carbon fibre microelectrodes as a basis for enzyme biosensors . Analytica Chimica Acta 303 (1995): 275-283.

Orozco, J.; Jorquera, C. J.; and Sánchez, C. F. Gold nanoparticle-modified ultramicroelectrode arrays for biosensing: A comparative assessment. Bioelectrochemistry 75 (2009): 176–181.

Pan, M.; Guo, X.; Cai, Q.; Li, G.; Chen, Y. A novel glucose sensor system with Au nanoparticles based on microdialysis and coenzymes for continuous glucose monitoring. Sensors and Actuators A 108 (2003): 258–262.

Pongsak Wattanacharoonroj. The Study of Enzyme Immobilization on the Electrode Biosensor by Sol-Gel Technology. Master's Thesis, Department of Chemical Engineering, Engineering, King Mongkut's University of Technology Thonburi, 2005.

Pournaghi-Azar, M.H.; and Habibi, B. Electropolymerization of aniline in acid media on the bare and chemically pre-treated aluminum electrodes A comparative characterization of the polyaniline deposited electrodes. Electrochimica Acta 52 (2007): 4222–4230.

Pritchard, J.; Law, K.; Vakurov, A.; Millner, P.; Higson, S. P.J. Sonochemically fabricated enzyme microelectrode arrays for the environmental monitoring of pesticides. Biosensors and Bioelectronics 20 (2004): 765–772.

Qian, L.; and Yang, X. Composite film of carbon nanotubes and chitosan for preparation of amperometric hydrogen peroxide biosensor. Talanta 68 (2006): 721–727.

Qu, F.; Yang, M.; Jiang, J.; Shen, G.; Yu, R. Amperometric biosensor for choline based on layer-by-layer assembled functionalized carbon nanotube and polyaniline multilayer film. Analytical Biochemistry 344 (2005): 108–114.

Razola, S.S.; Ruiz, B.L.; Diez, N.M.; Mark, H.B., Jr.; Kauffmann, J-M. Hydrogen peroxide sensitive amperometric biosensor based on horseradish peroxidase entrapped in a polypyrrole electrode. Biosensors and Bioelectronics 17 (2002): 921-928.

Revzin, A.F.; Sirkar, K.; Simonian, A.; Pishko, M.V. Glucose, lactate, and pyruvate biosensor arrays based on redox polymer/oxidoreductase nanocomposite thin-films deposited on photolithograghically patterned gold microelectrodes. Sensors and Actuators B 81 (2002): 359-368.

Rosatto, S.S.; Kubota, L.T.; and Neto G.D.O. Biosensor for phenol based on the direct electron transfer blocking of peroxidase immobilising on silica-titanium. Analytica Chimica Acta 390 (1999): 65-72.

Rosatto, S. S.; Sotomayor, P. T.; Kubota, L. T.; Gushikem, Y. SiO2/Nb2O5 sol_/gel as a support for HRP immobilization in biosensor preparation for phenol detection. Electrochimica Acta 47 (2002): 4451-4458.

Ruzgas, T.; Csoregi, E.; Emneus, J.; Gorton, L.; Varga, G.M. Peroxidase-modified electrodes: Fundamentals and application. Analytica Chimica Acta 330 (1996): 123-138.

Ruzgas, T.; Emneus, J.; Gorton, L.; Marko-Varga G. The development of a peroxidase biosensor for monitoring phenol and related aromatic compounds. Analytica Chimica Acta 311(1995): 245-253.

Sarac, A.S.; Evans, U.; Serantoni, M.; Clohessy, J.; Cunnane, V.J. Electrochemical and morphological study of the effect of polymerization conditions on poly(terthiophene). Surface and Coatings Technology 182 (2004): 7–13.

Schwarz, J.; Kaden, H.; and Enseleit, U. Voltammetric examinations of ferrocene on microelectrodes and microarrayelectrodes. Electrochemistry Communications 2 (2000): 606–611.

Shi, A. W.; Qu, F. L.; Yang, M. H.; Shen , G. L.; Yu, R. Q. Amperometric H2O2 biosensor based on poly-thionine nanowire/HRP/nano-Au-modified glassy carbon electrode. Sensors and Actuators B 129 (2008): 779–783.

Shuler, M. L.; and Kargi, F. Bioprocess Engineering: Basic concepts. 2nd ed. Upper Saddle River: Prentice Hall PTR.

Simm, A.O.; Jones, S.W.; Banks, C.E.; Compton, R.G. Novel methods for the production of silver microelectrode arrays: Their characterization by atomic force microscopy and application to the electro-reduction of halothane. Analytical Sciences 21 (2005): 667- 671.

Songa, E.A.; Arotiba, O.A.; Owino, J. H.O.; Jahed, N.; Baker, P. G.L.; Iwuoha, E. I. Electrochemical detection of glyphosate herbicide using horseradish peroxidase immobilized on sulfonated polymer matrix. Bioelectrochemistry, (2009).

Stanca, S.E.; Popescu , I. C.; and Oniciu, L. Biosensors for phenol derivatives using biochemical signal Amplification. Talanta 61 (2003): 501-507.

Stephanis, C.G.; Hatiris, J.G.; and Mourmouras, D.E. The process (mechanism) of erosion of soluble brittle materials caused by cavitation. Ultrasonics Sonochemistry 4 (1997): 269-271.

Sulak, M.T.; Erhan, E.; and Keskinler, B. Amperometric Phenol Biosensor Based on Horseradish Peroxidase Entrapped PVF and PPy Composite Film Coated GC Electrode. Appl Biochem Biotechnol (2009).

Tang, J.; Wang, B.; Wu, Z.; Han, X.; Dong, S.; Wang, E. Lipid membrane immobilized horseradish peroxidase biosensor for amperometric determination of hydrogen peroxide. Biosensors and Bioelectronics 18 (2003): 867-872.

Tatsuma, T.; Gondaira, M.; and Watanabe, T. Peroxidase- Incorporated Polypyrrole Membrane Electrodes. Anal. Chem. 64 (1992): 1183-1187.

Thanachasai, S.; Rokutanzono, S.; Yoshida, S.; Watanabe, T. Novel Hydrogen Peroxide Sensors Based on Peroxidase-Carrying Poly{pyrrole-co-[4-

(3-pyrrolyl) butanesulfonate]} Copolymer Films. Analytical Sciences 18 (2002).

Thanachasai, S.; Yoshida, S.; and Watanabe, T. Effect of Fabrication Parameters on the Enzyme Loading and Sensor Response of Enzyme-Carrying Conductive Polymer Electrodes. Analytical Sciences 19 (2003).

Thomas, F.G. and Henze, G. Introdction to Voltammetric Analysis Theory and Practice. Australia: CSIRO publishing.

Tian, F.; Xu, B.; Zhu, L.; Zhu, G. Hydrogen peroxide biosensor with enzyme entrapped within electrodeposited polypyrrole based on mediated sol–gel derived composite carbon electrode. Analytica Chimica Acta 443 (2001): 9–16.

Umana, M. and Waller, J. Protein-Modified Electrodes. The Glucose Oxidase/Polypyrrole System. Anal. Chem. 58 (1986): 2979-2983.

Vidal, J. C.; Ruiz, E. G.; and Castillo, J. R. Recent advances in electropolymerized conduting polymers in amperometric biosensors. Microchim. Acta 143 (2003): 93-111.

Waltman, R. J. and Argon, J. B. Electrically conducting polymers: a review of the electropolymerization reaction, of the effects of chemical structure on polymer film properties, and of applications towards technology. CAN. J. CHEM. 64 (1986): 76-95.

Wang, B. and Dong, S. Sol–gel-derived amperometric biosensor for hydrogen peroxide based on methylene green incorporated in Nafion film. Talanta 51 (2000): 565–572.

Wang, B.; Zhang, J. ; Cheng, G. ; Dong S. Amperometric enzyme electrode for the determination of hydrogen peroxide based on sol–gel/hydrogel composite film. Analytica Chimica Acta 407 (2000): 111–118.

Wang, J. Analytical Electrochemistry. 2nd Ed. U.S.A.: Wiley-VCH, 2000.

Wang, P.; Li, S.; and Kan, J. A hydrogen peroxide biosensor based on polyaniline/FTO. Sensors and Actuators B 137 (2009): 662–668.

Xu, Q.; Mao, C.; Liu, N. N.; Zhu, J. J.; Sheng, J. Direct electrochemistry of horseradish peroxidase based on biocompatible carboxymethyl chitosan–gold nanoparticle nanocomposite. Biosensors and Bioelectronics 22 (2006): 768–773.

Yang, J.; and Martin, D.C. Microporous conducting polymers on neural microelectrode arrays I Electrochemical deposition. Sensors and Actuators B 101 (2004): 133–142.

Yang, Y.; Yang, G.; Huang, Y.; Bai, H.; Lu, X. A new hydrogen peroxide biosensor based on gold nanoelectrode ensembles/multiwalled carbon nanotubes/chitosan film-modified electrode. Colloids and Surfaces A: Physicochem. Eng. Aspects, (2009).

Zhang, S.; Zhao, H.; and John, R. Development of a generic microelectrode array biosensing system. Analytica Chimica Acta 421 (2000): 175–187.

Zhang, S.; Zhao, H.; and John, R. A dual-phase biosensing system for the determination of phenols in both aqueous and organic media. Analytica Chimica Acta 441 (2001): 95–105.

Zhao, X.; Mai, Z.; Kang, X.; Zou, X. Direct electrochemistry and electrocatalysis of horseradish peroxidase based on clay–chitosan-gold nanoparticle nanocomposite. Biosensors and Bioelectronics 23 (2008): 1032–1038.

Zoski, C. G. Handbook of Electrochemistry. Elsevier, (2009).

ศูนย์วิทยทรัพยากร
จุฬาลงกรณ์มหาวิทยาลัย

APPENDICES

ศูนย์วิทยทรัพยากร
จุฬาลงกรณ์มหาวิทยาลัย

Appendix A

Raw Data

Data of cyclic voltammetry were very much about 6,000 to 10,000 values for one graph. For this reason, the data of cyclic voltammogram were not shown.

Follows tables showed the response current which got from steady state responses of amperometry techniques at -0.05V. These data were information from finding of optimum electropolymerization conditions.

Table A.1 Amperometric current response (at -0.05V) from preliminary experiment of biosensors at different solution.

Solution Type	$I_{Bare\ GCE}$ (nA)	$I_{PPY/GCE}$ (nA)	$I_{HRP+PPY/GCE}$ (nA)
PBS	-6.58	-45.83	-33.161
30μM H_2O_2	-4.29	-33.77	-45.36
50 μM Phenol	-3.89	-23.99	-41.24
30 μM H_2O_2 /50 μM Phe	-1.99	-27.43	-72.78
50 μM H_2O_2 /50 μM Phe	-2.92	-37.56	-138.42
100 μM H_2O_2 /50 μM Phe	-2.58	-36.62	-75.08

Table A.2 Amperometric current response (at -0.05V) of micro-biosensors at different cycles coating of HRP-PPY.

Cycle	I_1 (nA)	I_2 (nA)	I_3 (nA)	I_{avg} (nA)	SD	RSD (%)	P value (relative to 20cyc.)
10	-32.39	-22.49	-14.95	-23.28	8.75	37.59	0.013
15	-47.26	-36.34	-20.19	-34.60	13.62	39.37	0.012
20	-68.09	-50.48	-38.96	-52.51	14.67	27.94	*
25	-55.07	-42.54	-33.23	-43.61	10.96	25.13	0.052
30	-23.98	-17.05	-12.77	-17.93	5.66	31.54	0.022

Table A.3 Amperometric current response (at -0.05V) of micro-biosensors at different scan rates of HRP-PPY coating.

Scan rate (mV/s)	I_1 (nA)	I_2 (nA)	I_3 (nA)	I_{avg} (nA)	SD	RSD (%)	P value (relative to 10mV/s)
5	-33.89	-26.53	-23.49	-27.97	5.35	19.12	0.045
10	-68.09	-50.48	-38.96	-52.51	14.67	27.94	*
20	-43.05	-40.09	-36.86	-40.00	3.09	7.74	0.203
30	-34.30	-24.65	-22.18	-27.05	6.41	23.68	0.035
50	-18.90	-18.96	-18.42	-18.76	0.30	1.58	0.056

Table A.4 Amperometric current response (at -0.05V) of micro-biosensors at different pyrrole concentration of HRP-PPY coating.

Py conc. (M)	I_1 (nA)	I_2 (nA)	I_3 (nA)	I_{avg} (nA)	SD	RSD (%)	P value (relative to 0.05M)
0.03	-20.11	-15.32	-7.76	-14.40	6.23	43.27	0.005
0.05	-43.05	-40.09	-36.86	-40.00	3.09	7.74	*
0.07	-33.70	-28.70	-17.67	-26.69	8.20	30.72	0.047
0.09	-20.12	-13.74	-10.39	-14.75	4.94	33.49	0.002

Table A.5 Amperometric current response (at -0.05V) of micro-biosensors at different HRP concentration of HRP-PPY coating.

HRP conc. (U/ml)	I_1 (nA)	I_2 (nA)	I_3 (nA)	I_{avg} (nA)	SD	RSD (%)	P value (relative to 250U/ml)
150	-14.89	-10.44	-10.39	-11.90	2.58	21.71	0.001
250	-43.05	-40.09	-36.86	-40.00	3.09	7.74	*
350	-35.14	-29.45	-26.54	-30.38	4.37	14.40	0.007
450	-31.84	-26.05	-21.35	-26.41	5.25	19.89	0.008

Table A.6 Amperometric current response (at -0.05V) of an optimum HRP-PPY/ 25 min sonicated PPD/GCE in different solutions.

Solution	I_1 (nA)	I_2 (nA)	I_3 (nA)	I_{avg} (nA)	SD	RSD(%)
PBS	-3.16	-2.71	-2.47	-2.78	0.35	12.76
50μM Phenol	-4.89	-4.00	-3.57	-4.15	0.67	16.22
50μM H_2O_2	-9.74	-8.52	-8.43	-9.13	0.87	9.48
50μM Phenol:50μM H_2O_2	-23.74	-21.84	-19.90	-21.83	1.92	8.80

Table A.7 Amperometric current response (at -0.05V) of a phenol calibration curve of a HRP-PPY/ 25 min sonicated PPD/GCE in 50 μM H_2O_2/PBS.

Phenol conc. (μM)	I_1 (nA)	I_2 (nA)	I_3 (nA)	I_4 (nA)	I_5 (nA)	I_{avg} (nA)	SD
2	-4.22	-4.02	-4.13	-3.88	-3.85	-4.02	0.1596897
4	-4.40						
6	-4.60						
8	-4.62						
10	-4.69						
20	-5.62						
40	-7.52						
60	-9.92						
80	-11.70						
100	-14.86						
200	-22.87						
400	-36.42						
600	-41.49						
800	-48.68						
1000	-37.82						

Table A.8 Amperometric current response (at -0.05V) of ten times measurements of a HRP-PPY/ 25 min sonicated PPD/GCE in 50 μM phenol/ 50 μM H_2O_2/PBS.

Times of measurement	Current response (nA)	% I
1	-28.50	100.00
2	-22.95	80.53
3	-22.47	78.86
4	-22.24	78.05
5	-21.57	75.71
6	-17.89	62.78
7	-16.69	58.59
8	-16.32	57.28
9	-16.09	56.47
10	-15.96	56.00

Table A.9 Amperometric current response (at -0.05V) of ten HRP-PPY microelectrode biosensors in 50 μM phenol/ 50 μM H_2O_2/PBS.

No. of biosensors	Current response (nA)
1	-14.25
2	-20.11
3	-24.25
4	-19.79
5	-15.67
6	-21.22
7	-16.36
8	-12.87
9	-17.41
10	-10.80
AVG I (nA)	-17.27
SD	4.12
RSD(%)	23.84

Table A.10 Amperometric current response (at -0.05V) for storage stability of a HRP-PPY microelectrode biosensor in 50 μM phenol/ 50 μM H_2O_2/PBS.

Storage time (days)	I (nA)	% I
Initial (fabrication day)	-17.41	100.00
1	-8.02	46.08
2	-7.74	44.46
5	-6.65	38.19
14	-5.49	31.55
30	-4.19	24.06

ศูนย์วิทยทรัพยากร
จุฬาลงกรณ์มหาวิทยาลัย

Appendix B

Conference

Panjai Rujisomnapa, Lerdluk Kaewvimol, Chanchana Thanachayanont, and Seeroong Prichanont. **"Fabrication of Microelectrode Arrays using Sonochemical Technique"** Extended Abstract for Conference at Kanchanaburi, Thailand with the name of ―The 19th Thailand Chemical Engineering and Applied Chemistry Conference" (TICHE) 2009 – Research Cooperation Between Academies and Industries in Thailand, 26-27 October 2009.

ศูนย์วิทยทรัพยากร
จุฬาลงกรณ์มหาวิทยาลัย

การประชุมวิชาการวิศวกรรมเคมีและเคมีประยุกต์แห่งประเทศไทย ครั้งที่ 19

ความร่วมมือทางการวิจัยระหว่างภาคการศึกษาและภาคอุตสาหกรรมในประเทศไทย

Research Cooperation Between Academies and Industries in Thailand

วันที่ 26-27 ตุลาคม 2552 ณ เฟลิกซ์ ริเวอร์ แคว รีสอร์ท กาญจนบุรี

ภาควิชาวิศวกรรมเคมี คณะวิศวกรรมศาสตร์และเทคโนโยลีอุตสาหกรรม

มหาวิทยาลัยศิลปากร

ได้รับเกียรติให้เป็นเจ้าภาพร่วมกับ

สมาคมวิศวกรรมเคมีและเคมีประยุกต์แห่งประเทศไทย

เพื่อจัดการประชุมวิชาการวิศวกรรมเคมีและเคมีประยุกต์แห่งประเทศไทย ครั้งที่ 19 ประจำปี 2552

ระหว่างวันที่ 26-27 ตุลาคม 2552 ณ เฟลิกซ์ ริเวอร์ แคว รีสอร์ท จ.กาญจนบุรี

Fabrication of Microelectrode Arrays using Sonochemical Technique

Panjai Rujisomnapa[1], Lerdluk Kaewvimol[1], Chanchana Thanachayanont[2], and Seeroong Prichanont[1,*]

1) Department of Chemical Engineering, Faculty of Engineering, Chulalongkorn University, Bangkok 10330

2) National Metal and Materials Technology Center (MTEC) a member of National Science and Technology Development Agency (NSTDA), Klong Luang, Pathumthani 12120

E-mail address: seeroong.p@chula.ac.th

Abstract

In this report, microelectrode arrays biosensor was produced by sonochemical fabrication. The arrays were formed by electropolymerization of an insulated polydiaminobenzene film on glassy carbon electrode (GCE). The electrochemical property of microelectrode arrays were characterized within this peper.

1. Introduction

In the past three decades, microelectrode array based biosensors have been used as devices for determining various electroactive species in the field of cellular biology. These biosensors showed advantageous characteristics in comparison to conventional biosensors such as small volume in reagents, quick response time, ease of fabrication, etc [1]. Even though microelectrode arrays can be fabricated by several approaches such as photolithography or laser ablation, but these are costly. Sonochemical fabrication is a simple and inexpensive approach. Previous researches have utilized sonochemically microelectrode arrays containing entrapped enzymes for an amperometric detection of glucose [2, 3], alcohol [4], and organophosphate pesticides [5, 6].

In this research, microelectrode arrays on glassy carbon electrode surface were fabricated using sonochemical procedure.

2. Experimental

2.1 Materials and Apparatus

Disodium hydrogen orthophosphate (Na_2HPO_4) and sodium dihydrogen orthophosphate (NaH_2PO_4) were purchased from Fisher Scientific. Sodium chloride (NaCl) and potassium sulfate (K_2SO_4) were purchased from Ajax Fine Chem. Potassium ferrocyanide ($K_4[Fe(CN)_6]$) was purchased from RANKEM. Acetic acid (CH_3COOH) was from Mallinckrodt Chemicals. Sodium acetate (CH_3COONa) was from Scharlau Chemie S.A. 1,2-Diaminobenzene dihydrochloride (PPD) was purchased from Fluka Analytical.

Electrochemical measurements of cyclic voltammetry were performed with a Glucosen potentiostat (Chulalongkorn University, Thailand). The electrochemical cell consists of a three-electrode system with a glassy carbon electrode (GCE), a platinum wire, and Ag/AgCl as working, counter, and reference electrodes, respectively.

2.2 Electrode preperation

5 mM of 1,2-diaminobenzene dihydrochloride was prepared in phosphate buffer solution pH 7.4 ($5.26x10^{-2}$ M Na_2HPO_4; $1.3 x10^{-2}$ M NaH_2PO_4; $5.1 x10^{-3}$ M NaCl). Next, the prepared solution was electropolymerised onto GCE by potentially cycling of the working electrode between 0 to +1.4V at 50 mV/s [7]. Sonochemical ablation of polydiaminobenzene modified insulated GCE was performed with the ultrasonic bath (CREST, model D, Malaysia).

3. Results and discussions

PPD was electropolymerized on GCE surface (Fig.1) by potential cycling between 0 to +1.4 V (vs. Ag/AgCl) for 10 cycles. The decreasing peak currents of the cyclic voltammetry demonstrate that the electrode surface became progressively insulated by the nonconductive polymer film. Cyclic voltammetry at a scan rate of 50mV/s of (i) the planar GCE, (ii) the polydiaminobenzene coated GCE, and sonochemically fabricated

microelectrode array at various times ((iii), (iv), and (v)) are shown in Fig.2. The PPD coated electrode shows no response current, in comparison to the high response obtained from thebare electrode. After 20 minutes sonochemical ablation of the nonconductive polymer layer, the electrode demonstrated low sigmoidal shaped current responses which probably indicated that mircroelectrode arrays were fabricated on GCE.

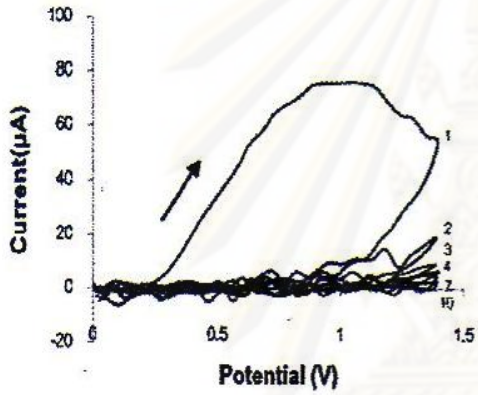

Fig1. Cyclic voltammetry for elecropolymerization of 5 mM 1,2-diaminobenzene dihydrocloride at a potential scan rate of 50 mV/s.

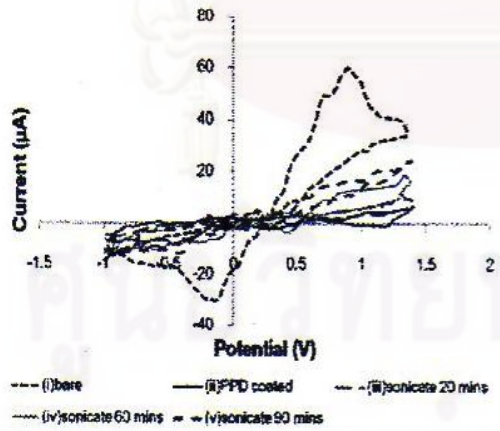

Fig.2 cyclic voltammetry of (i) bare GCE, (ii) insulating polymer coated GCE, (iii) a 20 mins. sonochemically fabricated microelectrode array, (iv) a 60 mins. sonochemically fabricated microelectrode array, and (v) a 90 mins. sonochemically fabricated microelectrode array; at scan rate of 50 mV/s.

4. Conclusion

The microelectrode arrays can be produced on glassy carbon electrode surface using sonochemical ablation of the coated nonconductive polymer layer. In the future work, we will immobilize enzyme within polyaniline on these microelectrode arrays and study the effects of electropolymerize conditions.

5. References

[1] Liu, J.; Bian, C.; Han, J.; Chen, S.; Xia, S. A silicon-based bulk micromachined amperometric microelectrode biosensor with consecutive platinization and polymerization of pyrrole. Sensors and Actuators B 106 (2005): 591–601.

[2] Barton, A. C.; Collyer, S. D.; Davis, F.; Gomall, D. D.; Law, K. A.; Lawrence, E. C.D.; Mills, D. W.; Myler, S.; Pritchard, J. A.; Thompson, M.; Higson, S. P.J. Sonochemically fabricated microelectrode arrays for biosensors offering widespread applicability: Part I. Biosensors and Bioelectronics 20 (2004): 328–337.

[3] Myler, S.; Davis, F.; Collyer, S. D.; Higson, S. P.J. Sonochemically fabricated microelectrode arrays for biosensors—part II Modification with a polysiloxane coating. Biosensors and Bioelectronics 20 (2004): 408–412.

[4] Myler, S.; Collyer, S.D.; Davis, F.; Gomall, D.D.; Higson, S. P.J. Sonochemically fabricated microelectrode arrays for biosensors Part III. AC impedimetric study of aerobic and anaerobic response of alcohol oxidase within polyaniline. Biosensors and Bioelectronics 21 (2005): 666–671.

[5] Pritchard, J.; Law, K.; Vakurov, A.; Millner, P.; Higson, S. P.J. Sonochemically fabricated enzyme microelectrode arrays for the environmental monitoring of pesticides. Biosensors and Bioelectronics 20 (2004): 765–772.

[6] Law, K. A.; and Higson, S. P.J. Sonochemically fabricated acetylcholinesterase micro-electrode arrays within a flow injection analyser for the determination of organophosphate pesticides. Biosensors and Bioelectronics 20 (2005): 1914–1924.

[7] Myler, S.; Eaton, S.; and Higson, S. P.J. Poly (o-phenylenediamine) ultra-thin-film composite membranes for enzyme electrodes. Analytica Chimica Acta 357 (1997): 55-61.

VITA

Miss Panjai Rujisomnapa was born in Bangkok, Thailand on December 3, 1985. She finished her secondary course from Satree Wat Mahaprutharam School in March, 2004. After that, she studied in the major of Chemical Engineering in Faculty of Engineering at King Mongkut's University of Technology Thonburi. She continued her further study for master's degree in Chemical Engineering at Chulalongkorn University in the Biochemical Engineering Research Group and achieved her Master's degree in April, 2010.

ศูนย์วิทยทรัพยากร
จุฬาลงกรณ์มหาวิทยาลัย